LIÈGE université

The University of Nottingham
UNITED KINGDOM · CHINA · MALAYSIA

Design of poly(HEMA) particles in supercritical carbon dioxide for protein delivery

Rahmet PARILTI

Thesis submitted for the degree of Doctor in Sciences

2017-2018



This thesis was financially supported by the Nanofar Erasmus Mundus Joint Doctorate programme in nanomedicine and pharmaceutical innovation and performed in collaboration between Center for Education and Research on Macromolecules (CERM), University of Liege (Belgium) and University of Nottingham (United Kingdom). CERM is indebted to Interuniversity Attraction Poles (IAP-7/5-FS2).

Thesis jury members

Prof. Carmen ALVAREZ-LORENZO	University of Santiago de Compostela
Prof. Mathias DESTARAC	University of Toulouse
Prof. Anne-Sophie DUWEZ	University of Liege (President)
Dr. Bruno GRIGNARD	University of Liege (Secretary)
Prof. Steve HOWDLE	University of Nottingham (Promoter)
Prof. Christine JEROME	University of Liege (Promoter)

Design of poly(HEMA) particles in supercritical carbon dioxide for protein delivery

by

Rahmet PARILTI

A vast majority of the polymer nanocarriers have been designed and developed for the controlled and targeted release of hydrophobic drugs. However, there are still some challenges to design appropriate carriers for the delivery of therapeutic proteins or peptides. Although the history of the protein/peptide based drugs dates back to insulin production, they have taken great attention since the last decades due to their possible broad range of therapeutic applications. They might offer more specific and safer therapies in comparison to small molecules drugs. Nonetheless, their encapsulation remains challenging especially to preserve their specific structure and activity in the formulations. For this purpose, hydrogel particles (nano-/microgels) have emerged as promising polymer carriers for such proteins.

This work focuses on the synthesis of nano-/microgels encapsulating therapeutic proteins and peptides in supercritical carbon dioxide which confers environmentally benign features to the synthesis method. More precisely, hydrogel particles were obtained by free-radical dispersion polymerisation of 2-hydroxyethyl methacrylate (HEMA) in supercritical carbon dioxide in presence of a cross-linker and a suitable stabiliser. Two kinds of stabilisers have been designed and studied, i.e. a photocleavable perfluorinated stabiliser and a fluorine-free stabiliser. The optimisation of the dispersion polymerisation conditions led to well-defined cross-linked particles. The process was robust enough to incorporate a drug or a peptide to encapsulate in one-pot synthesis into the particle network.

In a subsequent step such drug loaded particles were dispersed successfully in aqueous media and shown sustained release of their content. This was demonstrated notably for the release of a bactericidal peptide.

Acknowledgements

First of all, I would like to gratefully thank to my supervisors Prof. Christine Jerome and Prof. Steve Howdle for giving me this opportunity to undertake this PhD in their groups and for their continued guidance, enthusiasm and help throughout my thesis.

I extend my gratitude to all my jury members, Prof. Carmen Alvarez-Lorenzo, Prof. Mathias Destarac, Prof. Anne-Sophie Duwez and Dr. Bruno Grignard, for accepting to be the members of my thesis jury and for the time they have devoted to review my thesis.

Also, I would like to thank to our collaborators Prof. Christine Dupont, Yasmine Adriaensen and Pierre Eloy in University Catholique Louvain for XPS measurements and their exceptional scientific contribution to my thesis.

I am grateful to Dr. David Alaimo, Dr. Raphael Riva, and Dr. Michael Alexandre for their time and invaluable advices about my research. Also to Jeremie Caprasse my project student for his great contribution in the antimicrobial peptide encapsulation part of the thesis.

I would like to thank also Alba Castanon, soon to be doctor, for the fruitful collaboration during my work in University of Nottingham. I would like to thank her for teaching me a lot and introducing me to the equipment. Especially sharing with me generously her hydrocarbon based stabilisers.

I owe a huge thanks to our technicians in CERM. All the time they have been very kind, helpful and resourceful. I would like to thank Valerie Collard for great SEM images. She devoted a lot of time and effort to take good pictures. I would like to thank Gregory Cartigny for ATR-IR, Martine Dejeneffe for ordering our chemicals and Charlotte Dannemark for technical support for DLS. Besides, I would like to thank them all for their countless help for many practical things in the lab.

I would like to thank workshop staff Peter Fields and Richard Wilson for their invaluable technical and safety support for high pressure equipments at University of Nottingham. They were always really kind and very rapid to fix many times my reactor and other equipments in B10. This also extends to Mark Guyler who helped keeping all the labs well-organised.

Also I would like to thank Sophie Boulanger, Enza Esposito and Helene Carson (University of Nottingham) for keeping us on track with administrative works.

Of course, I would like to thank to the members of the labs that I had to chance to work during my PhD both in CERM and B10. They have been very kind, welcoming and supportive. I learned and grew a lot from their experience and guidance. As well as their friendship made these years so much fun and unforgettable times of my life. This includes also my NanoFar friends which I had incredible times during NanoFar schools and meetings. I was very happy to be part of this great PhD programme. I wish for all of my friends the best for their future and hopefully to be in touch for the upcoming years. I should say that you all have a very special place in my heart and you will be greatly missed and remembered.

Certainly, my deepest gratitude goes to my parents and my big family. Even I am far away I always feel their presence and support. Their eternal guidance is beyond words. Especially I would like to mention my dearest dears, the new members of our family, my nieces!! They brought a great joy and happiness to our family. May God bless all of my family with the greatest things! Wish we live long, happy, prosper life like always all together.

Babam ve annem başta olmak üzere benden maddi ve manevi desteklerini hiçbir zaman esirgemeyen tüm aileme canı yürekten teşekkür ediyorum. Sizler olmadan bu meşakkatli yolculuğu asla başaramazdım. Sizleri tüm kalbimle seviyorum. Sizin gibi bir aileye ve de hayatta sahip olduğum bütün herşey için Allah'a şükrediyorum.

Rahmet PARILTI

İnsanlar, kendi hayatları binâsının mimârlarıdır. Bu binâyı kurmak husûsunda gösterecekleri ustalık veya acemilik, onları mes'ud veya bedbaht eyler. Gayret et ki, hayatını kurarken sana saadet ve huzur getirecek iyilik, güzellik, hak, hakîkat ve fazîlet malzemesini kullanmak hünerini gösteresin.

Samiha Ayverdi

Table of Contents

Chapter 1: Introduction 1
1. Protein delivery 3
1.1 Why do we need to encapsulate them? 5
1.1.1 Low physical & chemical stability 6
1.1.2 Effect of administration methods 7
1.2 What should we consider when we are designing a protein delivery system? 9
2. Hydrogels 10
2.1 How can hydrogels be prepared as nano-sized particles? 14
2.1.1 Cross-linking of natural/synthetic polymer precursors 16
2.1.2 Synthesis of nanogels *via* heterogeneous polymerisation processes 25
3. Supercritical fluids 30
3.1 Supercritical carbon dioxide ($scCO_2$) 33
3.1.1 Polymerisations in $scCO_2$ 34
3.1.2 Stabiliser design 35
3.1.3 Emulsion polymerisation in $scCO_2$ 37
3.1.4 Dispersion polymerisation in $scCO_2$ 38
References 42
Aim of the thesis 53
Chapter 2: Mild synthesis of poly(HEMA)-networks as well-defined nanoparticles in supercritical carbon dioxide 55
1. Introduction 59
2. Experimental Part 63
2.1 Materials 63
2.2 Methods 63
2.2.1 Synthesis of macroRAFT agent (PEO-CTA) 63
2.2.2 Synthesis of diblock stabilisers (PEO-*b*-PFDA) 64
2.2.3 Synthesis of poly (2-hydroxyethyl methacrylate) network nanoparticles in $scCO_2$ 65
2.3 Characterisations 66
2.3.1 Cloud point measurements of the diblock copolymers 67
3. Results and discussions 68
3.1 Synthesis of the stabilisers 68

3.2 Dispersion polymerisation of 2-hydroxyethyl methacrylate (HEMA) in supercritical carbon dioxide ($scCO_2$) 70
3.2.1 Effects of the temperature and pressure 70
3.2.3 Effect of the stabiliser concentration 73
3.2.4 Effect of the stabiliser composition 74
4. Conclusions 75
References 76
Chapter 3: Sulindac encapsulation and release from functional poly(HEMA) microparticles prepared in supercritical carbon dioxide 79
1. Introduction 83
2. Experimental Part 86
2.1 Materials 86
2.2 Methods 87
2.2.1 Synthesis of the Sulindac encapsulated poly(HEMA) networks in $scCO_2$ 87
2.2.2 UV photolysis of the particles 87
2.2.3 Release behavior 88
2.2.4 Grafting of Fluoresceinamine on the particles *via* reductive amination 88
2.3 Characterisations 89
3. Results and discussions 90
3.1 One-pot sulindac encapsulation by *in-situ* dispersion polymerisation of HEMA 90
3.2 Determination of the encapsulation efficiency and release behaviour of hydrogel 95
3.3 Grafting on the particle surfaces 98
4. Conclusions 100
References 101
Chapter 4: Encapsulation of antimicrobial peptides in poly(HEMA) networks in supercritical carbon dioxide 103
1. Introduction 107
2. Experimental 110
2.1 Materials 110
2.2 Methods 111
2.2.1 Synthesis of the poly(HEMA) networks in $scCO_2$ 111
2.2.2 UV photolysis of the particles 111
2.2.3 Antibacterial Test 112
2.2.4 Grafting of targeting peptide *via* reductive amination 113
2.3 Characterisations 113

3. Results and discussion 114
3.1 Synthesis of the photocleavable stabiliser 114
3.2 Poly(HEMA) networks in supercritical carbon dioxide ($scCO_2$) 115
3.3 Antibacterial test 120
3.3.1 Free Bradykinin and Pro^3-TL 120
3.3.2 Antibacterial tests on empty and loaded particles 121
3.4 Surface Functionalisation 126
4. Conclusions 127
References 128
Chapter 5: Hydrocarbon based stabilisers for the synthesis of poly(HEMA) cross-linked particles in supercritical carbon dioxide 131
1. Introduction 135
2. Experimental 138
2.1 Materials 138
2.2 Methods 138
2.2.1 Synthesis of O-ethyl-S-(1-methoxycarbonyl) ethyl dithiocarbonate 138
2.2.2 Synthesis of PVAc-s-PVPi copolymers 139
2.2.3 Dispersion polymerisation in $scCO_2$ 139
2.2.4 Hydrolysis of the stabiliser and stabilized particles 140
2.3 Characterisations 141
3. Results and discussions 143
3.1 Synthesis of the stabilisers *via* RAFT polymerisation 143
3.1.1 Cloud point measurements 146
3.2 Dispersion polymerisation of HEMA in $scCO_2$ 148
3.2.1 Effect of stabiliser composition and molecular weight 150
3.2.2. Effect of cross-linker content 154
3.2.3 Copolymerisation with MMA and N-VP 156
3.3 Hydrolysis of the stabiliser towards hydrogel microparticles 158
3.3.1 Swelling of the homo/copolymer networks in water 161
4. Conclusions 162
References 163
Chapter 6: General conclusions and perspectives 165
General conclusions and perspectives 167
Annex 173

High pressure equipments 173
Abstract 175
1. ToP Industrie High pressure reactor (University of Liege) 177
1.1 Cleaning of the high-pressure reactor 179
2. High pressure equipments (University of Nottingham) 180
2.1 MKIII clamp-seal autoclave 180
2.2 High pressure variable volume view cell 183

List of Abbreviations

Ethylene glycol dimethacrylate	EGDMA
1H,1H,2H,2H-Heptadecafluorodecyl acrylate	FDA
Glycidyl methacrylate	GMA
Glycerol monomethacrylate	GMMA
2-hydroxyethyl acrylate	HEA
2-hydroxymethyl methacrylate	HEMA
N-vinyl pyrrolidone	N-VP
Vinyl acetate	VAc
Vinyl pivalate	VPi
Poly (ethylene oxide)	PEO
Poly(heptadecafluorodecyl acrylate)	PFDA
Poly (2-hydroxyethyl methacrylate)	Poly(HEMA)
Poly (N-isopropylacryl amide)	P(NIPAAM)
Poly (N-vinyl pyrrolidone)	P(NVP)
Poly (methyl methacrylate)	PMMA
Poly(vinyl acetate)	PVAc
Poly (vinyl alcohol)	P(VOH)
Poly(vinyl pivalate)	PVPi
Supercritical carbon dioxide	$scCO_2$
hv	Photosensitive moiety
C_v	Coefficient of variance

Chapter 1

Introduction

1. Protein delivery

Proteins are biomacromolecules that are obtained by condensation of carboxylic acid of one amino acid with the amino group of a subsequent amino acid residue thus amide bonds (peptide bonds). Formation of peptide bond is depicted in the figure below (Figure 1).

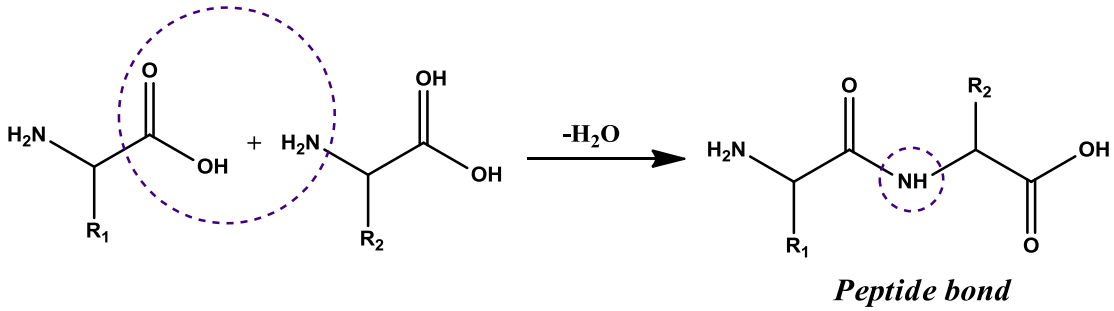


Figure 1: Formation of peptide bond by condensation of two amino acid units resulting into dipeptide.

Dipeptides then converted to polypeptides by successful condensation of many more amino acids (AAs) and subsequently these peptide chains fold into three-dimensional conformation and form the protein. Amino acids are amphoteric which means they are acidic and basic at the same time, as well soluble in water. There are nine essential amino acids that should be provided to the body with nutrients they are namely; Histidine (His), Isoleucine (Ile), Leucine (Leu), Lysine (Lys), Methionine (Met), Phenylalanine (Phe), Threonine (Thr), Tryptophan (Try), and Valine (Val).[1]

Proteins undertake many vital actions in the body; such as being catalyst in the biochemical reactions, signal transduction, supporting the cell membranes as a structural component or they act as transfer agents for molecules. So, as it can be understood mutation and alterations in proteins results in many diseases and disorders.[2]

Importance of the proteins for human beings was also highlighted by the human genome studies; most of our genes were found to be responsible for protein encoding.[3] Having said the importance of proteins for human body, it was also revealed that they can be used as therapeutics to treat many kinds of diseases for instance genetic and degenerative disorders, protein malfunction and enzyme deficiencies. When the peptide/protein based drugs are compared to conventional drugs, they are more active, and they exhibit either low or no drug-drug interactions. [4] As an example, protein-based drugs offer momentary actions which make them safer than existing therapies such as gene therapy, where random or permanent genetic alterations occurs.[2] Considering all the advantages of proteins, a vast number of studies turned to formulate active pharmaceutical ingredients based on peptide/proteins.

The history of the protein based drugs dates back to 1920s. First and one of the well-known protein pharmaceutical is Insulin, which is used by people who suffers from Type 1-diabetes. Even though insulin was the only therapeutic protein in the beginning, now this area of pharmaceutical research has been growing very rapidly thanks to the developments in the biotechnological production methods.[4]

Regarding the synthesis methods, traditionally small molecule drugs are vastly produced by organic chemistry. In the case of protein drugs, they are isolated either from animal or human resources. However, with recombinant DNA technology, the biologically active materials for treatments, proteins (i.e. enzyme inhibitors or activators, antibodies, vaccines or function regulators) being the majority of them, now can be produced by cloning and fermentation. The protein drugs that are produced by recombinant DNA technology offer many advantages in comparison to protein drugs produced by isolation from the native

resources. For instance, they can be synthesized and purified to higher levels with higher efficiency which makes them more affordable. As well as, they can be produced in excessive amounts. Besides, this production method eliminates the exposure to the diseases that could arise from purified source i.e animal/human diseases. Moreover, recombinant DNA technology also permits modification of the protein/peptide structure. Therefore, it is anticipated that the recombinant DNA expression for protein production is a very powerful and facile technique, that it can replace the non-recombinant protein drugs along with high demanding conventional organic chemistry to produce conventional drugs.[5], [6] So considering these facts, the protein pharmaceuticals can be launched in the market faster than ever before.[7] For instance, the well-known two pharmaceutical companies, Sanofi and Abbott, developed and marketed peptide based drugs reaching to billion dollars world-wide sales. Up-to-date more than 60 peptide/protein drugs are commercially available. Around 140 of them are investigated in clinical trials and more than 500 are in the pre-clinical phase. [8]

To sum up, we can state that the successful expansion of the field has been confirmed by increasing number of FDA approved protein drugs over the time. These drugs have been used in several treatments for wide range of diseases, such as cancer, infectious, autoimmune, and AIDS/HIV. Also, many more peptide/protein based drugs are being developed to address different treatments.[9]

1.1 Why do we need to encapsulate them?

In this section we aimed to address the most common problems exerted by protein drugs and why we need to encapsulate them to deliver them in active form, and in sufficient amounts to the targeted site. We have included some sub-topics to make the subject easier

to follow for the readers. However, we have to indicate this is non-exhaustive view on the subject.

1.1.1 Low physical & chemical stability

It has been shown that peptides/proteins based therapeutics hold a great promise for several disease treatments, yet they exhibit some challenges for their purification, separation, more importantly for their storage, and formulations. As a result, they differ from small organic molecules. Peptides/proteins show lower physical and chemical stability. The instability of them stems from their highly specific composition and structure. Briefly we can explain these two phenomena as follows:

Physical instability: Proteins are large polymeric substances (i.e. polypeptides) that folds into secondary, tertiary and quaternary superstructures thanks to secondary interactions. Therefore, physical instability involves structural change which is not observed for the small drugs.

The loss of tertiary structure is called as **denaturation** and upon loss of the structure the proteins are **inactivated**. Denaturation can be induced by changes in temperature (increase/decrease) pH, and organic solvents. Denaturation further results into **adsorption** on the surfaces and **aggregation** with other molecules. Protein aggregation leads to protein delivery systems to fail together with limiting commercialization of the products. Protein aggregation is also harmful for its environment by causing mutations in forming protein fibrils. When this aggregation occurs *in vivo* it results into some of the most known diseases such as Alzhemier's, Parkinson and Huntington diseases as well as Down Syndrome.[10]

Aggregation of proteins can be induced by several reasons. Physical aggregation occurs simply because of protein-protein interactions; whereas chemically occurs due to covalent bond formation. In addition to those, some processing steps, such as fermentation, refolding, heat-treatment, shear/shaking, freeze-thawing and drying can generate protein aggregation. Therefore we have to pay attention to prevent harsh synthetic and processing methods in order to maintain the proteins/peptides specific properties.

Chemical instability: As the name implies, this type of instability is caused by the chemical modifications occurring in the protein composition. These modifications could be bond formation or cleavage resulting into new chemical composition. These modifications can occur *via* hydrolysis, oxidation and different decomposition reactions. In both cases, physical and chemical instability, leads to either inactivation; or differentiation in the protein activity.[11]

1.1.2 Effect of administration methods

Further on this point, in comparison to conventional small molecule drugs proteins are easily degraded by enzymes *via* proteolysis. Also denaturation can occur during storage or administration. As a consequence, effect of administration method on the protein stability should be also considered. [12] Administration methods can be broadly divided into two main categories, namely invasive and non-invasive. Invasive methods are consisted of paranteral routes which are intravenous, intramuscular and subcutaneous injections, whereas non-invasive methods include oral, transdermal, nasal and pulmonary routes.

Parenteral routes signify the administration by injections as intravenous, subcutaneous and muscular. Since proteins have low stability in gastro-intestinal tract (GIT) and low permeability through the biological membranes, the most suitable administration methods

were considered as the parenteral routes.[7] Intravenous injections can circumvent the pre-systemic degradation of the protein drugs and could reach the concentration *in vivo* to have therapeutic effect. [13]

On the basis of this, protein based pharmaceuticals are conventionally administered by subcutaneous injections, such as insulin. Insulin is administered maybe several times per day to reach therapeutic effect. Additionally, in the case of people with chronic diseases the treatment should continue for their life time. Therefore, the patience compliance cannot be met. Mainly formulations for injections are based on solution and suspension of the protein for the ease of storage, and stability of the active agent. However, these formulations do not lead to control and site-specific delivery of the proteins. Moreover, their systemic effect is often very low. For example, in the case of insulin the patient response cannot exceed a day.

Due to patience compliance and acceptability oral delivery is one of the main choice of administration for numerous commercially available drugs, whilst it is not applicable for protein based drugs. The reason behind, there are numerous physiological, enzymatic, and chemical barriers that should be overcome by drugs along the oral route. Generally, conventional small organic drug molecules can prevail over these barriers. On the other hand, peptides/proteins are shown to be very sensitive towards all of these factors. In details, oral bioavailability of peptides/proteins is extremely low due to extreme pH variation, enzymatic degradation by gastrointestinal fluid, and poor intrinsic permeability to intestinal epithelium.[14]

The large size and the hydrophilicity of protein drugs lead to low absorption by the biological membranes, making oral and transdermal administrations ineffective.

Nonetheless, there are also different non-invasive administrations such as nasal, pulmonary, ocular etc. which are also under investigation for protein drugs. We can briefly say even though oral delivery is a preferred mean of administration for many drugs all the administration methods, except the oral delivery, stand as more viable routes for protein based drugs. [15]

To summarize, in order to circumvent the aforementioned problems present for protein based pharmaceuticals, (rapid degradation and inactivation, low bioavailability, storage and formulation instability) researches are focused on the idea of encapsulating them where it can possibly reduce the number of administration and provide controlled site-specific release of the substance.[16]

1.2 What should we consider when we are designing a protein delivery system?

In order to address the listed drawbacks of therapeutic proteins, researchers focused on encapsulating them in a proper carrier for their targeted delivery. There are several parameters to consider when designing a protein delivery system. The main goal of the encapsulation system is to deliver the proteins in sufficient amounts without causing immune response to the targeted site while retaining their specific activity. The therapeutic activity of proteins is largely dependent on their specific conformational structure. Hence, it is very important to keep their sensitive and flexible structure unchanged in the delivery systems. Besides, the chemical and physical stability, immunogenic and pharmacokinetic properties should not be altered.

In general an appropriate protein delivery system should meet the criteria summarized below[17]:

i. To have sufficient amounts of protein drug in vivo over an intended time scale

ii. Able to protect the protein drug from degradation during circulation

iii. Site-specific delivery thus increasing efficiency of the protein drug

Various types of polymer nanocarriers were studied in the literature for biomedical applications, such as nano- or microparticles, micelles, and hydrogel particles. However, drug delivery systems based on polymer micelles, and polymersomes generally exhibit inferior physical stability, and limited control of the therapeutic protein loading as compared to nanogels.[18] Thus, among these classes of polymeric carriers, 3D-network hydrogels, either in bulk or as particles (nanogels), stand out one of the most interesting delivery method. Specifically, designing nano- or micro- sized hydrogel particles offers superior properties, such as larger surface area, network like interior structure, makes them more advantageous in comparison to previously mentioned drug-carrier systems.[19]

2. Hydrogels

Hydrogels are described as three-dimensional polymer networks that are obtained from cross-linking of hydrophilic polymers. Due to the hydrophilic groups in the monomer unit such as –OH, –CONH–, $–CONH_2–$, and $–SO_3H$ they are hydrated in an aqueous medium but remain insoluble due to cross-linking. Hence, they are able to absorb and retain large amounts of water without losing the shape whereby resulting into hydrogel form.

Hydrogel matrices can be produced from natural polymers and their derivatives, such as pullulan, alginate, chitosan, and hyaluronic acid; while among the synthetic polymers, poly(ethylene glycol) (PEG) which is also referred as poly(ethylene oxide) (PEO) in the literature, poly(n-isopropylacryl amide) P(NIPAAM), poly(N-vinyl pyrrolidone) P(NVP),

poly(vinyl alcohol) (PVOH), poly(methacrylic acid) (PMAA) and poly(hydroxyethyl methacrylate) poly(HEMA) are the most commonly used polymers.[20] Hydrogels can also combine several functionalities by copolymerisation; or building interpenetrated double polymeric networks.[21] Hydrogels so far found many applications in biomedical field such as tissue engineering, diagnostic, drug delivery and they are commercially available as soft contact lenses. As far as drug delivery systems are concerned, studies in nanomedicine are focusing on the development of efficient technologies to prepare these relatively complex hydrogel systems as nano- or microparticles (referred as nano-/microgels) using either natural or synthetic starting materials.

In this framework, poly(HEMA) stands as the milestone in hydrogel matrices. It is a hydrophilic polymer exhibiting good optical and mechanical properties, showing low toxicity and irritant effect and was found biocompatible for many application sites. Therefore, since its advent in the field in 1960s, there are great numbers of publications using homo- or copolymers of poly(HEMA) hydrogels and increasing day by day as well as its application areas.[22] Poly(HEMA) hydrogels have found many applications in biomedical field, such as in dental, ophthalmic applications; orfor the immobilization of drugs, cells, and enzymes. Also it is extensively used in drug delivery applications especially for encapsulation of the hydrophilic drugs, which gained a considerable attention in the recent years.

Poly(HEMA) hydrogels made the biggest impact on the ocular applications, majority of the commercially available soft contact lenses are based on this hydrogel matrix. This area is growing rapidly with more studies investigating poly(HEMA) based copolymers in order to finely tune the hydrogel properties. For instance, Seo *et al.* studied poly(HEMA) hydrogels modification with a variety of comonomers such as N-vinyl pyrrolidone (N-VP), methacrylic

acid (MAA), glycidyl methacrylate (GMA), and glycerol monomethacrylate (GMMA) to probe the alteration of mechanical properties of resulting soft contact lenses (Figure 2). They investigated these copolymer hydrogel matrices as soft-contact lens material. Besides, to probe the mechanical and surface wettability properties in order to address the patients' compliance for extended wear of contact lenses.[23] Moreover, this type of contact lens was investigated for the delivery of triamcinolone acetonide (TA) which is a corticosteroid for the treatment of ocular allergy. In this study, poly(HEMA) copolymer hydrogels obtained *via* thermal or photopolymerisation of HEMA in the presence of either methacrylic acid (MA) or N-vinyl pyrrolidone (NVP) as a comonomer in different concentrations. Obtained hydrogels were loaded with a model drug triamcinolone acetonide (TA) and the release behaviour from loaded hydrogels was probed. Highest TA loading and release were achieved by the MA-rich copolymer hydrogels. [24] Much recently, Kapoor et al. incorporated Cyclosporine A (cyclic polypeptide) in the contact lens based on poly(HEMA) hydrogel matrix for ocular disease treatments. They have investigated formation of 100% Cyclosporine particles inside the poly(HEMA) hydrogels by introducing the drug in high concentration to the monomer mixture. As they have anticipated, the release behaviour of the drug could be altered by simply changing the loading percentage, however the size of the drug particles in poly(HEMA) matrix lowered the transmittance. Anyhow, this approach could be very beneficial for different application where the transmittance is not that important.[25] Hackl *et al.* have investigated copolymer hydrogels based on 2-hydroxyethyl methacrylate (HEMA) and 2-hydroxyethylacrylate (HEA) for the delivery of a small protein, lysozyme. Specifically, they investigated the effect of copolymerisation on the mechanical properties, swelling, morphology and the release rate of lysozyme from the resultant hydrogel matrix. They reported that by introducing HEA a more hydrophilic monomer

content into the polymer matrix enhanced the protein loading and the release rate. Moreover, it was shown that the released protein retained its native conformation. They have concluded this study by showing that they can simply adjust the properties i.e swelling, loading/release rate for desired application by altering the HEMA-HEA comonomer compositions.[26]

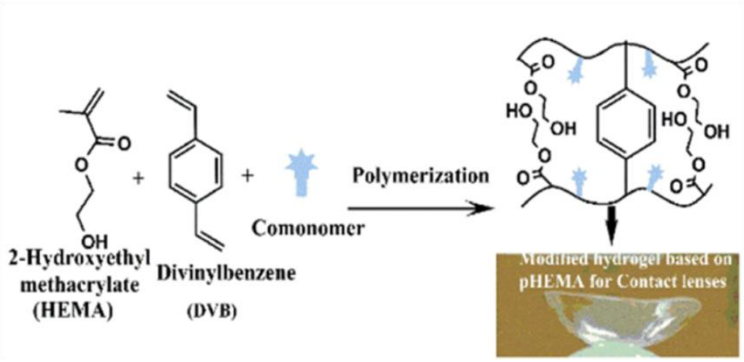


Figure 2: Copolymerisation of HEMA with different comonomers altering the mechanical properties of the resulting poly(HEMA) hydrogel matrix.[23]

Moreover, poly(HEMA) hydrogels can be used as scaffolds for tissue engineering and restorative materials for dental applications. For instance, Mackova *et al.*, studied porous hydrogels based on copolymers of 2-hydroxyethyl methacrylate (HEMA), 2-(acethylthio)ethyl methacrylate (ATEMA), and zwitterionic 2-methacryloyloxyethyl phosphorylcholine (MPC) for tissue engineering applications. Due to residual impurity of ethylene glycol dimethacrylate (EGDMA) in HEMA monomer, poly(HEMA) gels are obtained. Therefore, to produce degradable hydrogel matrix, modification of the ATEMA content in the copolymer results into reductively degradable networks with disulfide bridges. The resultant copolymer matrix was found to be non-toxic and promising material as subcutaneous implant i.e support for human mesenchymal stem cells.[27]

Copolymer networks of 2-hydroxyethyl methacrylate (HEMA) with trimethylolpropane trimethacrylate (TMPT) were also investigated as reconstructive materials for dental applications in which water soluble antimicrobials were encapsulated. In details, hydrogel composed of 50:50 monomer feed ratio loaded successfully with quaternary ammonium compound (QAC), Cetylpyridinium chloride (CPC) and led to extended release of the compound.[28] Interestingly enough, copolymer hydrogels of poly(HEMA) with poly(NIPAAM) show a temperature responsive behaviour thanks to the NIPAAM moieties , i.e. a quite valuable property for myoblast sheet engineering, offering a suitable support for cell sheet production thanks to enhanced cell adhesion and viability properties.[29]

Besides playing on copolymerisation, emulsion polymerisation processes have also been used to design hydrogels with high porosity. Super porous hydrogels based on copolymers of HEMA were synthesized by high internal phase emulsion (HIPE) polymerisation and were investigated as scaffolds for tissue engineering.[30]–[32] Similar macroporous 3D poly(HIPEs) of HEMA networks were also implemented for different interesting applications such as biomedical devices, bioreactors, biological and chemical material separation, as well as adsorbents in biomedicine or environmental applications.[33]

2.1 How can hydrogels be prepared as nano-sized particles?

Getting these hydrogels in the form of micro-/nano- scale size particles offers several advantages as compared to their bulk counterpart.[34] Particles of polymer networks that have submicronic size, prepared either by physical or chemical cross-linking are referred as nano/microgels. Those hydrogel particulate systems were proven to be very promising candidates as drug carriers owing to their high loading capacity and stability. Besides, they can be designed to response to environmental factors such as pH and temperature. Their

surfaces can be modified with different functional groups for targeting or imaging agents in order to achieve site specific delivery or diagnostic applications. It has also been shown that nanogels can be used for intracellular delivery[35] and that they are able to cross through the blood brain barrier.[36] The most important issue is that the nanogels prevent the guest molecule from the degradation by metabolic systems.[37]

Hydrogel particles also hold an advantage for their administration methods. They can be used for different administration routes both invasive and non-invasive to name few parenteral routes, oral, nasal, intra-ocular and topical.[38] For instance, as it is illustrated in the Figure 3, in comparison to bulk hydrogels, the nano- or microgels can be injected (A). In the case of bulk hydrogels implants should be surgically placed. Moreover they can fill the cavities more precisely (B), besides also different types of nano-/microgels can be mixed in the suspension to be injected.

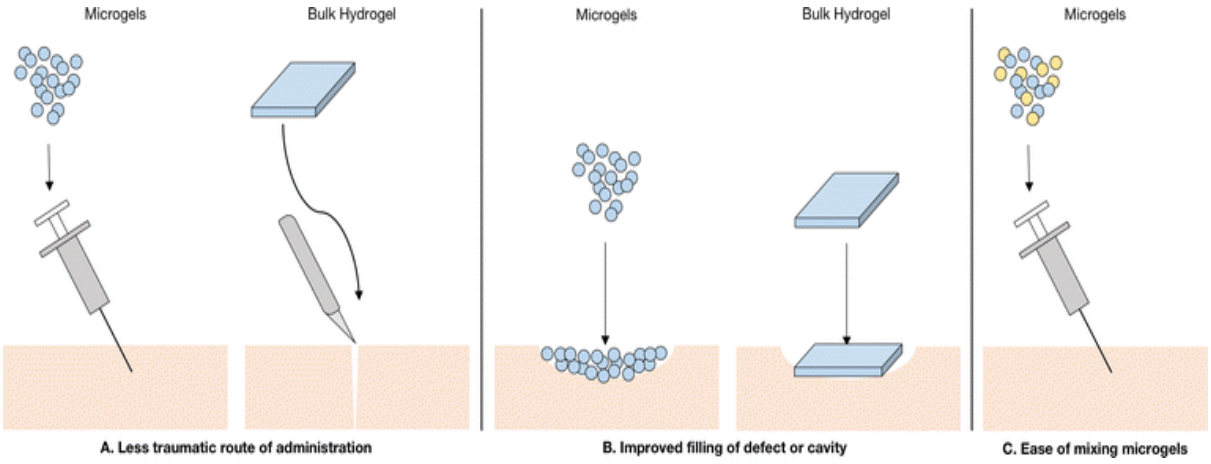


Figure 3: Comparison of the administration methods for nano and microgels to the bulk hydrogels.[39]

Nanogels can be prepared by mainly two different methods: one is based on cross-linking of amphiphilic polymer precursors through physical or chemical cross-links, the second is the preparation by heterogeneous polymerisations such as emulsion and precipitation

polymerisation methods using hydrophilic monomers and a suitable cross-linker in the reaction medium. The key feature for both methods of production of gels is to introduce cross-links in order to obtain 3D network which makes the nanogel insoluble yet swellable by water.

2.1.1 Cross-linking of natural/synthetic polymer precursors

Amphiphilic random copolymers precursors for the production of nanogels are composed of hydrophilic polymer framework which is functionalised by hydrophobic groups to introduce amphiphilic behaviour. By choosing proper cross-linking method we can "lock" the self-assembly of these amphiphilic copolymers in water whereby forming nanogels which are characterised by their nano size and their swelling behaviour in aqueous solutions.[40] Nanogels composed of natural polymers (i.e pullulan, chitosan, alginate, etc.) are vastly formed by supramolecular cross-linking which will be exemplified in following subsections.

Moreover, the nanogels can be also obtained from smart synthetic random or diblock polymer precursors which show stimuli-responsive behaviour according to the environment such as pH and temperature. For example, the supramolecular self-assembly of a thermoresponsive diblock copolymer will occur at high temperature thanks to the hydrophobic interaction of the temperature responsive component and after cross-linking, reducing the temperature allows the core to become hydrophilic and swell in water to form nanogel. Cross-linking of preformed polymers can be obtained by either physical or covalent bonds. Physical cross-linking occurs thanks to the secondary interactions such as hydrogen bonding and hydrophobic interactions or if the polymer contains electric charges along the chain, cross-linking can be also induced by electrostatic interactions.[41] In these cases, self-association leads to simultaneous cross-linking of amphiphilic macromolecules due to the

presence of hydrophobic groups/electron charges on the polymer chains. Thus, nanogels can be obtained by supramolecular cross-linking having size in nanometre range where it can be controlled by simply adjusting the concentration and formulation processes.[42]

a) Self assembly of amphiphilic random or diblock copolymers

One of the most studied methods for the preparation of nanogels is the physical self-assembly of the polymers by means of hydrophobic interactions, electrostatic interaction and hydrogen bonding with other polymer chains leading to controlled aggregation *via* tuning the polymer concentration in the solution and external environmental parameters, such as temperature and pH value. This self-association of the hydrophilic polymers is widely investigated and there are promising candidates especially for encapsulation of protein drugs. One of the most known examples for the nanogel obtained by means of self-assembly either physical or chemicals cross-linking was obtained by hydrophobic interactions of amphiphilic polysaccharides. Figure 4 represents the self-assembly of a hydrophilic polysaccharide modified with hydrophobic groups which leads self-association to form physically cross-linked nanogels.

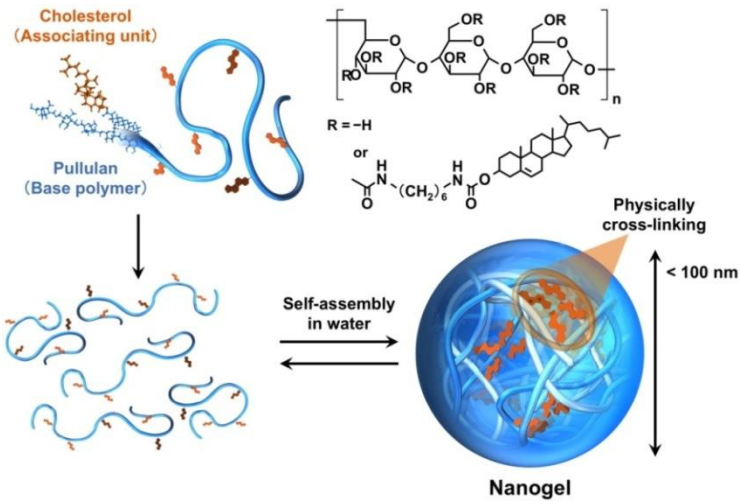
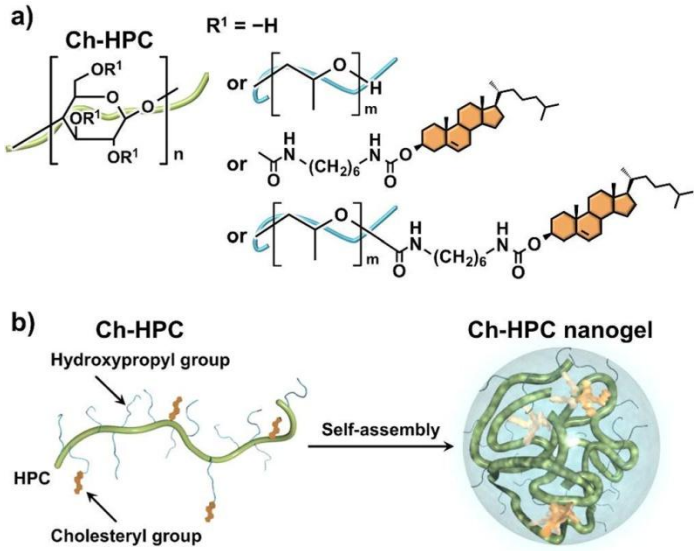


Figure 4: Nanogel formation from self-assembly of hydrophilic polymer (pullulan) functionalised by hydrophobic groups (cholesterol units).

The polysaccharides chains are modified with cholesterol units and so have sufficient amphiphilicity to form crosslinks by interchain hydrophobic interactions in aqueous medium, thus leading to formation of nanogels by self-assembly in water. These nanogels were widely investigated specifically for protein delivery applications. For instance, pullulan was functionalised with cholesterol in order to introduce hydrophobic domains. This hydrophobic polysaccharide derivative was able to form nanogels upon sonication with relatively small sizes around 25 nm and uniformity.[43] These nanogels were investigated for their use to encapsulate prostaglandin E1 (PGE1) for wound healing caused by chronic skin ulcers. A square skin wound was treated with both cholesterol-bearing pullulan (CHP) with and without prostaglandin E1 (PGE1) groups. It has been shown that CHP-PGE1 nanogels led to significant decrease of the wound size.[44] Previously insulin, interleukin-12 (IL-12), antigen proteins for cancer vaccine, and nasal vaccine were successfully incorporated in these types of pullulan nanogels. Nevertheless, it has been reported that due to physical cross-linking, cholesterol modified pullulan nanogels showed poor stability. Therefore, chemical cross-linking was necessary to be introduced to maintain the structure. Cholesterol bearing pullulan was further substituted by acryloyl groups (CHPOA). The nanogels were obtained thanks to the dual cross-linking by covalent ester bonds and physical interaction of with CHPOA and four-armed PEG modified with thiol group (PEG-SH). The obtained nanogels had a size between 50-150 nm depending on the acryloyl substitution and feed ratio of PEG-SH. Nanogels showed 18 hours half-life which was 15 times longer half-life than the aforementioned pullulan based nanogels (1.2 hours).[45]

Another example, hydroxypropyl cellulose (HPC) was also functionalised with cholesterol (Ch) to self-assemble into nanogels (Ch-HPC) in water by hydrophobic interactions of

cholesterol groups as it is illustrated previously in the Figure 5. The hydrodynamic volume of the nanogels was dictated by the degree of substitution of cholesterol groups on the polymer chain. The resulting nanogels had sizes between 60-83 nm. These formed Ch-HPC nanogels were used as a building block to obtain macroscopic gels. These materials are also referred as tectonic materials in the literature.[46]



Scheme 5: (a) Structure of Ch-HPC. (b) Schematic illustration of the self-assembly of Ch-HPC to form nanogels[46].

Besides, synthetic amphiphilic copolymers can be obtained by copolymerisation of hydrophilic monomer with a monomer bearing hydrophobic groups to induce supramolecular self-assembly. For example, Ryu et al. have synthesized random copolymer composed of OEG-methacrylate copolymerisation with pyridyl disulfide (PDS) derived methacrylate *via* reversible addition-fragmentation chain transfer (RAFT) polymerisation. Owing to the PDS side-chain functionalities, the resultant amphiphilic copolymer self-assembles in water with a size of the nanoaggregate determined by the number of PDS groups. Moreover, to form the nanogels, the PDS groups on the amphiphilic copolymer

precursor were cross-linked using disulfide cross-linking. By changing the composition and/or molecular weight of the copolymer, the size of self-assemblies in water could be varied. They reported nanogels have shown sizes between 5-120 nm. In addition to that they also probed the effect of temperature on the nanoaggregates, the low LCST behaviour of the OEG units led to larger aggregates at high temperatures.[47]

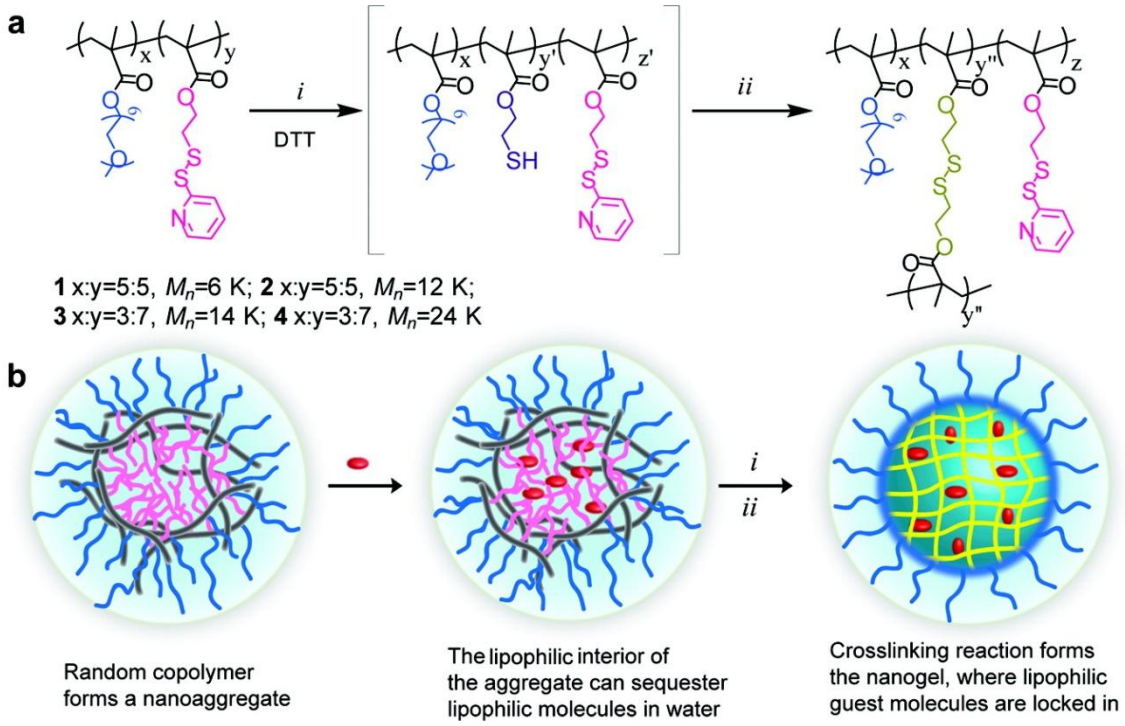


Figure 6: Synthesis of the PEG-PDS nanogels8a) schematic illustration of the nanogel formation and encapsulation.[47]

This amphiphilic copolymer precursor was further investigated for host-guest encapsulation in the presence of salt. The salt-ions effectively altered the size of the nanogel as well as encapsulation efficiencies in the formed nanogel. [48] In another example, Aktan et al. synthesized nanogels from poly(ethylene glycol)-methacrylate-based maleimide-bearing copolymer. Thermoresponsive copolymer was self-assembled into nanosized aggregates in water upon heating to its lower critical solution temperature (LCST) at 55°C, and they cross-linked the nanoaggregates using the thiol−maleimide conjugation.[49]

b) Supramolecular cross-linking by electrostatic interactions

For the formation of nanogels by electrostatic interactions, alginate is one of the widely studied example. Alginate is highly water soluble biopolymer which limits its application as a drug carrier. Alginate chains can be modified with hydrophobic groups to enhance it stability *in vivo*. More importantly since it is an anionic polysaccharide, bearing carboxylate groups, alginate can be cross-linked by multi-valent cations to form hydrogels.[50] Conventionally divalent calcium (Ca^{2+}) cations are employed for cross-linking and resulting hydrogels are referred also as calcium-alginate hydrogels. Generally they are employed for encapsulation of living cells, growth factors and cytokines.[17] The size of the alginate micro/nanogels are determined by the alginate solution concentration, counter-ion solution concentration and the speed of addition of the counter-ions to the alginate solution.[51] To illustrate this, Xue *et al.* synthesized doxorubicin (DOX) loaded alginate nanogels through very simple method as described as follows: Anionic sodium alginate (carboxylic groups) was mixed with cationic doxorubicin (amine groups) via electrosratic interactions. Subsequent cross-linking was performed *in situ* with the aid of calcium ions affording DOX-loaded alginate nanogels having size about 210 nm. The figure below (Figure 7) depicts the formation of DOX loaded alginate nanogel and its internalisation by the cell.[52]

Alginate is inherently a pH sensitive biopolymer which makes it a very promising candidate for oral delivery of hydrophilic drugs such as protein and peptides. However, the alginate nanogels are found to exhibit low encapsulation and burst release of the drugs during particle formation. Therefore, to control the size of the nanogel and its porosity stands as a great challenge. Owing to this fact, much recently microfluidic approaches are tried to tune the structure.[53]

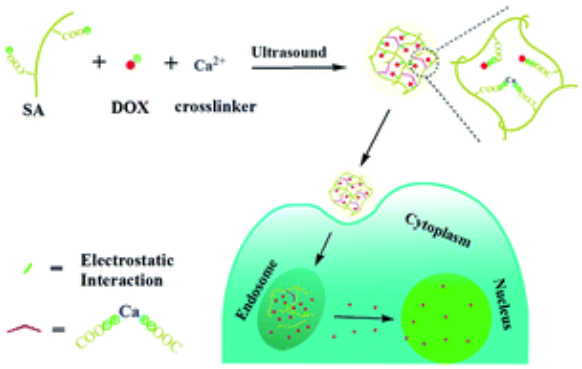


Figure 7: Doxorubicin (DOX) loaded alginate nanogel preparation and its cell-uptake. [52]

Similarly, chitosan, a polysaccharide bearing primary amino groups, can form hydrogels by cross-linking using the coordination of metal ions or by covalent cross-linking. By physical means, chitosan is able to gel by itself by adjusting the pH, or by simply blending with poly(vinyl alcohol) (PVOH). Moreover, chitosan is positively charged in acidic medium where it can form hydrogels by electrostatic interaction either with anionic polymers, or with phosphates and sulphate ions.[54] Similar processes as described for alginate are followed to control the size of these cross-linked assemblies in the nanometer range. Under constant stirring, the alkaline solution of the polyanion (i.e tripolyphosphate) is added onto acidic solution of chitosan. The nanogels formed simultaneously as a consequence of electrostatic interaction of oppositely charged groups. The resultant nanogels are in the size range of 300-400 nm bearing positive charges on the surface.

Advantageously, the charges on the chitosan can be altered by changing the pH and this alters the properties of the resulting hydrogel changing the ratio of shrinking/swelling in different pH environments. Therefore, the hydrogels obtained by chitosan are suitable for gastric environment. Also it enhances the bioavailability of lipophilic drugs in gastrointestinal tract thanks to its mucoadhesive properties.[55] For instance, Azadi *et al.* prepared methotrexate-loaded chitosan nanogels *via* ionic gelation using a polyanion,

negatively-charged tripolyphosphate (TPP). The nanogels were formed thanks to the inter- and intra-molecular electrostatic interactions as it was mentioned earlier. These nanogels were intended for drug delivery for brain.[56]

In the case of synthetic polymers, the metal-ionomer complexes can form nanogels in electrostatic manner, too. Ionomers can be complexed by oppositely charged multivalent metal ions whereby resulting into nanogels. For instance, methoxy poly(ethylene glycol)-grafted-polyethyleneimine (PEG-*g*-PEI) is a cationic ionomer which self-assemble to micellar templates upon complexation with Zn^{2+} ions. However, the nanoobject should be cross-linked in order to form stable nanogel structure. Therefore, PEI was functionalized by L-histidine to induce covalent cross-linking through disulphide bonds. Abolmaalii *et al.* studied this nanogel synthesis and loading with methotrexate (MTX) and loaded nanogels lowered the viability of HepG2 cells (MTX-resistant hepatocellular carcinoma).[57]

In summary, the supramolecular self-assembly of either natural or synthetic amphiphilic polymers results into the formation of micro/nano-sized hydrogels thanks to physical interactions such as hydrophobic interactions, electrostatic interaction or hydrogen bonding. The cross-linking occurs without addition of a cross-linker which prevents adverse effect on trapped biomolecules. Traditionally, the production method of self-assembly is performed in water and in mild conditions. However, the nanogels obtained from supramolecular cross-linking might not meet the criteria for the mechanical properties, such as strength and stability *in vivo* which may limit their applications.[58] Furthermore, these self-assemblies occur in specific range of concentration (sensitive to dilution), therefore the efficiency of the guest-molecule encapsulation is low.

c) Cross-linking of natural polymer precursors in emulsion

As we have explained in the previous sections, nanoparticles of hydrogels can be obtained from preformed natural/synthetic polymers either by self-assembly when they are amphiphilic, or by nanogelation in diluted conditions if they bear electrical charges along the polymer chain.

Beside, a third process can be followed to prepare hydrogel nanoparticles of natural polymer precursors which is based on the use of a heterogeneous system. The cross-linking of preformed natural polymer precursors dissolved in the aqueous phase of a reverse emulsion results into gel particles with a size controlled by the size of the emulsion droplets, i.e. dependent on the added stabilisers. For instance, folate-chitosan based nanogels were prepared by inverse microemulsion cross-linking by using genipin as a natural cross-linker and Triton-X 100 used as a stabiliser. Nanogels were obtained by mixing three water-in-oil (W/O) microemulsions of chitosan, genipin (cross-linker) and folate using cyclohexane, n-hexanol and water respectively. Obtained nanogels were collected by precipitation in ethanol and washed several times with ethanol and phosphate buffer solution (PBS) then filtrated and dried by vacuum. Nanogels were obtained with small size, between 35 -45 nm, as evidenced by transmission electron microscopy (TEM) images. This nanogel was loaded with 5-fluorouracil and showed a promising release behaviour in different pH conditions.[59] The same group also studied the nanogel preparation using similar inverse microemulsion (Figure 8) but replacing genipin by dicarboxylic acids as a cross-linker (i.e PEG diacid/tartaric acid). The obtained nanogels had a size lower than 50 nm and were loaded with high efficiency with 5-fluorouracil.[60]

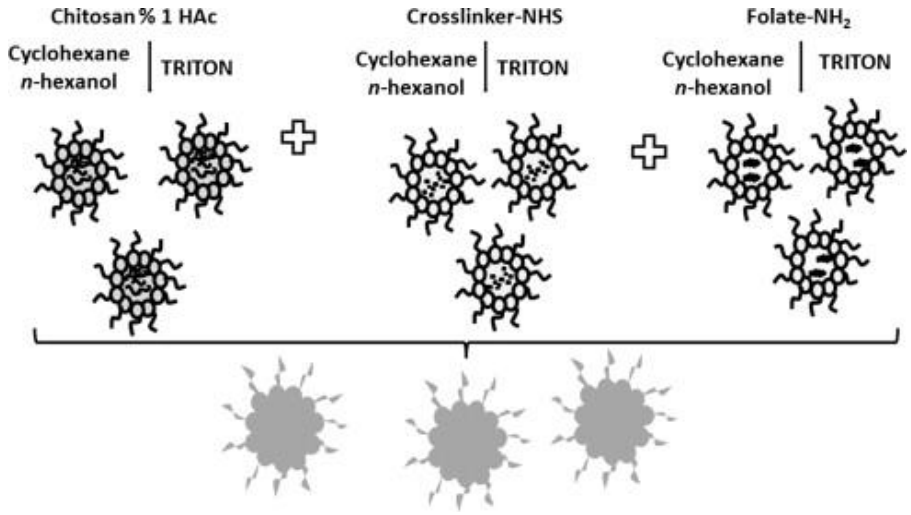


Figure 8: Chitosan nanogel preparation procedure.[60]

Even if this process allows good control of the particles size, the purification steps to recover the synthesized nanogels from the heterogeneous reaction mixture, that include washing with an organic solvent (i.e ethanol), dialysis against water followed by additional washing and drying under vacuum, make this process less straightforward as compared to self-assembly processes discussed above.

2.1.2 Synthesis of nanogels *via* heterogeneous polymerisation processes

Heterogeneous polymerisation processes result in particle formation with varying sizes and morphologies that can be controlled by the processes conditions. Therefore, they constitute potentially relevant methods for the synthesis of nanogels. These polymerisation processes are divided into four groups which are namely emulsion, suspension, precipitation, and dispersion polymerisations. The difference between these processes rely on the initial phase of the starting mixture, kinetics, the mechanism of particle formation and the particle morphology.[61] These polymerisation processes are widely used for different industrial applications such as cosmetic, food, agricultural and pharmaceutical and significantly employed for the particle production for drug delivery applications.

a) Emulsion polymerisation

Emulsion polymerisation is a heterogeneous polymerisation process that starts from an emulsion of a monomer in a non-miscible solvent stabilised by the addition of surfactants. To collect polymer particles, monomer droplets are stabilised by the surfactant in a non-miscible solvent that constitute the continuous phase. Then, the polymerisation occurs within the droplets leading to formation of polymer particles with a size dictated by the initial droplet size.

Emulsion polymerisation is divided into different groups with respect to droplet size namely macro-, mini/nano- and microemulsions. In macroemulsion the droplet size is around 400 nm, in miniemulsion between 100-400 nm and for microemulsion is between 10-100 nm (Figure 9).[62] Depending on the nature of the hydrophilic or hydrophobic nature of the monomer, water-in-oil (W/O) or oil-in-water (O/W) emulsions can be envisioned to produce polymer nanoparticles.

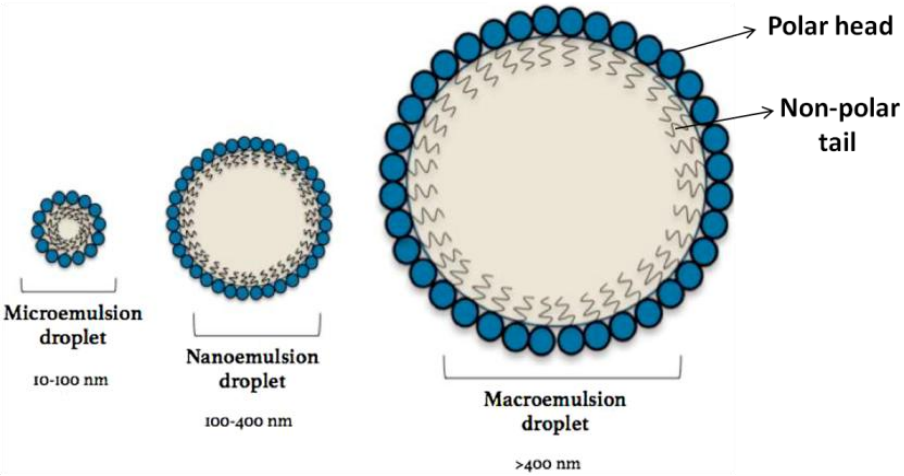


Figure 9: Types of emulsion polymerisation with respect to the formed droplet size.[62]

As an example, cross-linked nanoparticles of copolymers of N-vinylcaprolactam (N-VCL) and 2-hydroxyethyl methacrylate (HEMA) were synthesized *via* free radical emulsion polymerisation in water in the presence of methylene bis(acrylamide) as cross-linker and

sodium dodecyl sulfate (SDS) as surfactant. The mixture was polymerised in inert atmosphere at 70°C under vigorous stirring for 20 hours. Particles were isolated by centrifugation; unreacted monomers and cross-linker were removed by immersing in water for 2 days. Subsequently centrifuged and dried under vacuum at 40°C for 1 day. The obtained poly(NVC-co-HEMA) particles had uniform size around 150 nm and spherical shape. These particles were then allowed to swell in water into nanogels and were investigated for the delivery of curcumin, an anti-cancer drug. The release studies of these temperature responsive nanogels showed a promise for curcumin delivery.[63]

Inverse emulsion refers to the water-in-oil (W/O) polymerisation technique in which the monomer is hydrophilic and mostly in aqueous solution is emulsified in a continuous oil phase whereby the polymerisation yields to submicronic particles. The particles are stabilised thanks to the surfactant (and a co-surfactant) inhibiting Ostwald ripening. Reverse emulsion polymerisation is widely used for the synthesis of nanogels.

For instance, nanogels composed of HEMA and methacrylic acid (MAA) (poly(HEMA-co-MAA)) were synthesized using reverse emulsion polymerisation in the presence of EGDMA as a cross-linker and poly(vinyl alcohol) (PVOH) as a stabiliser. The polymerisation carried out at 70°C for 24 hours. In order to remove unreacted monomer and cross-linker the particles were washed with methanol and NaOH solutions. After several times purification, the particles were suspended and dialysed against water and harvested by freeze-drying. The obtained nanogels sizes varied according to the stabiliser (PVOH) concentration between 292 nm to 1.5 µm as it was measured from corresponding SEM images (Figure 10). Figure 9 is a representative SEM image of freeze-dried sample. Poly(HEMA-*co*-MMA) nanogels were loaded with Ovalbumin (OVA) by impregnation method. The resultant

nanogels showed pH responsive nature and were used for oral vaccine delivery. Interestingly, the surface of the as-obtained nanogels was modified with mannan to enhance the internalization by macrophages. [64]

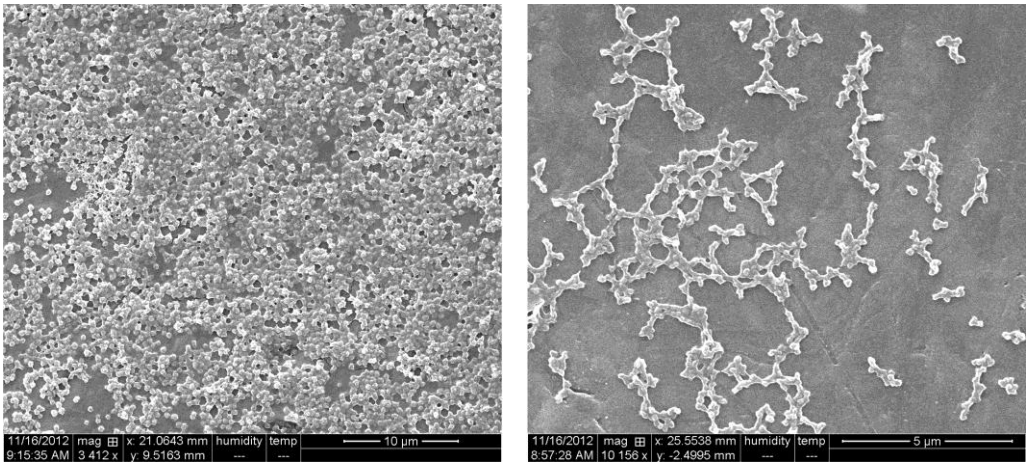


Figure 10: SEM images of the poly(HEMA-co-MAA) pH responsive nanogels.[64]

b) Precipitation and dispersion polymerisation

According to the IUPAC, precipitation polymerisation is defined as a polymerisation in which monomer and initiator are dissolved in the continuous phase where it acts as a non-solvent for the corresponding polymer after reaching a certain molecular weight. Dispersion polymerisation behaves like precipitation polymerisation; initially it is a homogenous mixture of monomer, initiator, stabiliser and the solvent in which the continuous phase is a poor solvent for the forming polymer.[65]

Dispersion polymerisation is a one-pot process affording highly monodisperse nano- or micron-size polymer particles. The Figure 11 depicts the stages of the dispersion polymerisation. Initially it starts as a homogenous mixture of monomer, initiator and stabiliser in the continuous medium **(1)**. After growing polymer chains **(2)** reaches to a certain molecular weight the polymer will precipitate out and the polymeric particles will be

formed by stabiliser either adsorbing or anchoring to the surface of the growing particles affording highly uniform particles **(3)**.[66]

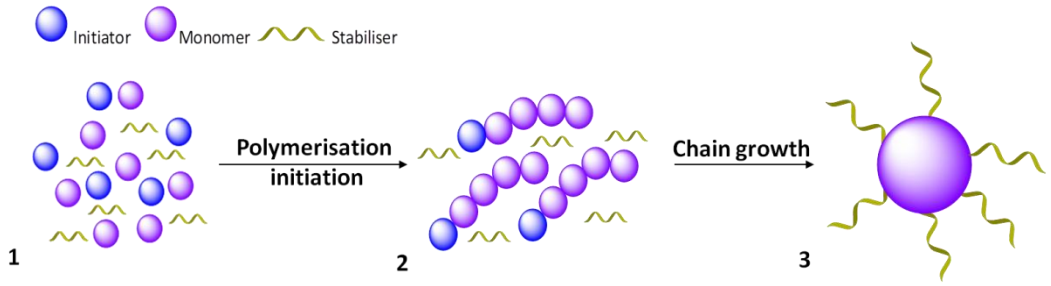


Figure 11: Schematic illustration of dispersion polymerisation mechanism.

Witting *et.al* have shown the synthesis of poly(N-isopropylacrylamide)-polyglycerol networks *via* precipitation polymerisation in water. Nanogels were obtained using acrylated dendritic polyglycerol (dPG) as a cross-linker and sodium dodecyl sulfate (SDS) as colloidal stabiliser. Transglutaminase 1 loaded nanogels were used for delivery of this protein through skin to the transglutaminase 1-deficient skin models where they observed restoration of skin using these loaded nanogels.[67] These nanogels were further investigated by Sahle et al. for the delivery of drugs through hair follicle. They have used the same method to obtain nanogels in water. The resultant nanogels had a size between 300-500 nm and showed a good penetration through hair follicle which was detected by model drug coumarin 6 incorporation and release from obtained nanogels.[68] Carmona-Moran *et.al* synthesized temperature responsive poly(N-vinylcaprolactam)-co-acrylic acid core-shell nanogels by free radical precipitation polymerisation in water, using N,N-methylenebis(acrylamide) as a cross-linker and sodium dodecyl sulphate (SDS) as a surfactant. Obtained nanogels were then loaded with non-steroidial anti-inflammatory drug (NSAID) Diclofenac. The average hydrodynamic diameter of the diclofenac-loaded (PVCL-co-AA) nanogels was approximately 300 nm at 25°C and shifted to 190 nm at 32°C. These

nanogels were then embedded in a gellan gum hydrogel film for transdermal delivery application. [69]

Briefly, we have listed some recent examples of the various types of homo- or copolymer nanogels synthesized by different heterogeneous polymerisation techniques. These polymerisation techniques are performed using an organic phase and additionally elevated temperatures are needed for the decomposition of the initiator. Therefore, they do not offer the most suitable synthesis medium to handle solvent or heat labile substances. Moreover, even the nanogels are successfully produced thanks to these facile techniques, post-polymerisation processes are needed for the particle harvesting, purification, removal of surfactants, and drying. To overcome these drawbacks of the heterogeneous polymerisation techniques for producing well-defined polymeric particles for different applications researchers focused on translating these techniques into green polymerisation medium supercritical carbon dioxide ($scCO_2$) which enable to produce dry powder formulations.

3. Supercritical fluids

Supercritical fluids are defined as any substance that are above their both critical temperature (T_c) and pressure (P_c) and close to their critical densities.[70] Phase diagram (Figure 12) shows where the pure substance is found to be solid, liquid, gas or supercritical.[71] Three phases (solid, liquid and gas) coexist in a particular point which is given by the triple point. Along the curve between triple point and critical point is called as boiling curve where equilibrium between liquid and its vapour is clearly observed. However, by increasing the temperature and pressure, density of the two phases are altered. In

details, density of the liquid will decrease due to thermal expansion while the density of the vapour phase will increase and will reach to a point (critical point) where the difference is indistinguishable. Thus, we can say that the critical point stands for the highest temperature and pressure in which the substance is found to be vapour and liquid.[72]

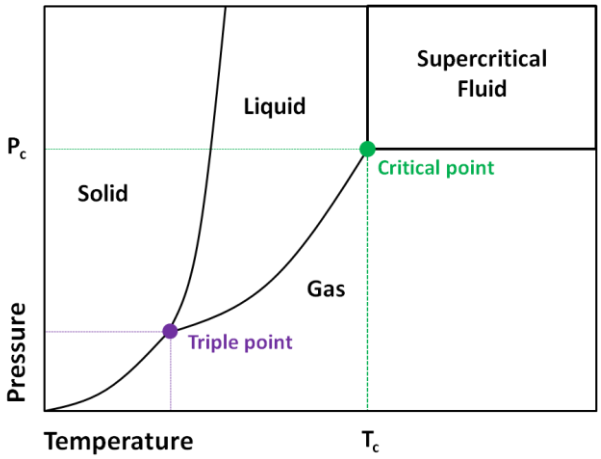


Figure 12: The phase diagram of a pure substance where it indicates the supercritical region.

SCFs exhibit properties that can be described as in between liquids and gases which are far from ideal gas behaviour. Their liquid like densities enable to dissolve solids while they have high diffusivity and low viscosity as gases which has a substantial effect on reaction kinetics.[73]

Moreover, the density and consequently the solvent properties of the SCFs are easily altered by compressing to different pressures.[70], [74] It should be noted that the variation in density of SCF does not cross the line indicated by triple point and the critical point (boiling curve) where liquid and gas phases coexist.[74] Table 1 compares the physical properties of liquids, supercritical fluids and gases respectively.

As it can be seen from the Table 1 the supercritical fluid properties relies in between liquids and gases. Supercritical fluids have low viscosities and they are highly compressible like

gases. Due to this fact their liquid like densities consequently solvent properties could easily altered by changing temperature and pressure.[73] This aspect of the SCFs is more pronounced in the critical region therefore solubility of the solids in SCFs is predominantly a function of pressure and temperature in or near the critical region.[75]

Table 1: Physical properties of liquid, supercritical fluid and gas.[72]

Physical Property	Liquid	Supercritical Fluid	Gas
Density (g/ml)	1	0.4	10^{-3}
Viscosity (Pa s)	10^{-3}	10^{-4}	10^{-5}
Diffusivity (cm^2/s^{-1})	10^{-5} - 10^{-6}	10^{-3}	0.1

In depth, the solubility of the solids in any given supercritical fluid is dependent on two parameters which are namely the free volume difference between solid and the SCF, and the intermolecular forces. More specifically the solvent-solvent, solute-solvent and solute-solute molecular interactions will define substance solubility along with free volume. Initial approximations indicate that a solute solubility is proportional to the SCF density. As previously said by varying temperature and pressure we can easily tune the solvent strength of the SCF[76] and this unique feature of SCFs found application for the extraction of molecules.

Even though there are several different SCFs are used such as ethylene, propane and water with no doubt supercritical carbon dioxide ($scCO_2$) has found the most applications both in academic and industrial scale due to its moderate critical points and thanks to its environmentally benign properties. Properties and application of supercritical carbon dioxide ($scCO_2$) is discussed further in details in following subsections.

3.1 Supercritical carbon dioxide ($scCO_2$)

Supercritical carbon dioxide ($scCO_2$) is a green solvent due to its environmentally benign properties, and offers a platform for designing green products or processes. $scCO_2$ enlisted as non-toxic solvent. it is reported upon skin or eye contact with CO_2 vapour has no harm.[77] Due to this fact, for Food and Drug Administration (FDA), CO_2 falls into the same group of solvents as water, they have no harmful effect when they are in contact with the human body in reasonable concentrations. More precisely, when a material is produced with a CO_2 process, if residual CO_2 is present, the material will not require further treatment.[78] Moreover, carbon dioxide is naturally abundant, non-flammable, inexpensive and recyclable solvent which makes it an excellent environmentally friendly alternative to conventional solvent. Furthermore, its critical point is easily accessible (T_c=31.1°C and P_c=73.8 bar). Additionally, density also as a consequence its solvent strength can be altered by simply adjusting the temperature and pressure.[79] One of the most significant advantage of CO_2 is that it can be removed from the reaction medium by simple depressurization which allows recovering the materials by precipitation without solvent residues. This stands as a great convenience compared even water-based designed processes. Consequently, it is considered to be a very promising alternative both for academic and industrial applications especially for pharmaceutical applications.[80]

$scCO_2$ is a good medium to handle solvent and heat labile substances. Thus, it is used as solvent or anti-solvent in handling pharmaceuticals. Most drugs are sparingly water soluble leading to low bioavailability therefore the dosage must be high to reach therapeutic effect. On the other hand, it is proved that if the drug size is reduced to micron range their water solubility is increased due to larger surface area. This method is called as micronization.

$scCO_2$ either as solvent/anti-solvent for micronization of drugs shown to be very beneficial compared to the existing systems such as milling, freeze-drying or spraying.[81] Or it can be used as a medium to encapsulate drugs in already prepared polymers by co-precipitation forming micro-/nano sized particles[82] or impregnation in scaffolds or implants.[83]

Among the pharmaceuticals, protein based drugs have a sensitive tertiary structure. Upon exposure to high temperatures or organic solvents proteins denaturate and as a consequence they lose their specific activity. Therefore, $scCO_2$ was investigated as a medium to encapsulate protein drugs.[84] However, these methods are limited by either drug or polymer solubility in $scCO_2$. That being so, producing particles in $scCO_2$ and in situ encapsulation of the pharmaceuticals specifically proteins is much more desirable from the production point of view. In addition to that to produce nano/microgels is not achievable by these techniques.

3.1.1 Polymerisations in $scCO_2$

There are two possible ways to address the excess use of volatile organic solvents used in polymerisation: (i) by designing processes without solvent or (ii) by replacing organic solvents by an environmentally acceptable alternative. By far, it has been shown that the solvent free procedures suffer from the high viscosity and insufficient mass transfer.[85] Owing to this fact, and to the aforementioned environmentally friendly properties of CO_2, it stands out as one of the best alternative. Although $scCO_2$ has been implemented in many fields either as a solvent or anti-solvent, it undeniably greatly impacts the fields of polymer synthesis and processing. Solubility of CO_2 in homo- or copolymers, or polymer blends lowers the glass transition temperature (T_g) allowing them to be processed easier. Homogenous polymerisation in $scCO_2$ is limited to a narrow range of $scCO_2$ soluble

polymers. Therefore, it has been used mostly to produce fluoropolymers.[86], [87] $scCO_2$ was found as an advantageous medium for heterogeneous polymerisations as demonstrated by the increasing number of articles and reviews.[88]–[91]

As far as free-radical polymerisations (FRP) in $scCO_2$ are concerned, chain transfer to solvent that lowers the molecular weight becomes unlikely to occur due to CO_2 inertness towards free-radicals.[92] As a consequence, $scCO_2$ was used to carry out FRP but also controlled radical polymerisation (CRP) , such as atom transfer radical polymerisation (ATRP)[93], nitroxide-mediated polymerisation(NMP)[94], [95] and RAFT polymerisation[96], [97] especially by heterogeneous processes such as precipitation, dispersion and emulsion.

3.1.2 Stabiliser design

CO_2 being a non-polar solvent of low dielectric constant, highly polar or high molecular weight materials show either very low or no solubility in CO_2. Most of common monomers are soluble in $scCO_2$ whereas their corresponding high molecular weight polymers have either very low or negligible solubility. Therefore, $scCO_2$ is a good candidate to conduct heterogeneous polymerisation processes such as aqueous emulsion, precipitation and dispersion polymerisation.[74]

One of the main key factors for successful dispersion polymerisation is the choice of surfactant. Surfactants can either adsorb or chemically graft on the growing polymers in the stage where they reach a certain molecular weight which they start to become insoluble. By adsorption or grafting, surfactant facilitates the formation of polymer particles avoiding their bulk precipitation.

As a consequence, studies focused on designing proper amphiphilic polymers or small molecules to be used in CO_2. These amphiphilic polymers are composed of two different segments, a CO_2-phobic part which interacts with the g rowing polymer particles and a CO_2-philic part that ensures the dispersion in CO_2 avoiding aggregation. It was postulated that the CO_2-phobic part of such block copolymer is interacting with the dispersed phase while the CO_2-philic part extends out in the medium. This was confirmed by in-situ small-angle X-ray scattering studies. Therefore, self-assembly of these amphiphilic copolymers results in the stabilisation of discrete polymer particles or in some cases, water droplets. Initial findings pointed that fluorinated or siloxane based polymers were exceptionally highly soluble in CO_2.[98] Therefore, the design of surfactants for CO_2 applications included one of them as the "CO_2-philic" sequence. DeSimone *et al.* has coined the term of CO_2-philic when showing that the amphipatic polymer poly(1,1-dihydroperfluorooctylacrylate) (PFOA) was used as a stabiliser (Figure 13) for the synthesis of poly(methyl methacrylate) (PMMA) particles in $scCO_2$.[99] This study was marked as the first successful attempt for the dispersion polymerisation in $scCO_2$.

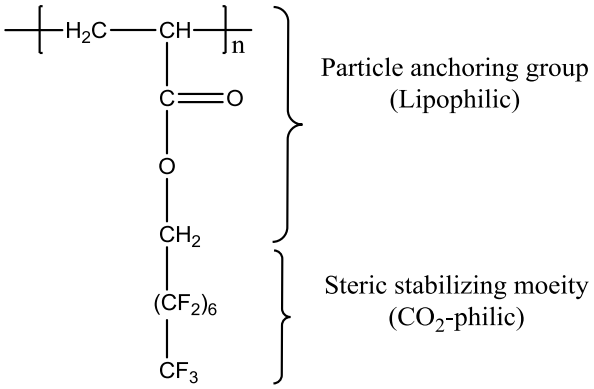


Figure 13: Amphipatic polymer that governs two different segments that are able to anchor to the growing particle where the fluorinated part ensures the solubility in $scCO_2$.[99]

In order to enhance the adsorption or the grafting on to the particles, block copolymers were designed as stabilisers where the second block, "CO_2-phobic", has an affinity towards growing particles.

Fluorinated and siloxane based polymers were previously stated that they are highly soluble due to interaction of CO_2 with C-F bond and Si-O-Si— moieties respectively. However, this was somehow limiting factor for CO_2-philic stabiliser design. In addition, CO_2 was shown to take part in Lewis Acid-base interaction with carbonyl groups of the compounds. Therefore, it opened a pathway for designing CO_2-philic hydrocarbon polymers that shows solubility in $scCO_2$ in reasonable temperature and pressure. Sarbu *et al.* has defined the guidelines designing hydrocarbon based polymers as a stabiliser for CO_2 applications.[100], [101] Since then, significant efforts have been devoted to synthesize this type of CO_2-philic hydrocarbon based polymers to be used in heterogeneous polymerisation in $scCO_2$[102]–[105]. Several types of copolymers stabilisers, either fluorinated, siloxane or hydrocarbon based were studied for the dispersion or emulsion polymerisations of a wide variety of monomers including MMA, HEMA, 2-ethoxyethyl methacrylate (EEMA), GMA, NIPAAM, N,N-dimethylacrylamide (DMA), N,N-dimethylaminoethyl methacrylate (DMAEMA), Styrene (Sty). These heterogeneous methods are leading to the formation of well-defined polymer particles when appropriate stabilisers and conditions are identified.

3.1.3 Emulsion polymerisation in $scCO_2$

Emulsion polymerisation can be performed in $scCO_2$ thanks to immiscibility of water in the medium. By this technique, particles can be produced by water in -CO_2 (W/CO_2) by means of a stabiliser able to stabilize water droplets in CO_2 (Figure 14).[88]

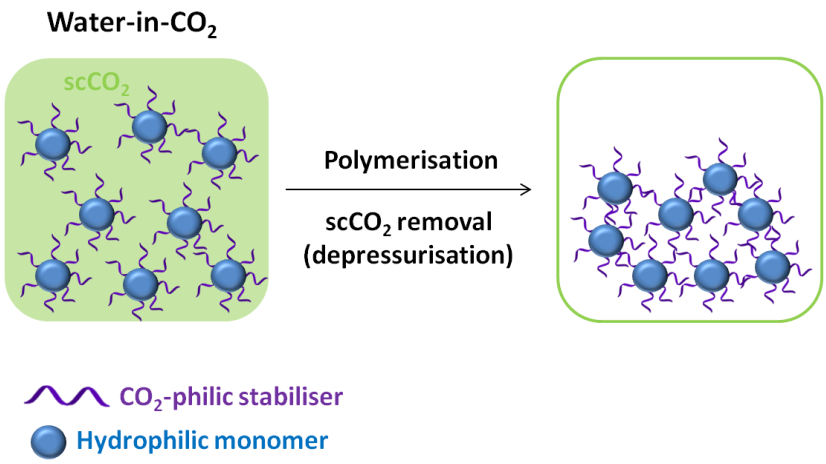


Figure 14: Illustration of particle polymer formation via W/CO_2 emulsion polymerisation. (Re-drawn from the reference).[88]

W/CO_2 emulsion polymerisation enables to produce hydrophilic particles. In comparison to macroemulsions, microemulsion in $scCO_2$ is harder to stabilise due to strong van der Waals attraction between water droplets. Therefore, the stabilisers must be carefully chosen. The amphiphilic CO_2-stabiliser forms a water/CO_2 core/shell micelle therefore if the components are water soluble the reaction will take place in water droplets (Figure 14). As a consequence those water droplets can be used as nanoreactors.[106] After successful emulsion polymerisation and CO_2 removal (depressurisation) water swollen hydrophilic polymer particles are collected. As an example, emulsion polymerisation of n-ethylacrylamide [107] and inverse emulsion polymerisation of acrylamide [108] in supercritical carbon dioxide were performed successfully leading to polymer particles in sub-micrometre range.

3.1.4 Dispersion polymerisation in $scCO_2$

Dispersion polymerisation in $scCO_2$ also affords discrete particle formation. Owing to high solubility of the fluorinated and siloxane based copolymers, they have been widely used as stabiliser for the dispersion polymerisation of a wide range of monomers such as

styrene[109]–[111], 1-vinyl-2-pyrrolidone[112], [113], glycidyl methacrylate[114], acrylonitrile [115], methyl methacrylate[116], [117] , 2-(dimethylamino ethyl methacrylate(DMAEMA)[118] and HEMA[119] , the synthesis of cross-linked polymer microspheres is scarcely reported even if such particle networks are also crucial for many different applications. We will specifically focus here, on the production of polymer networks by this heterogeneous process.

Cooper *et al.* has pioneered the synthesis of cross-linked particles in $scCO_2$. They have reported for the first time, the synthesis of well-defined cross-linked polymer microspheres from divinyl benzene (DVB) and ethylvinyl benzene monomers mixture (poorly soluble in $scCO_2$) with and without stabiliser in $scCO_2$. The poly(divinyl benzene) (PDVB) particles obtained without stabiliser by suspension polymerisation method whereas in the presence of stabiliser particles were produced by emulsion polymerisation. In both cases, particles were harvested as dry, white, free-flowing powders. In the case of emulsion polymerisation, they have used a diblock copolymer composed of a fluorinated poly(methyl methacrylate) (PFMA) block and a second block of conventional PMMA as surfactant. Even in the absence of stabiliser the particles were found to have discrete spherical shape due to very high amount of cross-linker (55% and 80% wt) which results into very rigid surface and prevents their agglomeration. In the absence of the stabiliser particles had size between 1.5- 5 µm whereas in the presence of stabiliser particles obtained with sizes lower than 0.5 µm. AS Cooper *et al.* has foreseen the heteregeneous polymerisation in $scCO_2$ opened a pathway for the facile synthesis of cross-linked polymer particles composed of water sensitive/soluble co-monomers which their production was often limited in conventional solvents. [120]

Cross-linking might improve the mechanical properties of polymers such as better strength, higher chemical and mechanical resistance, more interestingly better thermal resistance. Therefore, Shin *et al.* investigated the preparation of cross-linked PMMA particles to enhance their thermal properties. They performed dispersion polymerisation in $scCO_2$ in presence of poly(heptadecafluorodecyl methacrylate) (PHDFDMA) as stabiliser along with a variety of cross-linking agents; EGDMA, 1,4-butanediol di(meth)acrylate (1,4-BD(M)A), and trimethylolpropane trimethacrylate. Cross-linked PMMA particles were obtained in the size range of 5-11 µm. By differential scanning calorimetry (DSC), they have observed a clear increase of the particles T_g in parallel to their cross-linking density. Furthermore, the EGDMA was found to be the most suitable cross-linking agent which led to the most thermally stable particles.[121]

Wang et.al reported on the synthesis of cross-linked microparticles of glycidyl methacrylate (GMA) in $scCO_2$ by using poly(dimethylsiloxane) monomethacrylate (PDMS-MA) macromonomer as stabiliser. In this work, thanks to stabiliser the polymerisation time of GMA was reduced to shorter times (4 hours)[122] compared to previous work of Shiho *et al.* where 20 hours of reaction time were required. [114]

Casimiro et al. have reported on the polymerisation of diethylene glycol dimethacrylate (DEGDMA) using commercially available perfluoropolyether oil known as Krytox 157FSL in scCO2. They were particularly interested in this monomer because P(DEGDMA) cross-linked microspheres can be used for immobilisation of enzymes or hormones. The performed dispersion polymerisation of DEGDMA led to highly cross-linked P(DEGDMA) particles with sizes between 1.2-2 µm. Likewise other examples, the use of $scCO_2$ eliminated the tedious

post-polymerisation work-up for purification compared to the conventional dispersion polymerisation. [123]

Hydrogels based on P(NIPAAM) exhibits LCST behaviour which has been implemented in several biomedical applications as drug delivery systems and tissue engineering. Hence, Temtem et.al have investigated the preparation of cross-linked P(NIPAAM) particles in scCO2 by precipitation polymerisation. In other words, the polymerisation performed in absence of stabiliser. They could achieve P(NIPAAM) discrete particles with a few agglomeration at higher cross-linker content i.e 2.5-4.5 % wt N,N-methylenebisacrylamide (MBAm).[124]

Following to this study, Costa *et al.* prepared cell-sized P(NIPAAM) hydrogel microbeads (microgels) to be used in biosensing applications. P(NIPAAM) microgels were synthesized using MBAm, di(ethylene) glycol dimethacrylate (DEGDMA) and glycerol dimethacrylate (GDMA) water soluble cross-linkers and Krytox as a stabiliser. The microgels obtained had sizes between 3.2-3.8 μm. As it is observed for the cross-linked networks, the mechanical properties could be easily adjusted by tuning the cross-linking density. Moreover, cytotoxicity assays reveal that the P(NIPAAM) microgels exhibit no toxic effect on fibroblast cell cultures which is very promising for biomedical applications.[125]

As we have seen the examples in previous sections, HEMA can be used in different biomedical applications either as homo-/copolymer. Thus, its successful polymerisation in non-toxic solvent $scCO_2$ is of great interest for pharmaceutical applications. Ma *et al.* focused on the dispersion polymerisation of HEMA. Even though Shiho et al. have reported the polymerisation of HEMA in $scCO_2$, they have used polystyrene and poly(1,1-dihydroperfluorooctyl acrylate) (PS-*b*-PFOA) stabiliser. However, Ma *et al.* work marked as

the first study to use stabiliser composed of poly(ethylene oxide)-*b*-poly(1,1,2,2-tetrahydroperfluorodecyl acrylate) (PEO-*b*-PFDA) block copolymer as stabiliser for dispersion polymerisation of HEMA in $scCO_2$, leading to poly(HEMA) particles with remarkably small size (between 200-400 nm). Although they did not use additional cross-linker in their work, the poly(HEMA) particles were obtained as cross-linked networks due to the presence of EGDMA as an impurity in the monomer. [126]

Furthermore, Alaimo et al. have synthesised a novel photocleavable diblock CO_2-philic stabiliser (PEO-*hv*-PFDA) for dispersion polymerisation of HEMA in CO_2. They have reported that after successful polymerisation of HEMA in $scCO_2$, particles with a size in the range of 350 nm are obtained. Subsequently, the fluorinated sequence of the stabiliser can be extracted from the particles surface when the particles were subjected to UV-photolysis. This opened up a promising platform for obtaining stabiliser-free particles. [127]

In conclusion, these pioneer works evidenced that heterogeneous polymerisations in $scCO_2$ in presence of a dedicated stabiliser, allows the formation of well-defined and small size particles of cross-linked polymers. In case of dispersion polymerisation, after venting the reactor, solvent-free particles are collected as a dry flowing powder without requiring stringent purification steps opening promising prospects for application in the field of healthcare and pharmaceutical formulations.

References

[1] J. Clayden, N. Greeves, and S. Warren, *Organic Chemistry*. 2004.

[2] Z. Gu, A. Biswas, M. Zhao, and Y. Tang, "Tailoring nanocarriers for intracellular protein delivery.," *Chem. Soc. Rev.*, vol. 40, no. 7, pp. 3638–55, Jul. 2011.

[3] M. L. Tan, P. F. M. Choong, and C. R. Dass, "Recent developments in liposomes, microparticles and nanoparticles for protein and peptide drug delivery," *Peptides*, vol. 31, no. 1, pp. 184–193, 2010.

[4] J. Renukuntla, A. D. Vadlapudi, A. Patel, S. H. S. Boddu, and A. K. Mitra, "Approaches for enhancing oral bioavailability of peptides and proteins," *International Journal of Pharmaceutics*, vol. 447, no. 1–2. 2013.

[5] W. Wang, "Instability, stabilization, and formulation of liquid protein pharmaceuticals," *Int. J. Pharm.*, vol. 185, no. 2, pp. 129–188, 1999.

[6] B. Leader, Q. J. Baca, and D. E. Golan, "Protein therapeutics: a summary and pharmacological classification.," *Nat. Rev. Drug Discov.*, vol. 7, no. 1, pp. 21–39, 2008.

[7] S. Frokjaer and D. E. Otzen, "Protein drug stability: a formulation challenge," *Nat. Rev. Drug Discov.*, vol. 4, no. 4, pp. 298–306, 2005.

[8] K. Fosgerau and T. Hoffmann, "Peptide therapeutics: Current status and future directions," *Drug Discov. Today*, vol. 20, no. 1, pp. 122–128, 2015.

[9] A. J. Almeida and E. Souto, "Solid lipid nanoparticles as a drug delivery system for peptides and proteins ☆," *Adv. Drug Deliv. Rev.*, vol. 59, pp. 478–490, 2007.

[10] W. Wang, "Protein aggregation and its inhibition in biopharmaceutics," *Int. J. Pharm.*, vol. 289, pp. 1–30, 2005.

[11] M. C. Manning, K. Patel, and R. T. Borchardt, "Stability of protein pharmaceuticals," *Pharm. Res.*, vol. 6, no. 11, pp. 903–918, 1989.

[12] R. Vaishya, V. Khurana, S. Patel, and A. K. Mitra, "Long-Term Delivery of Protein Therapeutics," *Expert Opin. Drug Deliv.*, vol. 12, no. 3, pp. 415–440, 2015.

[13] L. Tang, A. M. Persky, G. Hochhaus, and B. Meibohm, "Pharmacokinetic aspects of biotechnology products," *J. Pharm. Sci.*, vol. 93, no. 9, pp. 2184–2204, 2004.

[14] J. H. Hamman, G. M. Enslin, and A. F. Kotz, "Oral Delivery of Peptide Drugs Barriers and Developments," *Biodrugs*, vol. 19, no. 3, pp. 165–177, 2005.

[15] W. S. Choi, K. G. G. Murthy, D. A. Edwards, R. Langer, and Al. M. Klibanov, "Inhalation delivery of proteins from ethanol suspensions.," *Proc. Natl. Acad. Sci. U. S. A.*, vol. 98, no. 20, pp. 11103–11107, 2001.

[16] L. M. Sanders and R. W. Hendren., *Protein Delivery Physical Systems*. Kluwer Academic Publishers, 2002.

[17] T. Vermonden, R. Censi, P. Di, and W. E. Hennink, "Hydrogels for protein delivery," *Chem. Rev.*, vol. 161, no. 2, pp. 680–692, 2012.

[18] S. J. Buwalda, T. Vermonden, and W. E. Hennink, "Hydrogels for Therapeutic Delivery : Current Developments and Future Directions," *Biomacromolecules*, 2017.

[19] X. Zhang, S. Malhotra, M. Molina, and R. Haag, "Micro- and nanogels with labile crosslinks – from synthesis to biomedical applications," *Chem. Soc. Rev.*, vol. 44, pp. 1948–1973, 2015.

[20] A. S. Hoffman, "Hydrogels for biomedical applications," *Adv. Drug Deliv. Rev.*, vol. 64, pp. 18–23, 2012.

[21] R. Censi, P. Di, T. Vermonden, and W. E. Hennink, "Hydrogels for protein delivery," *Chem. Rev.*, vol. 161, no. 2, pp. 680–692, 2012.

[22] J.-P. Montheard, M. Chatzopoulos, D. Chappard, T. T. Yu, and M. S. Shoichet, "2-Hydroxyethyl Methacrylate (HEMA): Chemical Properties and Applications in Biomedical Fields," *J. Macromol. Sci. Part C Polym. Rev.*, vol. 26, no. August 2014, pp. 1507–1514, 1992.

[23] E. Seo, S. Kumar, J. Lee, J. Jang, J. H. Park, M. C. Chang, I. Kwon, J.-S. Lee, and Y. Huh, "Modified hydrogels based on poly(2-hydroxyethyl methacrylate) (pHEMA) with higher surface wettability and mechanical properties," *Macromol. Res.*, vol. 25, no. 7, pp. 704–711, 2017.

[24] E. Garcia-Millan, S. Koprivnik, and F. J. Otero-Espinar, "Drug loading optimization and extended drug delivery of corticoids from pHEMA based soft contact lenses hydrogels via chemical and microstructural modifications," *Int. J. Pharm.*, vol. 487, no. 1–2, pp. 260–269, 2015.

[25] Y. Kapoor, P. Sekar, A. Chauhan, Y. Kapoor, P. Sekar, and A. Chauhan, "Incorporation of Drug Particles for Extended Release of Cyclosporine A from poly-Hydroxyethyl Methacrylate

Hydrogels," *Eur. J. Pharm. Biophar-maceutics Eur. J. Pharm. Biopharm.*, vol. 120, no. February, pp. 73–79, 2017.

[26] E. V. Hackl, V. V. Khutoryanskiy, and I. Ermolina, "Hydrogels based on copolymers of 2-hydroxyethylmethacrylate and 2-hydroxyethylacrylate as a delivery system for proteins: Interactions with lysozyme," *J. Appl. Polym. Sci.*, vol. 134, no. 18, pp. 1–13, 2017.

[27] H. Macková, Z. Plichta, H. Hlídková, O. Sedláček, R. Konefal, Z. Sadakbayeva, M. Dušková-Smrčková, D. Horák, and Š. Kubinová, "Reductively Degradable Poly(2-hydroxyethyl methacrylate) Hydrogels with Oriented Porosity for Tissue Engineering Applications," *ACS Appl. Mater. Interfaces*, vol. 9, no. 12, pp. 10544–10553, 2017.

[28] H. Kitagawa, K. Takeda, R. Kitagawa, N. Izutani, S. Miki, N. Hirose, M. Hayashi, and S. Imazato, "Development of sustained antimicrobial-release systems using poly(2-hydroxyethyl methacrylate)/trimethylolpropane trimethacrylate hydrogels," *Acta Biomater.*, vol. 10, no. 10, pp. 4285–4295, 2014.

[29] C. Villa, F. Martello, S. Erratico, A. Tocchio, M. Belicchi, C. Lenardi, and Y. Torrente, "P(NIPAAM–co-HEMA) thermoresponsive hydrogels : an alternative approach for muscle cell sheet engineering," *J. Tissue Eng. Regen. Med.*, vol. 11, pp. 187–196, 2017.

[30] A. C. Nalawade, R. V. Ghorpade, S. Shadbar, M. S. Qureshi, N. N. Chavan, A. A. Khan, and S. Ponrathnam, "Inverse high internal phase emulsion polymerization (i-HIPE) of GMMA, HEMA and GDMA for the preparation of superporous hydrogels as a tissue engineering scaffold," *J. Mater. Chem. B*, vol. 4, no. 3, pp. 450–460, 2016.

[31] M. Ovadia and M. S. Silverstein, "High porosity, responsive hydrogel copolymers from emulsion templating," *Polym. Int.*, no. August, 2015.

[32] T. J. Long, C. C. Sprenger, S. R. Plymate, and B. D. Ratner, "Prostate cancer xenografts engineered from 3D precision-porous poly(2-hydroxyethyl methacrylate) hydrogels as models for tumorigenesis and dormancy escape," *Biomaterials*, vol. 35, no. 28, pp. 8164–8174, 2014.

[33] I. N. Savina, G. C. Ingavle, A. B. Cundy, and S. V. Mikhalovsky, "A simple method for the production of large volume 3D macroporous hydrogels for advanced biotechnological, medical and environmental applications," *Sci. Rep.*, vol. 6, no. 1, p. 21154, 2016.

[34] J. K. Oh, R. Drumright, D. J. Siegwart, and K. Matyjaszewski, "The development of microgels/nanogels for drug delivery applications," *Prog. Polym. Sci.*, vol. 33, no. 4, pp. 448–477, Apr. 2008.

[35] H. Tan, H. Jin, H. Mei, L. Zhu, W. Wei, Q. Wang, and F. Liang, "PEG-urokinase nanogels with enhanced stability and controllable bioactivity," *Soft Matter*, vol. 8, pp. 2644–2650, 2012.

[36] S. Kalaiarasi, P. Arjun, S. Nandhagopal, J. Brijitta, A. Muthamil, S. Gnana, P. Vincent, and R. Rajesh, "Development of biocompatible nanogel for sustained drug release by overcoming the blood brain barrier in zebrafish model," *J. Econ. Financ. Adm. Sci.*, vol. 14, no. 2, pp. 157–169, 2016.

[37] A. V. Kabanov and S. V. Vinogradov, "Nanogels as pharmaceutical carriers: Finite networks of infinite capabilities," *Angew. Chemie - Int. Ed.*, vol. 48, no. 30, pp. 5418–5429, 2009.

[38] N. S. Zarekar, V. J. Lingayat, and V. V. Pande, "Nanogel as a Novel Platform for Smart Drug Delivery System," *Nanosci. Nanotechnol. Res.*, vol. 4, no. 1, pp. 25–31, 2017.

[39] A. L. Liu and A. J. García, "Methods for Generating Hydrogel Particles for Protein Delivery," *Ann. Biomed. Eng.*, vol. 44, no. 6, pp. 1946–1958, 2016.

[40] R. T. Chacko, J. Ventura, J. Zhuang, and S. Thayumanavan, "Polymer nanogels: a versatile nanoscopic drug delivery platform.," *Adv. Drug Deliv. Rev.*, vol. 64, no. 9, pp. 836–51, Jun. 2012.

[41] H. K. S. Yadav, N. Anwar, A. Halabi, and G. A. Alsalloum, "Nanogels as Novel Drug Delivery Systems - A Review Properties of Nanogels Keywords : Introduction Advantages of Nanogels," *Insight Pharma Res.*, pp. 1–8, 2017.

[42] H. Zhang, Y. Zhai, J. Wang, and G. Zhai, "New progress and prospects: The application of nanogel in drug delivery," *Mater. Sci. Eng. C. Mater. Biol. Appl.*, vol. 60, pp. 560–568, 2016.

[43] K. Akiyoshi, S. Deguchi, N. Moriguchi, S. Yamaguchi, and J. Sunamoto, "Self-aggregates of hydrophobized polysaccharides in water. Formation and characteristics of nanoparticles," *Macromolecules*, vol. 26, no. 12, pp. 3062–3068, Jun. 1993.

[44] H. Kobayashi, O. Katakura, N. Morimoto, K. Akiyoshi, and S. Kasugai, "Effects of Cholesterol-Bearing Pullulan (CHP) -Nanogels in Combination with Prostaglandin E1 on Wound Healing," *Wiley Period.*, vol. 1, pp. 55–60, 2009.

[45] A. Shimoda, S. ichi Sawada, A. Kano, A. Maruyama, A. Moquin, F. M. Winnik, and K. Akiyoshi, "Dual crosslinked hydrogel nanoparticles by nanogel bottom-up method for sustained-release delivery," *Colloids Surfaces B Biointerfaces*, vol. 99, pp. 38–44, 2012.

[46] Y. Tahara, M. Sakiyama, S. Takeda, T. Nishimura, S. Mukai, S. Sawada, Y. Sasaki, and K. Akiyoshi, "Self-Assembled Nanogels of Cholesterol-Bearing Hydroxypropyl Cellulose: A Thermoresponsive Building Block for Nanogel Tectonic Materials," *Langmuir*, vol. 32, pp. 12283–12289, 2016.

[47] J.-H. Ryu, R. T. Chacko, S. Jiwpanich, S. Bickerton, R. P. Babu, and S. Thayumanavan, "Self-cross-linked polymer nanogels: a versatile nanoscopic drug delivery platform.," *J. Am. Chem. Soc.*, vol. 132, no. 48, pp. 17227–35, Dec. 2010.

[48] L. Li, J. H. Ryu, and S. Thayumanavan, "Effect of hofmeister ions on the size and encapsulation stability of polymer nanogels," *Langmuir*, vol. 29, no. 1, pp. 50–55, 2013.

[49] B. Aktan, L. Chambre, R. Sanyal, and A. Sanyal, "'Clickable' Nanogels via Thermally Driven Self-Assembly of Polymers: Facile Access to Targeted Imaging Platforms using Thiol-Maleimide Conjugation," *Biomacromolecules*, vol. 18, no. 2, pp. 490–497, 2017.

[50] S. Choudhary, J. M. Reck, A. J. Carr, and S. R. Bhatia, "Hydrophobically modified alginate for extended release of pharmaceuticals," *Polym. Adv. Technol.*, no. May, pp. 1–7, 2017.

[51] M. Hamidi, A. Azadi, and P. Rafiei, "Hydrogel nanoparticles in drug delivery.," *Adv. Drug Deliv. Rev.*, vol. 60, no. 15, pp. 1638–49, Dec. 2008.

[52] Y. Xue, X. Xia, B. Yu, X. Luo, N. Cai, S. Long, and F. Yu, "A green and facile method for the preparation of a pH-responsive alginate nanogel for subcellular delivery of doxorubicin," *RSC Adv.*, vol. 5, no. 90, pp. 73416–73423, 2015.

[53] S. Bazban-Shotorbani, E. Dashtimoghadam, A. Karkhaneh, M. M. Hasani-Sadrabadi, and K. I. Jacob, "Microfluidic Directed Synthesis of Alginate Nanogels with Tunable Pore Size for Efficient Protein Delivery," *Langmuir*, vol. 32, no. 19, pp. 4996–5003, 2016.

[54] F. Croisier and C. Jérôme, "Chitosan-based biomaterials for tissue engineering," *Eur. Polym. J.*, vol. 49, no. 4, pp. 780–792, 2013.

[55] Z. Zhang, R. Zhang, L. Chen, Q. Tong, and D. J. McClements, "Designing hydrogel particles for controlled or targeted release of lipophilic bioactive agents in the gastrointestinal tract," *Eur. Polym. J.*, vol. 72, pp. 698–716, 2015.

[56] A. Azadi, M. Hamidi, and M. Rouini, "Methotrexate-loaded chitosan nanogels as ' Trojan Horses ' for drug delivery to brain : Preparation and in vitro / in vivo characterization," *Int. J. Biol. Macromol.*, vol. 62, pp. 523–530, 2013.

[57] S. S. Abolmaali, A. M. Tamaddon, S. Mohammadi, Z. Amoozgar, and R. Dinarvand, "Chemically crosslinked nanogels of PEGylated poly ethyleneimine (l-histidine substituted) synthesized via metal ion coordinated self-assembly for delivery of methotrexate: Cytocompatibility, cellular delivery and antitumor activity in resistant cells," *Mater. Sci. Eng. C*, vol. 62, pp. 897–907, 2016.

[58] L. S. Moreira Teixeira, J. Feijen, C. A. van Blitterswijk, P. J. Dijkstra, and M. Karperien, "Enzyme-catalyzed crosslinkable hydrogels: Emerging strategies for tissue engineering," *Biomaterials*, vol. 33, no. 5, pp. 1281–1290, 2012.

[59] M. A. Pujana, L. Pérez-álvarez, L. C. C. Iturbe, and I. Katime, "Water soluble folate-chitosan nanogels crosslinked by genipin," *Carbohydr. Polym.*, vol. 101, pp. 113–120, 2014.

[60] M. A. Pujana, L. Pérez-álvarez, L. Carlos, C. Iturbe, and I. Katime, "pH-sensitive chitosan-folate nanogels crosslinked with biocompatible dicarboxylic acids," *Eur. Polym. J.*, vol. 61, pp. 215–

225, 2014.
[61] R. Arshady, “Suspension, emulsion, and dispersion polymerization: A methodological survey,” *Colloid Polym. Sci.*, vol. 270, no. 8, pp. 717–732, 1992.
[62] S. P. Callender, J. A. Mathews, K. Kobernyk, and S. D. Wettig, “Microemulsion utility in pharmaceuticals: Implications for multi-drug delivery,” *Int. J. Pharm.*, vol. 526, no. 1–2, pp. 425–442, 2017.
[63] K. Sudhakar, K. M. Rao, M. C. S. Subha, and K. C. Rao, “Temperature-responsive poly (N-vinylcaprolactam- co-hydroxyethyl methacrylate) nanogels for controlled release studies of curcumin,” *Des. Monomers Polym.*, vol. 18, no. 8, pp. 705–713, 2015.
[64] M. Duran-Lobato, B. Carrillo-conde, Y. Khairandish, and N. A. Peppas, “Surface-Modified P(HEMA- co -MAA) Nanogel Carriers for Oral Vaccine Delivery: Design, Characterization, and In Vitro Targeting Evaluation,” *Biomacromolecules*, vol. 15, pp. 2725–2734, 2014.
[65] S. Slomkowski, J. V. Alemán, R. G. Gilbert, M. Hess, K. Horie, R. G. Jones, P. Kubisa, I. Meisel, W. Mormann, S. Penczek, and R. F. T. Stepto, “Terminology of polymers and polymerization processes in dispersed systems (IUPAC Recommendations 2011),” *Pure Appl. Chem.*, vol. 83, no. 12, pp. 2229–2259, Jan. 2011.
[66] Abe, A, A.-C. Albertsson, K. D. W. H. De Jeu, H. K. S. Kobayashi, K. L. L. Leibler, T. E. L. I. Manners, M. M. E. M. Terentjev, M. V. B. Voit, and G. W. U. Wiesner, *Advances in Polymer Science Editorial Board :* 2009.
[67] M. Witting, M. Molina, K. Obst, R. Plank, K. M. Eckl, H. C. Hennies, M. Calderón, W. Frieß, and S. Hedtrich, “Thermosensitive dendritic polyglycerol-based nanogels for cutaneous delivery of biomacromolecules,” *Nanomedicine Nanotechnology, Biol. Med.*, vol. 11, no. 5, pp. 1179–1187, 2015.
[68] F. F. Sahle, M. Giulbudagian, and J. Bergueiro, “Dendritic polyglycerol and N-isopropylacrylamide based thermoresponsive nanogels as smart carriers for controlled delivery of drugs through the hair follicle,” vol. 9, pp. 172–182, 2017.
[69] C. A. Carmona-Moran, O. Zavgorodnya, A. D. Penman, E. Kharlampieva, S. L. Bridges, R. W. Hergenrother, J. A. Singh, and T. M. Wick, “Development of gellan gum containing formulations for transdermal drug delivery : Component evaluation and controlled drug release using temperature responsive nanogels,” *Int. J. Pharm.*, vol. 509, no. 1–2, pp. 465–476, 2016.
[70] M. Poliakoff, S. M. Howdle, and S. G. Kazarian, “Vibrational Spectroscopy in Supercritical Fluids: From Analysis and Hydrogen Bonding to Polymers and Synthesis,” *Angew. Chemie Int. Ed. English*, vol. 34, no. 12, pp. 1275–1295, Jul. 1995.
[71] J. A. Darr and M. Poliakoff, “New Directions in Inorganic and Metal-Organic Coordination Chemistry in Supercritical Fluids,” *Chem. Rev.*, vol. 99, no. 2, pp. 495–541, 1999.
[72] R. S. Oakes, A. A. Clifford, and C. M. Rayner, “The use of supercritical fluids in synthetic organic chemistry,” *J. Chem. Soc. Perkin Trans. 1*, no. 9, pp. 917–941, 2001.
[73] A. I. Cooper and J. M. DeSimone, “Polymer synthesis and characterization in liquid / supercritical carbon dioxide,” *Curr. Opin. Solid State Mater. Sci.*, vol. 1, no. 6, pp. 761–768, 1996.
[74] A. I. Cooper, “Polymer synthesis and processing using supercritical carbon dioxide,” *J. Mater. Chem.*, vol. 10, no. 2, pp. 207–234, 2000.
[75] J. M. Dobbs, J. M. Wong, R. J. Lahiere, and K. P. Johnston, “Modification of supercritical fluid phase behavior using polar cosolvents,” *Ind. Eng. Chem. Res.*, vol. 26, no. 1, pp. 56–65, 1987.
[76] M. McHugh and V. Krukonis, “Thermodynamic Modeling of Supercritical Fluid_Solute Phase Behavior,” *Supercrit. Fluid Extr. - Princ. Pract.*, pp. 99–134, 1994.
[77] Praxair, “Praxair Material Safety Data Sheet,” *Emerg. Overv.*, no. July, pp. 1996–1997, 2007.
[78] E. J. Beckman, “Supercritical and near-critical CO2 in green chemical synthesis and processing,” *J. Supercrit. Fluids*, vol. 28, no. 2–3, pp. 121–191, 2004.
[79] K. P. Johnston, “Block copolymers as stabilizers in supercritical fluids,” *Curr. Opin. Colloid*

Interface Sci., vol. 5, no. 5–6, pp. 350–355, 2000.

[80] F. Rindfleisch, T. P. DiNoia, and M. a. McHugh, "Solubility of polymers and copolymers in supercritical CO2," *J. Phys. Chem.*, vol. 100, no. 38, pp. 15581–15587, 1996.

[81] N. Esfandiari, "Production of micro and nano particles of pharmaceutical by supercritical carbon dioxide," *J. Supercrit. Fluids*, vol. 100, pp. 129–141, 2015.

[82] M. J. Cocero, Á. Martín, F. Mattea, and S. Varona, "Encapsulation and co-precipitation processes with supercritical fluids: Fundamentals and applications," *Journal of Supercritical Fluids*, vol. 47, no. 3. pp. 546–555, 2009.

[83] M. Champeau, J. M. Thomassin, T. Tassaing, and C. Jérôme, "Drug loading of polymer implants by supercritical CO<inf>2</inf> assisted impregnation: A review," *J. Control. Release*, vol. 209, pp. 248–259, 2015.

[84] M. J. Whitaker, J. Hao, O. R. Davies, G. Serhatkulu, S. Stolnik-Trenkic, S. M. Howdle, and K. M. Shakesheff, "The production of protein-loaded microparticles by supercritical fluid enhanced mixing and spraying," in *Journal of Controlled Release*, 2005, vol. 101, no. 1–3 SPEC. ISS., pp. 85–92.

[85] M. F. Kemmere, "Supercritical Carbon Dioxide for Sustainable Polymer Processes," *Supercrit. Carbon Dioxide Polym. React. Eng.*, pp. 1–14, 2006.

[86] L. Du, J. Y. Kelly, G. W. Roberts, and J. M. DeSimone, "Fluoropolymer synthesis in supercritical carbon dioxide," *J. Supercrit. Fluids*, vol. 47, no. 3, pp. 447–457, 2009.

[87] J. M. Desimone, Z. Guan, and C. S. Elsbernd, "Synthesis of fluoropolymers in supercritical carbon dioxide.," *Science*, vol. 257, no. 5072, pp. 945–7, 1992.

[88] C. Boyère, C. Jérôme, and A. Debuigne, "Input of supercritical carbon dioxide to polymer synthesis : An overview," *Eur. Polym. J.*, vol. 61, pp. 45–63, 2014.

[89] E. Girard, T. Tassaing, J. D. Marty, and M. Destarac, "Structure-Property Relationships in CO2-philic (Co)polymers: Phase Behavior, Self-Assembly, and Stabilization of Water/CO2 Emulsions," *Chem. Rev.*, vol. 116, no. 7, pp. 4125–4169, 2016.

[90] Knez, E. Markočič, M. Leitgeb, M. Primožič, M. Knez Hrnčič, and M. Škerget, "Industrial applications of supercritical fluids: A review," *Energy*, vol. 77, pp. 235–243, 2014.

[91] R. Campardelli, L. Baldino, and E. Reverchon, "Supercritical fluids applications in nanomedicine," *J. Supercrit. Fluids*, vol. 101, pp. 193–214, 2015.

[92] J. L. Kendall, D. a. Canelas, J. L. Young, and J. M. DeSimone, "Polymerizations in Supercritical Carbon Dioxide.," *Chem. Rev.*, vol. 99, no. 2, pp. 543–564, Mar. 1999.

[93] J. Xia, T. Johnson, S. G. Gaynor, K. Matyjaszewski, and J. DeSimone, "Atom transfer radical polymerization in supercritical carbon dioxide," *Macromolecules*, vol. 32, no. 15, pp. 4802–4805, 1999.

[94] J. Ryan, F. Aldabbagh, P. B. Zetterlund, and M. Okubo, "First nitroxide-mediated free radical dispersion polymerizations of styrene in supercritical carbon dioxide," *Polymer (Guildf).*, vol. 46, no. 23, pp. 9769–9777, 2005.

[95] P. B. Zetterlund, F. Aldabbagh, and M. Okubo, "Controlled/living heterogeneous radical polymerization in supercritical carbon dioxide," *J. Polym. Sci. Part A Polym. Chem.*, vol. 47, no. 15, pp. 3711–3728, 2009.

[96] A. M. Gregory, K. J. Thurecht, and S. M. Howdle, "Controlled Dispersion Polymerization of Methyl Methacrylate in Supercritical Carbon Dioxide via RAFT," *Macromolecules*, vol. 41, no. 4, pp. 1215–1222, Feb. 2008.

[97] M. Zong, K. J. Thurecht, and S. M. Howdle, "Dispersion polymerisation in supercritical CO 2 using macro-RAFT agents w," *Chem. Commun.*, pp. 5942–5944, 2008.

[98] R. Fink and E. J. Beckman, "Phase behavior of siloxane-based amphiphiles in supercritical carbon dioxide," *J. Supercrit. Fluids*, vol. 18, no. 2, pp. 101–110, 2000.

[99] J. M. Desimone, E. E. Maury, Y. Z. Menceloglu, J. B. McClain, T. J. Romack, and J. R. Combes, "Dispersion polymerizations in supercritical carbon dioxide.," *Science (80-.).*, vol. 265, no. 5170, pp. 356–359, 1994.

[100] T. Sarbu, T. J. Styranec, and E. J. Beckman, "Design and Synthesis of Low Cost , Sustainable CO2-philes," *Ind. Eng. Chem. Res.*, vol. 39, pp. 4678–4683, 2000.

[101] T. Sarbu, T. Styranec, and E. J. Beckman, "Non-fluorous polymers with very high solubility in supercritical CO2 down to low pressures," *Lett. to Nat.*, vol. 405, pp. 165–168, 2000.

[102] N. A. Birkin, N. J. Arrowsmith, E. J. Park, A. P. Richez, and S. M. Howdle, "Synthesis and application of new CO2-soluble vinyl pivalate hydrocarbon stabilisers via RAFT polymerisation," *Polym. Chem.*, vol. 2, no. 6, p. 1293, 2011.

[103] H. Lee, E. Terry, M. Zong, N. Arrowsmith, S. Perrier, K. J. Thurecht, and S. M. Howdle, "Successful dispersion polymerization in supercritical CO2 using polyvinylalkylate hydrocarbon surfactants synthesized and anchored via RAFT.," *J. Am. Chem. Soc.*, vol. 130, no. 37, pp. 12242–3, Sep. 2008.

[104] B. Tan, H. M. Woods, P. Licence, S. M. Howdle, and A. I. Cooper, "Synthesis and CO2 Solubility Studies of Poly (ether carbonate)s and Poly (ether ester) s Produced by Step Growth Polymerization," *Macromolecules*, vol. 38, pp. 1691–1698, 2005.

[105] X. Liu, M. Wang, S. Harrisson, A. Debuigne, J. D. Marty, and M. Destarac, "Enhanced Stabilization of Water/scCO2Interface by Block-Like Spontaneous Gradient Copolymers," *ACS Sustain. Chem. Eng.*, vol. 5, no. 11, pp. 9645–9650, 2017.

[106] X. Zhang, S. Heinonen, and E. Levänen, "Applications of supercritical carbon dioxide in materials processing and synthesis," *RSC Adv.*, vol. 4, no. 105, pp. 61137–61152, 2014.

[107] W. Ye and J. M. Desimone, "Emulsion Polymerization of N -Ethylacrylamide in Supercritical Carbon Dioxide," *Macromolecules*, vol. 38, pp. 2180–2190, 2005.

[108] F. A. Adamsky and E. J. Beckman, "Inverse emulsion polymerization of acrylamide in supercritical carbon dioxide," *Macromolecules*, vol. 27, no. 1, pp. 312–314, 1994.

[109] N. Baran, S. Deniz, M. Akgün, I. N. Uzun, and S. Dinçer, "Dispersion polymerization of styrene in supercritical carbon dioxide using monofunctional perfluoropolyether and silicone-containing fluoroacrylate stabilizers," *Eur. Polym. J.*, vol. 41, no. 5, pp. 1159–1167, 2005.

[110] D. A. Canelas and J. M. DeSimone, "Dispersion Polymerizations of Styrene in Carbon Dioxide Stabilized with Poly(styrene- b -dimethylsiloxane)," *Macromolecules*, vol. 30, no. 19, pp. 5673–5682, 1997.

[111] H. Yuvaraj, H. S. Hwang, M. H. Woo, E. J. Park, H. S. Ganapathy, Y. S. Gal, and K. T. Lim, "Dispersion polymerization of styrene in supercritical CO2 stabilized by random copolymers of 1H,1H-perfluorooctyl methacrylate and 2-dimethylaminoethyl methacrylate," *J. Supercrit. Fluids*, vol. 42, no. 3 SPEC. ISS., pp. 359–365, 2007.

[112] T. Carson, J. Lizotte, and J. M. Desimone, "Dispersion Polymerization of 1-Vinyl-2-pyrrolidone in Supercritical Carbon Dioxide," *Macromolecules*, vol. 33, no. 6, pp. 15–18, 2000.

[113] A. Galia, A. Giaconia, V. Iaia, and G. Filardo, "Synthesis of hydrophilic polymers in supercritical carbon dioxide in the presence of a siloxane-based macromonomer surfactant: Heterogeneous polymerization of 1-vinyl-2 pyrrolidone," *J. Polym. Sci. Part A Polym. Chem.*, vol. 42, no. 1, pp. 173–185, 2004.

[114] H. Shiho and J. M. DeSimone, "Dispersion Polymerization of Glycidyl Methacrylate in SupercriticalCarbon Dioxide," *Macromolecules*, vol. 34, pp. 1198–1203, 2001.

[115] H. Shiho and J. M. DeSimone, "Dispersion Polymerization of Acrylonitrile in Supercritical Carbon Dioxide," *Macromolecules*, vol. 33, no. 5, pp. 1565–1569, Mar. 2000.

[116] H. M. Woods, C. Nouvel, P. Licence, D. J. Irvine, and S. M. Howdle, "Dispersion polymerization of methyl methacrylate in supercritical carbon dioxide using a silicone-containing fluoroacrylate stabilizer.," *Macromolecules*, no. 38, pp. 3271–3282, 2005.

[117] T. D. McAllister, L. D. Farrand, and S. M. Howdle, "Improved Size Control for the Dispersion Polymerization of Methyl Methacrylate in Supercritical Carbon Dioxide," *Macromol. Chem. Phys.*, pp. 1–8, 2016.

[118] W. Wang, M. R. Giles, D. Bratton, D. J. Irvine, S. P. Armes, V. W. Weaver, and S. M. Howdle, "The homo and copolymerisation of 2- (dimethylamino) ethyl methacrylate in supercritical

carbon dioxide," *Polymer (Guildf).*, vol. 44, pp. 3803–3809, 2003.
[119] H. Shiho and J. M. DeSimone, "Dispersion polymerization of 2-hydroxyethyl methacrylate in supercritical carbon dioxide," *J. Polym. Sci., Part A Polym. Chem.*, vol. 38, no. 20, pp. 3783–3790, 2000.
[120] A. I. Cooper, W. P. Hems, and A. B. Holmes, "Synthesis of cross-linked polymer microspheres in supercritical carbon dioxide," *Macromol. Rapid Commun.*, vol. 19, pp. 353–357, 1998.
[121] J. Shin, W. Bae, and H. Kim, "Synthesis of cross-linked poly(methyl methacrylate) via dispersion polymerization in supercritical carbon dioxide," *Colloid Polym. Sci.*, vol. 288, no. 3, pp. 271–282, 2010.
[122] W. Wang, R. M. T. Griffiths, A. Naylor, M. R. Giles, D. J. Irvine, and S. M. Howdle, "Preparation of cross-linked microparticles of poly(glycidyl methacrylate) by dispersion polymerization of glycidyl methacrylate using a PDMS macromonomer as stabilizer in supercritical carbon dioxide," *Polymer (Guildf).*, vol. 43, no. 25, pp. 6653–6659, 2002.
[123] T. Casimiro, A. M. Banet-Osuna, A. M. Ramos, M. N. Da Ponte, and A. Aguiar-Ricardo, "Synthesis of highly cross-linked poly(diethylene glycol dimethacrylate) microparticles in supercritical carbon dioxide," *Eur. Polym. J.*, vol. 41, no. 9, pp. 1947–1953, 2005.
[124] M. Temtem, T. Casimiro, F. J. Mano, and A. Aguiar-ricardo, "Green synthesis of a temperature sensitive hydrogel," *Green Chem.*, vol. 9, pp. 75–79, 2007.
[125] E. Costa, T. Casimiro, C. Lobato, M. Teresa, and A. Aguiar-ricardo, "Tailoring thermoresponsive microbeads in supercritical carbon dioxide for biomedical applications," *J. Supercrit. Fluids*, vol. 56, no. 3, pp. 292–298, 2011.
[126] Z. Ma and P. Lacroix-desmazes, "Dispersion polymerization of 2-hydroxyethyl methacrylate stabilized by a hydrophilic / CO 2 -philic poly (ethylene diblock copolymer in supercritical carbon dioxide," *Polym. J.*, vol. 45, pp. 6789–6797, 2004.
[127] D. Alaimo, B. Grignard, C. Kuppan, Y. Adriaensen, M. J. Genet, C. Dupont-Gillain, J.-F. Gohy, C.-A. Fustin, C. Detrembleur, and C. Jérôme, "A photocleavable stabilizer for the preparation of PHEMA nanogels by dispersion polymerization in supercritical carbon dioxide," *Polym. Chem.*, vol. 8, no. 3, pp. 581–591, 2017.

Aim of the thesis

Aim of the thesis

So far various polymer nanocarriers have been used in the targeted delivery and controlled release of hydrophobic drugs. However, there are still challenges to efficiently encapsulate and deliver more complex drugs such as therapeutic proteins and peptides. For this purpose, 3D hydrophilic nanoparticle networks, nanogels, are extensively studied. In the previous introductive section, we reviewed the most studied nanogels production methods and showed their advantages and limitations. We also highlighted the potential of the dispersion polymerisation in $scCO_2$ as an emergent technique to prepare polymer network particles of small size.

Therefore, we aim to develop a facile one-pot synthesis to design poly(HEMA) nano-/microgels for protein delivery by using free-radical heterogeneous polymerisation in supercritical carbon dioxide ($scCO_2$) as green polymerisation medium. Indeed, $scCO_2$ enables to produce dry powder formulations without any solvent residues whereby also reducing post-polymerisation purification for the obtained formulation.

As shown is the introduction, the key factor for achieving well-defined particles in this medium is the stabiliser. Therefore, we use initially an already reported fluorinated block copolymer, PEO-*b*-PFDA, known to give good performances in getting well-defined small particles of poly(HEMA) in $scCO_2$, and we focus in the Chapter 2 on determining mild synthesis conditions, especially low temperature, for the synthesis of the cross-linked poly(HEMA) particles. These mild synthesis conditions were aimed to enable the handling of solvent-sensitive and heat- labile therapeutic agents.

Then, we aim to obtain stabiliser-free particles leading to water dispersable poly(HEMA) nanohydrogels. For this purpose, we synthesize a CO_2-philic diblock copolymer bearing a photocleavable junction. Upon UV-photolysis, the hydrophobic part of the stabiliser will be removed to leave the surface stabiliser-free. The efficiency of this photocleavable stabiliser to synthesize well-defined loaded poly(HEMA) particles in presence of a model drug (Chapter3) and antimicrobial peptide (Chapter 4) will be probed by redispersing them in water and studying the drug/peptide release.

Finally, we aim at investigating fluorine-free hydrocarbon based stabilisers to obtain cross-linked poly(HEMA) particles as an alternative to the fluorinated diblock stabiliser (Chapter 5). In this case, the hydrocarbon based stabiliser present on the surface will be hydrolysed to provide alcohols improving water solubility and leading to poly(HEMA) nanohydrogels.

Chapter 2

Mild synthesis of poly(HEMA)-networks as well-defined nanoparticles in supercritical carbon dioxide

Rahmet Parilti, David Alaimo, Bruno Grignard, Frank Boury, Steven M. Howdle and Christine Jérôme, *J. Mater. Chem. B*, 2017, **5**, 5806–5815.

Abstract

Free-radical dispersion polymerisation of 2-hydroxyethyl methacrylate was carried out in supercritical carbon dioxide ($scCO_2$) in presence of stabilisers based on polyethylene oxide (PEO) and poly(heptadecafluorodecyl acrylate) (PFDA). Dispersion polymerisation in the presence of this diblock stabiliser resulted into poly(HEMA) spherical particles with the size of 316 nm. Furthermore, the effect of the CO_2-phobic block (PEO) in diblock copolymer was investigated by using three different chain lengths (1000, 2000, 5000 g/mol). By optimizing the stabiliser composition and structure, mild reaction conditions have been identified allowing to obtain well-defined spherical cross-linked poly(HEMA) particles with a mean diameter of unprecedented low size (216 nm) at temperature as low as 35°C.

1. Introduction

Nanoparticles (NPs) of either natural or synthetic polymers have been widely explored for their promising biomedical applications as nano-sized carriers for controlled and targeted delivery of therapeutic agents. They possess unique physical and chemical properties such as high stability, small size, low toxicity and easily tailored chemistry which makes them good candidate for controlled delivery systems. Thus far anticancer drugs, vaccines, and oligonucleotides containing delivery systems have been investigated[1]**.** These emerging therapies had a major impact in medicine and improved the efficacy of the performance of currently available drugs.[1,2] Recent studies are focused on designing nanocarriers for controlled release and delivery of protein- or peptide-based therapeutics due to their specific and variety of vital actions in the body.[3,4] Besides, proteins offer efficient treatments compared to existing therapies such as gene therapy[5]**.** However, there are several important issues that should be considered regarding proteins; they have a sensitive tertiary structure which is easily degraded by temperature and upon exposure to solvents can lead to the loss of their activity**.**[5,6] Therefore different production methods have been investigated in order to preserve the specific structure and activity of proteins [7,8] one of them being supercritical carbon dioxide ($scCO_2$) processes.[9] Indeed, supercritical carbon dioxide is a cheap solvent with non-toxicity and non-flammability with easily accessible critical point (31.1°C and 73.8 bar) which makes it also desirable for large-scale productions.[10,11] Therefore, it has emerged as an alternative medium for conventional solvents due to its environmentally benign properties.

2-hydroxyethyl methacrylate (HEMA) based particles have been reported to exhibit potential applications in the biomedical field. [12,13] Hydrogels of poly(HEMA) present excellent biocompatibility and can act as potential carriers in drug delivery, dental, ophthalmic, and neural tissue engineering applications.[14,15] Typically, particles based on homo- or copolymers of poly(HEMA) are synthesised in water or water/organic solvent mixtures which necessitates several additional steps for purification and drying of the obtained products.[16] Furthermore, polymer particles that are produced for pharmaceutical applications face several obstacles, such as the type of solvent that can be used and the level of residual solvent that is permitted in final products. The high affinity of polymers toward organic solvents prohibits complete separation. On the other hand, polymers exhibit inherently low or no solubility in $scCO_2$ thus making it a very good anti solvent for particle production as well.[17] Upon depressurization $scCO_2$ goes to gaseous state so that the polymers can be isolated from the reaction media by simple depressurization without solvent residues which allows dry powder formulations that have superior stability when compared to liquid formulations.[9] Owing to these facts, much more effort has been devoted to use CO_2 as a green polymerisation medium and producing particles carrying a therapeutic agent in their core.[9] It has been reported that a wide range of monomers are soluble in $scCO_2$ whereas their corresponding high molecular-weight polymers are insoluble[11] except amorphous or low crystalline fluoropolymers[13,16,18–25], silicones[22,26,27] and low molar mass polyvinyl alkanoate[28–30] (poly(vinyl acetate), PVAc) and poly(vinyl pivalate, PVPi) that were found to have significant solubility in $scCO_2$ under moderate conditions (<100 °C, <400 bar). Therefore, $scCO_2$ is a good medium to conduct heterogeneous polymerisation processes such as suspension, emulsion and dispersion polymerisation.[11] Heterogeneous

polymerisation techniques led to particle formation with different size and morphologies.[31] Dispersion polymerisation is defined as a polymerisation in which monomer, initiator and stabiliser are dissolved in the continuous phase acting as a non-solvent for the corresponding polymer[32], and is especially interesting because it leads to micron sized particles in single batch and many commodity polymers can be produced in large scale by this method.[33] Upon precipitation of the polymer chains, a suitable stabiliser is adsorbed or grafted on the forming particles resulting into long range repulsion between particles and preventing their coagulation. Therefore, a successful dispersion is highly dependent on choosing a ideal stabiliser.[34]

Recently Mc. Allister *et al.* have produced well-defined poly(methylmethacrylate) (PMMA) particles in $scCO_2$ by free radical dispersion polymerisation using poly(dimethyl siloxane) end-capped by a methacrylate moiety (PDMS-MA) as a stabiliser. [35] With such reactive PDMS, they probed the effect of the PDMS-MA concentration ranging from 1-20wt% on the PMMA particles size. As a rule, increasing the PDMS-MA concentration leads to the decrease of the PMMA particle size from 3.8 µm to 0.6 µm. This effect is attributed to the stabilisation of a larger surface area of formed PMMA at higher PDMS concentration. Thus, a higher number of small PMMA particles can be obtained. Accordingly, the stabiliser concentration is also an important parameter to produce well-defined particles with desired diameter.

In this case, non-crystalline fluorinated-based (co)polymers were found to be very efficient stabilisers for the dispersion polymerisation in $scCO_2$.[13,16,18–25] These polymers present unique physico-chemical properties due to their low surface energy, high thermal and chemical stability.[36,37] As well as their relatively high solubility in $scCO_2$ these polymers have

found applications in the dispersion polymerisation of many vinyl monomers such as methacrylate derivatives[13,16,38–42] (MMA, HEMA, or others methacrylate esters), acrylonitrile[20,43], *N*-vinylpyrrolidone[25,44], styrene[22] resulting into well-defined spherical particles.

Consequently, we aim to develop a novel dispersion polymerisation process for the one-pot encapsulation of therapeutic proteins in $scCO_2$ which would be highly beneficial both for manufacturing and medical point of view. In a previous study [45], some of us reported on the synthesis of perfluorinated stabilisers, composed of hydrophilic poly(ethylene oxide) (PEO) and fluorinated acrylate (1H,1H,2H,2H-heptadecafluorodecyl acrylate, PFDA) sequences combined in different architectures, i.e. random, diblock and palm-tree copolymers and their use as a stabiliser for dispersion polymerisation of HEMA in α,α,α-Trifluorotoluene (TFT). The effect of the stabiliser and monomer concentration were investigated for different architectures of PEO/PFDA copolymers. Stabilisers that were constituted of block architecture, i.e. diblock and palm-tree, reduced the interfacial tension at water/TFT interface significantly compared to the random copolymer. Nevertheless, spherical and monodisperse particles of poly(HEMA) networks have been obtained by dispersion polymerisation regardless of the copolymer architecture of the stabiliser used at 80 °C degrees in TFT. It has been shown that the size of the particles can be adjusted by changing the stabiliser concentration, so that nanoparticles (300nm) could be obtained.

Here, we study these promising perfluorinated copolymers, especially the PEO-*b*-PFDA diblock copolymer, as stabilisers for the synthesis of cross-linked poly(HEMA) nanoparticles in $scCO_2$ in place of TFT to investigate the feasibility of using this green polymerisation medium. In addition, we use mild conditions of temperature to be compatible with proteins

stability, i.e. going down to the body temperature. Therefore, the effect of temperature and pressure on the size, morphology of the particles was investigated as well as the composition and concentration of the stabiliser.

2. Experimental Part

2.1 Materials

Poly(ethylene glycol) monomethyl ether (PEO, Fluka, Mn=2000 g/mol), Poly(ethylene glycol) monomethyl ether (PEO, Aldrich, Mn=1000 g/mol and Mn=5000 g/mol), 1H,1H,2H,2H-Heptadecafluorodecyl acrylate (FDA, Aldrich, 96%), 2,2'-Azobis(2-methylpropionitrile) (AIBN, Aldrich, 98%), S-Dodecyl-S'-(α,α'-dimethyl-α''-acetic acid)trithiocarbonate (DDMAT, Aldrich, 98%), α,α,α -Trifluorotoluene (TFT, Aldrich, 99+%), 1,1,2-trichlorotrifluoroethane (CFC-113, Aldrich, 99.8%), Deuterated Chloroform ($CDCl_3$, Eurisotop, Chloroform D+0.03% Tetramethysilane (TMS), >99.8) 2,2'-Azobis(4-methoxy-2,4-dimethylvaleronitrile) (V-70,Wako), 2-hydroxyethyl methacrylate (HEMA, Aldrich, 97%), Ethylene glycol dimethacrylate (EGDMA, Aldrich, 98%,), Carbon dioxide (I5122,CO2 N27 purity > 99,999%, Air Liquide, Belgium). Ultrapure water was produced by MilliQ plus 188 apparatus (Millipore). The diblock copolymers exhibiting similar PFDA block but different PEO block length thus different molar mass and composition, were synthesized by RAFT as described previously.[45]

2.2 Methods

2.2.1 Synthesis of macroRAFT agent (PEO-CTA)

A conventional synthesis was followed to prepare the macroRAFT agent (PEO-CTA).45 It is briefly described below for PEO 2000g/mol, the quantities were adjusted for PEO 1000 and

5000g/mol. Prior to the reaction, 5 g of poly (ethylene oxide) (2000 g/mol) was dried 3 times by azeotrope cycles with dry toluene and stored under nitrogen atmosphere. A round-bottom flask was charged with 1.82 g of RAFT agent S-Dodecyl- S'-(α,α'-dimethyl-α''-acetic acid)trithiocarbonate (DDMAT) (0.005 mol: 2 eq.), 1.03 g of N,N'-dicyclohexylcarbodiimide (DCC) (0.005 mol: 2 eq.), 0.06 g of 4-(dimethylamino)pyridine (DMAP) (0.0005 mol: 0.2 eq.) and 40 ml dry THF. The mixture was then transferred onto dried PEO under nitrogen pressure with the aid of stainless steel capillary. The final mixture was left for stirring at ambient temperature for 120 hours with moderate stirring rate. The macroRAFT agent was recovered by precipitation in diethyl ether followed by filtration and drying under vacuum. The macroRAFT agents were analyzed by ^{1}H NMR and Size Exclusion Chromatography using dimethyl formamide (DMF) as eluent. ^{1}H NMR: (250 MHz, $CDCl_3$) δ 7.26 (NMR solvent), 4.24 ($CH_2\underline{CH_2}$- OC(O)C$(CH_3)_2$– of PEO), 3.63 (broad peak, -CH_2 of PEO), 3.37 (-CH_3 chain-end of PEO), 3.23 (–SC(S)S$\underline{CH_2}CH_2$, CTA), 1.68 (–C$(CH_3)_2$- SC(S)S–, CTA), 1.61 (–C(S)S– $CH_2\underline{CH_2}CH_2$–,CTA), 1.22 (–$CH_2\underline{(CH_2)_9}CH_3$, CTA), 0.87 -0.82 (–$CH_3$ CTA chain-end). SEC-DMF: Đ=1.05 for PEO_{22}-CTA, PEO_{45}-CTA and Đ=1.02 PEO_{113}-CTA).

2.2.2 Synthesis of diblock stabilisers (PEO-*b*-PFDA)

Conventional synthesis of the diblock copolymer was adjusted from previously published method[13] and extended to 3 different molecular weight macroRAFT agents (PEO-CTA). The procedure and amounts were selected as follows: PEO-CTA (0.537 mmol) was dissolved in 38 g of TFT in a round-bottom flask. To this solution 19.32 mmol of FDA was added DP_{th}=(n([FDA]/[PEO-CTA]=36). After the addition of the monomer and a solution of 0.108 mmol (0.0177 g) of AIBN in 2 g of TFT was added, the flask was sealed with a 3-way stopcock and subjected to nitrogen bubbling in order to eliminate traces of oxygen. Thereafter, the

flask was placed in an oil bath at 65°C and left for stirring with moderate stirring rate for 48 h. The conversion was determined by ^{1}H-NMR by taking a crude sample at the end of reaction. Polymerisation ran to full conversion. The polymer was then recovered by precipitation in methanol followed by filtration and drying under vacuum. The resultant diblock copolymers were further characterized by ^{1}H NMR.^{1}H NMR : (250 MHz, $CDCl_3$) δ 7.26 (NMR solvent), 4.40 (broad peak, C(O)–O– $\underline{CH_2}$, PFDA block), 3.67 (broad peak, CH_2–CH_2–O, PEO block), 3.39 (-CH_3 chain-end of PEO), 2.51 (-$C(CH_3)_2$-CH_2-$\underline{CH_2}$ backbone and O-CH_2-$\underline{CH_2}$ PFDA), 1.77 (-$C(CH_3)_2$-$\underline{CH_2}$ PFDA backbone), 1.63 (s, 6H, –C(CH3)2- SC(S)S–, CTA), 1.57 (–C(S)S– $CH_2\underline{CH_2}CH_2$–,CTA), 1.20 (–$CH_2\underline{(CH_2)_9}CH_3$, CTA), 0.92 ($CH_3$, CTA chain-end).

2.2.3 Synthesis of poly (2-hydroxyethyl methacrylate) network nanoparticles in $scCO_2$

Dispersion polymerisations of 2-hydroxyethyl methacrylate were carried out in a high pressure stainless steel cell (82 ml, ToP Industrie) connected to a syringe pump (ISCO model no. 260D) equipped with a mechanical stirrer, a pressure transducer, a rupture disc, an internal thermocouple, a heating mantel and a digital control unit which enables instant monitoring of the pressure, temperature and stirring rate (more information on the used high pressure equipment can be found in Annex 1.1).

In a conventional dispersion, the amounts are used as follows: the cell was charged with 8.2 ml of HEMA (10% v/v CO_2), 82 µl of EGDMA (cross-linker, 1% v/v monomer), 0.82 g of stabiliser (in the case of 10% w/$v_{monomer}$), 0.1 g of AIBN (or 0.187 g V-70, 1% w/v monomer). The cell was securely sealed and a small amount of CO_2 was introduced. After the heating mantel was clamped, the stirring rate and temperature were set with the control unit. Temperature and pressure were increased step-wise and the reactor was stabilised at the

desired conditions. The reaction was run overnight at 400 rpm. At the end of the reaction, for the depressurization, initially stirring was stopped and the heating jacket removed and the reactor is allowed to cool down to ambient temperature. Thereafter, the reactor is depressurized gradually by opening an outlet valve. The depressurization rate is not systematically controlled. The pressure release is kept slow enough to avoid particle spraying out or polymer flushing in the outlet pipes. Therefore, the speed can be estimated to be between 5 to 10 bars per minute. After total depressurization, the cell was opened and the product was collected as a dry powder. Obtained products were stored in the ambient temperature in a plastic container.

2.3 Characterisations

^{1}H-NMR spectra were recorded with a 400 MHz Brucker spectrometer. ^{1}H NMR spectra of macroinitiator was recorded in deuterated chloroform ($CDCl_3$) NMR solvent having tetramethylsilane (0.03%TMS) as an internal reference, and for diblock fluorinated copolymers were recorded in 1,1,2-trichlorotrifluoroethane(CFC-113) and $CDCl_3$ mixture. Size exclusion chromatography (SEC) was carried out in DMF (flow rate 1 mL/min) at 40 °C using a Water 600 autosampler liquid chromatography equipped with a differential refractometer index detector. All the particles were analyzed with scanning electron microscopy (SEM, JEOL JSM 840-A) to evaluate their morphology and average particle sizes. Samples were prepared on SEM stubs and coated with Pt (30 nm). Average diameter of the particles (D_n) is determined from a conventional SEM images by measuring of randomly selected individual particles with the aid of VistaMetrix software (Version 1.33.0). Coefficient of variance (C_v) is an indicator of size distribution of the particles. It is calculated

from the standard deviation (σ) divided by the average diameter size (D_n) that is calculated from the SEM images. **Eq. 1:** $C_v = (\sigma/D_n)*100$

2.3.1 Cloud point measurements of the diblock copolymers

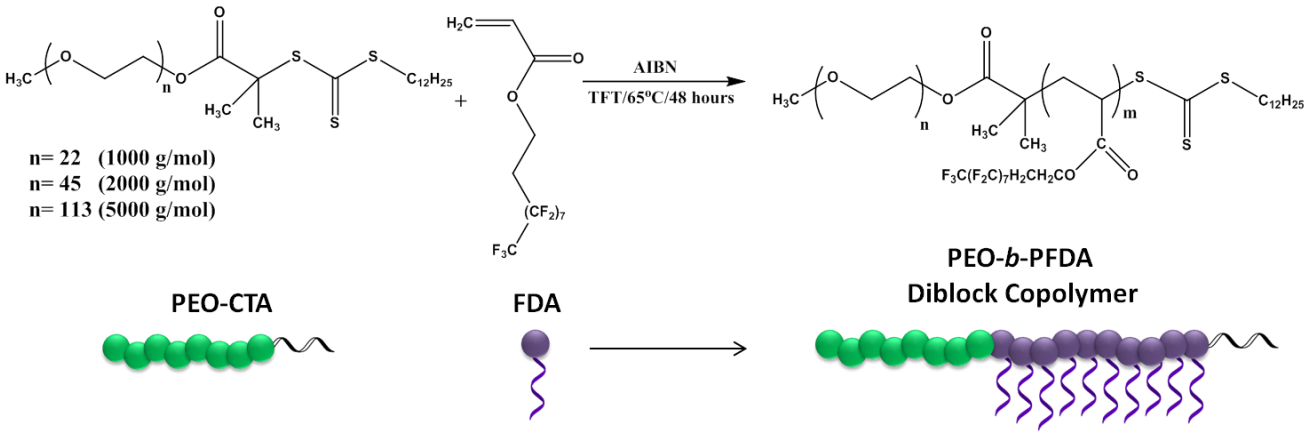
The solubility of the diblock copolymers indicates their potential to be used as a stabiliser for dispersion polymerisation in $scCO_2$. Cloud point in $scCO_2$ can be defined as the pressure in which the polymer starts to precipitate out from the solution at a given temperature[46]. Cloud points of synthesised block copolymers were determined by using high pressure variable volume view cell equipment (see Annex 2.2) that was produced by University of Nottingham.[47] The cell supports a maximum pressure of 345 bar. For a typical cloud point measurement 3g (15% wt monomer/ CO_2) of monomer, 150 mg of stabiliser (5%wt stabiliser/monomer) and 20 g of CO_2 were used. Stabiliser was dissolved in given amount of CO_2 was then transferred to the view cell by using a small stainless-steel CO_2 bomb. The weight of the bomb was recorded before and after addition to calculate the exact amount of CO_2 in the cell.

The cell was heated up to the desired temperature and allowed to stabilise. Thereafter, the hydraulic piston was slowly moved forward to increase the pressure in the cell until a single phase was observed through the sapphire window. At this pressure, the light at the end of the view cell becomes visible. The piston was moved back again slowly to decrease the pressure in a controlled manner to observe the pressure at which the medium is no longer a single phase. A cloudy mixture is observed due to precipitation of the polymer from the solution mixture and the light at the back of the view cell is not visible anymore. Cloud points were taken at 35, 45, 55, 65 and 75 °C and each point was repeated for 3 times. The cloud points are reported as an average value of these 3 repetitions.[30]

3. Results and discussions

3.1 Synthesis of the stabilisers

Dispersion polymerisation requires the use of an efficient stabiliser to control the morphology, the size and the stability of the formed particles. In order to investigate the effect of the PEO block length of the stabiliser on the particle formation in $scCO_2$, a series of PEO-*b*-PFDA diblock copolymers of different compositions have been synthesized following the RAFT polymerisation process by using PEO based chain transfer agent (PEO-CTA) of three different molecular weights (Scheme 1).



Scheme1: Synthesis of fluorinated diblock copolymers as CO_2-philic stabiliser *via* reversible addition-fragmentation chain transfer (RAFT) polymerisation.

Commercially available monomethoxy polyethylene glycol (Me-O-PEO-OH) of 1000 g/mol, 2000 g/mol and 5000 g/mol were used for the synthesis of PEO_{22}-CTA, PEO_{45}-CTA, and PEO_{113}-CTA, respectively, by adapting the previously reported procedure of Alaimo *et al.* [45]. The ^{1}H-NMR spectra analysis of the macroCTAs allowed us to determine the functionalisation yield of the PEO chain-end by comparing the $-CH_3$ end-group of alkyl chain of chain transfer agent (CTA) resonating around δ=0.87 ppm with the $-CH_2$ groups of the PEO repeating units resonating around δ= 3.6 ppm. Functionalization yields were found to be

82.1 % 88.3 % and 84.8% for PEO_{22}-CTA, PEO_{45}-CTA, and PEO_{113}-CTA, respectively, showing the robustness of the functionalization process which appears equally efficient whatever the molar mass of the PEO at least up to 5000 g/mol.

The RAFT polymerisation of FDA was then performed with the three PEO-CTAs according to previously reported conditions for PEO_{45}-CTA[13] and targeting the same polymerisation degree for the PFDA block of all the three resulting diblock copolymers. The diblock copolymers composition and molecular weight were determined by ^{1}H-NMR comparing the intensity of PFDA methylene groups (δ 4.40 ppm) and characteristic peak of PEO (around δ 3.6 ppm) [13,45]. The results are summarized in Table 1. Since the length of the PEO block varies while the PFDA block is the same, the three diblock stabilisers have a HRF increasing from ~0.6 to ~3.2. The fluorinated block being responsible for the solubilisation of the copolymer in CO_2, the solubility might be affected by increasing the length of the PEO block. The cloud points of the three diblock copolymers have thus been measured at 35°C (Table 1), the minimum temperature targeted for the dispersion synthesis of poly(HEMA) networks. At that temperature, the cloud point of both PEO_{22}-*b*-$PFDA_{38}$ and PEO_{45}-*b*-$PFDA_{37}$ was found to be roughly similar.

Table 1: Characteristics of synthesized PEO-*b*-PFDA diblock copolymers

Stabiliser	M_nPEO-CTA (g/mol)	DP_{th} [a]	HFR [b]	M_nPFDA [c] (g/mol)	$M_n$total (g/mol)	Cloud point [d] (bar)
PEO_{22}-*b*-$PFDA_{38}$	1364	36	0.58	19684	21048	106.8
PEO_{45}-*b*-$PFDA_{37}$	2364	36	1.216	19166	21530	104.9
PEO_{113}-*b*-$PFDA_{38}$	5364	36	3.23	19684	25048	-----

[a]Theoretical degree of polymerisation of the PFDA block=(n[FDA]/[PEO-CTA]); [b] Hydrophilic/Fluorinated ratio of the copolymer=[EO]/[FDA]); [c] Experimental molecular weight of PFDA block calculated by ^{1}H-NMR spectroscopy, M_w(FDA)=518 g/mol; [d] Minimal solubilisation pressure in CO_2 for a copolymer concentration of (5%wt stabiliser/monomer) measured at 35°C, for PEO_{113}-*b*-$PFDA_{38}$ was found to be insoluble at the view cell pressure limit 345 bar (5000 psi).

Indeed, decreasing the length of PEO does not constitute a barrier to the dissolution of the PFDA and thus of the stabiliser. In contrast, increasing the length of the PEO to 5000 g/mol significantly decreases the copolymer solubility, so that the cloud point of the less fluorinated diblock PEO_{113}-*b*-$PFDA_{38}$ copolymer could not be measured by our set-up since it remains insoluble at 35°C and 345 bar, i.e. the pressure limit of the view cell required for such measurements.

3.2 Dispersion polymerisation of 2-hydroxyethyl methacrylate (HEMA) in supercritical carbon dioxide ($scCO_2$)

3.2.1 Effects of the temperature and pressure

Particles formation by dispersion polymerisation processes is often guided by the stabiliser. This holds also for $scCO_2$. Indeed, the free-radical polymerisation of HEMA in $scCO_2$ in absence of stabiliser leads to the formation of aggregated polymer product as shown by Figure 1-1. However, in presence of a PEO-*b*-PFDA diblock copolymer, well-defined poly(HEMA) particles are obtained as previously described by Ma *et al*.[13] and Alaimo *et al*.[48].

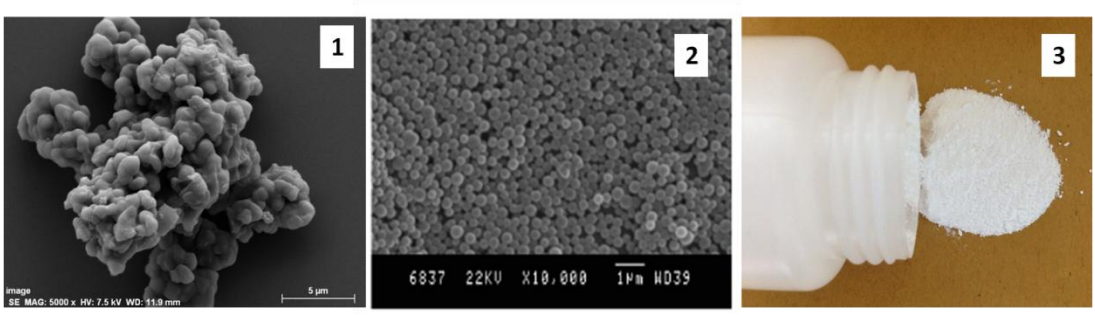


Figure 1: SEM images of poly(HEMA) powder collected after dispersion polymerisation of HEMA: (1) in absence of stabiliser and (2) in the presence of PEO_{45}-*b*-$PFDA_{37}$ (0.82g) stabiliser. Reactor feed: monomer (HEMA) 8.2 ml), cross-linker (EGDMA) 82µl) and initiator (AIBN) 0.1g). (3) Representative image of the free-flowing dry powder obtained by dispersion polymerisation in supercritical carbon dioxide in presence of a stabiliser. Collected straight after polymerisation from the high-pressure reactor without further treatment or purification.

Accordingly, by applying the synthesis conditions reported by Ma *et al.* , i.e. 65°C and 385 bar, and using the PEO_{45}-*b*-$PFDA_{37}$ stabiliser, poly(HEMA) particles were obtained with diameters in nanometre range (316 nm, Figure 1-2). In that case, after polymerisation and depressurization of the reactor, a nice free-flowing powder easy to handle is directly collected in the dry state (Figure 1-3).

Motivated by finding mild conditions to produce poly(HEMA) networks as particles below 300 nm, we firstly studied the possibility to decrease the dispersion polymerisation temperature of a HEMA/bis-acrylate cross-linker mixture, to 35-40°C.

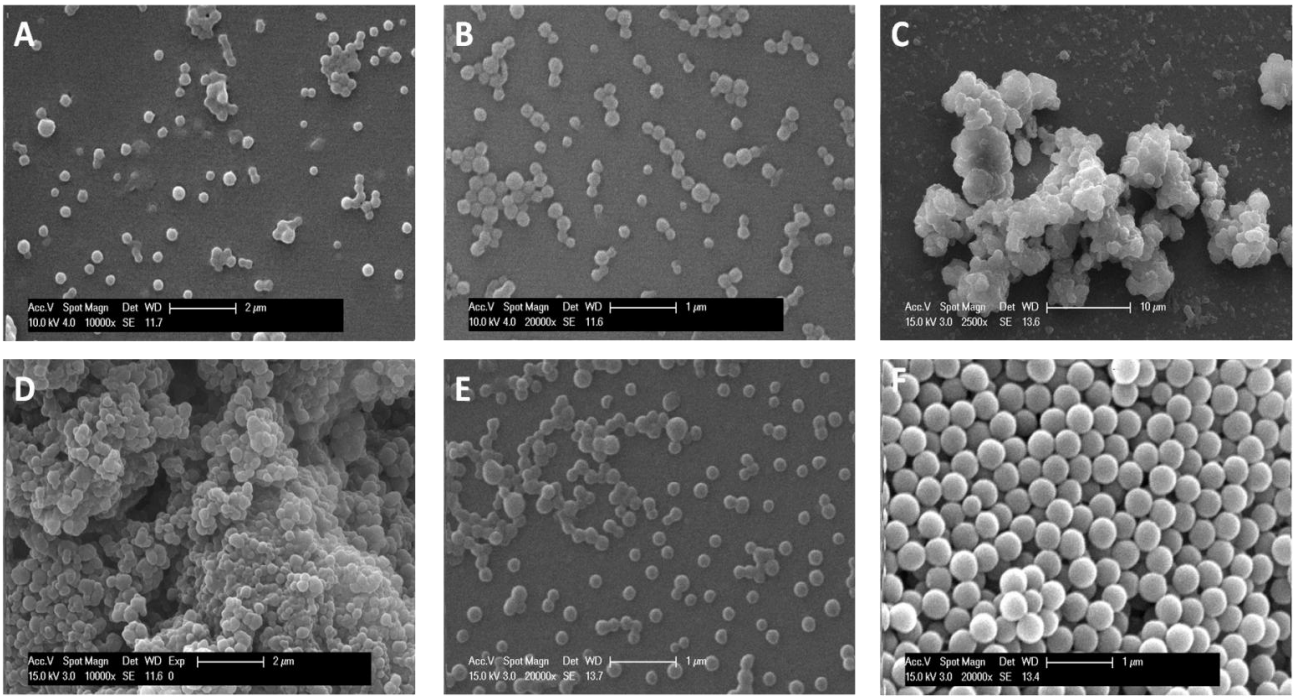


Figure 2: SEM images of collected poly(HEMA) networks after dispersion polymerisation in $scCO_2$ carried out at A) 40°C/385 bar; B) 40°C/300 bar; C) 40°C/300 bar, with 5% $w_{stabiliser}/v_{monomer}$; D) 35°C/300 bar with PEO_{22}-*b*-$PFDA_{38}$ stabiliser, E) 35°C/300 bar with PEO_{45}-*b*-$PFDA_{37}$;, F) 35°C/300 bar with PEO_{113}-*b*-$PFDA_{38}$ stabiliser; for all the polymerisations stirring rate was kept constant at 400 rpm and same feed ratios for monomer (HEMA, 8.2 ml), cross-linker (EGDMA, 82µl), initiator (V-70, 0.187g), and PEO_{45}-*b*-$PFDA_{37}$ stabiliser (0.82g) were used unless otherwise it is noted (For details see experimental section and Table 5).

For that purpose, the AIBN free radical initiator was replaced by 2,2'-Azobis(4-methoxy-2,4-dimethylvaleronitrile) (V-70) that exhibits a lower dissociation temperature and performed the HEMA dispersion polymerization in the same conditions as used above, i.e. with the PEO_{45}-*b*-$PFDA_{37}$ stabiliser and at 385 bar.

Initially the pressure was kept constant and the temperature lowered down to 40°C (V-70/40°C/385 bar) (Table 2 entry A and Figure 2-A). In these conditions, particles with a mean diameter of 369 nm and a well-defined spherical morphology have been obtained. Compared to the Figure 1-2, the particle size has increased from 316 to 369 nm. It should be noted that under a constant pressure of 385 bar, the CO_2 density is increased from 864,9 kg/m3 to 949,7 kg/m^3 by decreasing the temperature from 65°C to 40°C [49]. This could modify the solubility of the stabilisers and the surface stabilisation of the growing particles in CO_2 therefore resulting into bigger particles[39].

In order to counter-balance this negative effect on the particles size of increasing the CO_2 density resulting of the temperature decrease, the pressure was then decreased to 300 bar keeping constant the temperature at 40°C (Table 2 Entry B, and Figure 2-B). A significant decrease of the particles size from 316 nm to 209 nm was observed leading to one of the smallest particles ever reported for poly(HEMA) dispersion polymerisation in $scCO_2$. This result is in accordance with the study of Shiho *et al.* [39] probing the effect of pressure on the poly(HEMA) particle size. They observed a similar increase of the particle size from 370 nm to 550 nm by increasing the pressure from 291 bar to 442 bar with PS-*b*-PFOA diblock copolymers as stabiliser. Another example of such effect was also reported by Canelas *et al*. for the synthesis of poly(styrene) particles using a PS-*b*-PDMS stabiliser [50] in which particle size increased 30% from 660 nm to 850 nm when initial pressure changed from 297 to 439

bar. Dispersion polymerisation of acrylonitrile with PS-*b*-PFOA in $scCO_2$ also showed an increase in the particle size by 60% from 270 nm to 430 nm when the pressure increases from 207 to 444 bar. [20] Decreasing further the temperature from 40°C to 35°C at 300 bar (Table 5, entry E) leads to nanoparticles still well below 250 nm as evidenced by Figure 3-E. These results clearly indicate that 35°C and 300 bar are very efficient conditions to obtain monodisperse spherical poly(HEMA) particles with remarkably small sizes.

3.2.3 Effect of the stabiliser concentration

The key-role of the stabiliser has been demonstrated above to obtain well-defined particles which was confirmed by a polymerisation performed in the absence of stabiliser (Figure 1-1) leading to the recovered ill-defined aggregates of coalesced particles. Nevertheless, minimizing the concentration of stabiliser is of interest in order to limit the fluorinated content engaged in the process and present at the nanoparticles surface in the collected particles. In a previous study Ma *et al*.[13] reported on the synthesis of poly(HEMA) particles having a size of 412 nm with a PEO_{45}-*b*-$PFDA_{39}$ stabiliser at a concentration as low as 3.5% w/v with respect to HEMA at 65°C and 370 bar. However they obtained 77.4% yield according to the polymer product they obtained[13].

Table 2: Conditions for the dispersion polymerisations of a HEMA/EGDMA mixture in $scCO_2$.

Image	Stabiliser	Stabiliser (%)	T (°C)	P (bar)	D_n [a] (nm)	C_v [b] (%)
A	PEO_{45}-*b*-$PFDA_{37}$	10	40	385	369	21
B	PEO_{45}-*b*-$PFDA_{37}$	10	40	300	209	19
C	PEO_{45}-*b*-$PFDA_{37}$	5	40	300	Aggregate	
D	PEO_{22}-*b*-$PFDA_{38}$	10	35	300	Aggregate	
E	PEO_{45}-*b*-$PFDA_{37}$	10	35	300	216	14
F	PEO_{113}-*b*-$PFDA_{38}$	10	35	300	400	8

The starting monomer, cross-linker and initiator concentrations were kept constant for all the dispersions as described in the experimental part. a- number average particle diameter determined by measuring the diameter of 100 particles using SEM images; b Coefficient of variance calculated according to the equation: Cv = (σ/Dn)*100.

Therefore, in our mild conditions (at 40°C and 300 bar), we have decreased the stabiliser concentration from 10wt% to 5 wt% (vs. the volume of monomer) for the dispersion polymerisation in order to investigate the impact on the size and the morphology of the nanoparticles.

While well-defined and small spherical nanoparticles were obtained in the case of 10% stabiliser concentration (Figure 2-B), ill-defined aggregates have been obtained at lower stabiliser concentration (Figure 2-C). In our conditions, 5% stabiliser concentration is insufficient to obtain well-defined particles.

With another stabiliser, i.e. PS-*b*-PFOA, Shiho *et al.* investigated the effect of stabiliser concentration on poly(HEMA) particles in $scCO_2$ (at 65°C and P=373±10 bar) in a range of concentration varying from 6-30%. They also evidenced the formation of large aggregate when the dispersion ran at a stabiliser concentration of 6% w/v with respect to HEMA.[39] Therefore, to keep discrete spherical particles as free flowing powders by working in the milder reaction conditions developed here as compared to the previous studies, a minimum stabiliser concentration of 10% w/v is required.

3.2.4 Effect of the stabiliser composition

With the goal to investigate the effect of the length of the CO_2-phobic block of the diblock copolymer, on the particles size and morphology, we have used the three stabilisers having the same PFDA block but different PEO block length of 1000 g/mol (PEO_{22}), 2000 g/mol (PEO_{45}) and 5000 g/mol (PEO_{113}) (Table 2) for the dispersion polymerisations of HEMA/EGDMA at 35°C and 300 bar. In contrast to results obtained with the PEO_{45}-*b*-$PFDA_{37}$ (Figure 2-E), when the PEO_{22}-*b*-$PFDA_{38}$ is used as stabiliser (Table 2, entry D) irregular shaped aggregates together with only a few amounts (430 mg over approximately 8.2 grams

of polymer) of free-flowing powder could be collected (Figure 2-D). Even if the solubility in $scCO_2$ is quite similar for these two stabilisers (Table 2-Cloud points), a significant impact of reducing the CO_2-phobic block length is observed on the poly(HEMA) stabilisation efficiency. When the block is not long enough, the stabiliser lacks efficiency. In case of the PEO_{113}-*b*-$PFDA_{38}$ (Table 2, Entry F) highly monodisperse well-defined nanoparticles are obtained (Figure 2-F) which are however larger (diameter 400 nm) as compared to PEO_{45}-*b*-$PFDA_{37}$. These results highlight the significant role of the CO_2-phobic block when designing an efficient stabiliser for $scCO_2$. In our study, a block length of 2000g/mol for PEO appears as optimal to get poly(HEMA) networks with a size close to 200nm.

4. Conclusions

The synthesis of poly(HEMA) nanoparticles was successfully performed in $scCO_2$ by using amphiphilic diblock copolymers based on PEO and PFDA. Discrete spherical poly(HEMA) networks were obtained with the lowest size of 209 nm. To the best of our knowledge, herein the mildest synthesis conditions were reported for the synthesis of the poly(HEMA) particles in $scCO_2$ which leads to monodisperse particles having size of 216 nm. The size of the particles can be controlled by the temperature, pressure and the composition of the amphiphilic block copolymer. We believe that this will pave the way for incorporation of temperature and solvent sensitive therapeutic agents. Thus, they can be introduced to the reaction mixture from the beginning for in-situ encapsulation. One-pot synthesis of loaded particles will be the highlight of the next chapters.

References

1 R. Chouhan and A. K. Bajpai, *J. Mater. Sci. Mater. Med.*, 2009, **20**, 1103–1114.

2 Y. Malam, M. Loizidou and A. M. Seifalian, *Trends Pharmacol. Sci.*, 2009, **30**, 592–599.

3 M. L. Tan, P. F. M. Choong and C. R. Dass, *Peptides*, 2010, **31**, 184–193.

4 S. Mura, J. Nicolas and P. Couvreur, *Nat. Mater.*, 2013, **12**, 991–1003.

5 Z. Gu, A. Biswas, M. Zhao and Y. Tang, *Chem. Soc. Rev.*, 2011, **40**, 3638–55.

6 M. J. Whitaker, J. Hao, O. R. Davies, G. Serhatkulu, S. Stolnik-Trenkic, S. M. Howdle and K. M. Shakesheff, in *Journal of Controlled Release*, 2005, vol. 101, pp. 85–92.

7 D. M. Cook, B. M. K. Biller, M. L. Vance, A. R. Hoffman, L. S. Phillips, K. M. Ford, D. P. Benziger, A. Illeperuma, S. L. Blethen, K. M. Attie, L. N. Dao, J. D. Reimann and P. J. Fielder, *J. Clin. Endocrinol. Metab.*, 2002, **87**, 4508–4514.

8 W. S. Choi, K. G. G. Murthy, D. A. Edwards, R. Langer and Al. M. Klibanov, *Proc. Natl. Acad. Sci. U. S. A.*, 2001, **98**, 11103–11107.

9 S. P. Cape, J. A. Villa, E. T. S. Huang, T. Yang, J. F. Carpenter and R. E. Sievers, *Pharm. Res.*, 2008, **25**, 1967–1990.

10 J. L. Kendall, D. a. Canelas, J. L. Young and J. M. DeSimone, *Chem. Rev.*, 1999, **99**, 543–564.

11 A. I. Cooper, *J. Mater. Chem.*, 2000, **10**, 207–234.

12 R. Filmon, F. Grizon, M. F. Baslé and D. Chappaard, *Biomaterials*, 2002, **23**, 3053–9.

13 Z. Ma and P. Lacroix-desmazes, *Polym. J.*, 2004, **45**, 6789–6797.

14 A. J. Cadotte and T. B. Demarse, *J. Neural Eng.*, 2005, **2**, 114–122.

15 S. Abraham, S. Brahim, K. Ishihara and A. Guiseppi-Elie, *Biomaterials*, 2005, **26**, 4767–4778.

16 H. S. Ganapathy, H. S. Hwang, M. Y. Lee, Y. T. Jeong, Y. S. Gal and K. T. Lim, *J. Mater. Sci.*, 2008, **43**, 2300–2306.

17 S.-D. Yeo and E. Kiran, *J. Supercrit. Fluids*, 2005, **34**, 287–308.

18 J. M. DeSimone, *Science*, 2002, **297**, 799–803.

19 C. Lepilleur and E. J. Beckman, *Macromolecules*, 1997, **30**, 745–756.

20 H. Shiho and J. M. DeSimone, *Macromolecules*, 2000, **33**, 1565–1569.

21 P. Christian, M. R. Giles, R. M. T. Griffiths, D. J. Irvine, R. C. Major and S. M. Howdle, *Macromolecules*, 2000, 9222–9227.

22 N. Baran, S. Deniz, M. Akgün, I. N. Uzun and S. Dinçer, *Eur. Polym. J.*, 2005, **41**, 1159–1167.

23 H. Yuvaraj, H. S. Hwang, M. H. Woo, E. J. Park, H. S. Ganapathy, Y. S. Gal and K. T. Lim, *J. Supercrit. Fluids*, 2007, **42**, 359–365.

24 M. R. Giles, R. M. T. Griffiths, A. Aguiar-Ricardo, M. M. C. G. Silva and S. M. Howdle,

Macromolecules, 2001, **34**, 20–25.

25 T. Carson, J. Lizotte and J. M. Desimone, *Macromolecules*, 2000, **33**, 15–18.

26 A. Galia, A. Giaconia, V. Iaia and G. Filardo, *J. Polym. Sci. Part A Polym. Chem.*, 2004, **42**, 173–185.

27 K. S. Oh, W. Bae and H. Kim, *Eur. Polym. J.*, 2008, **44**, 415–425.

28 H. Lee, E. Terry, M. Zong, N. Arrowsmith, S. Perrier, K. J. Thurecht and S. M. Howdle, *J. Am. Chem. Soc.*, 2008, **130**, 12242–3.

29 E. J. Park, A. P. Richez, N. a. Birkin, H. Lee, N. Arrowsmith, K. J. Thurecht and S. M. Howdle, *Polymer (Guildf).*, 2011, **52**, 5403–5409.

30 N. A. Birkin, N. J. Arrowsmith, E. J. Park, A. P. Richez and S. M. Howdle, *Polym. Chem.*, 2011, **2**, 1293.

31 R. Arshady, *Colloid Polym. Sci.*, 1992, **270**, 717–732.

32 S. Slomkowski, J. V. Alemán, R. G. Gilbert, M. Hess, K. Horie, R. G. Jones, P. Kubisa, I. Meisel, W. Mormann, S. Penczek and R. F. T. Stepto, *Pure Appl. Chem.*, 2011, **83**, 2229–2259.

33 Abe, A, A.-C. Albertsson, K. D. W. H. De Jeu, H. K. S. Kobayashi, K. L. L. Leibler, T. E. L. I. Manners, M. M. E. M. Terentjev, M. V. B. Voit and G. W. U. Wiesner, *Advances in Polymer Science Editorial Board :*, 2009.

34 C. Boyère, C. Jérôme and A. Debuigne, *Eur. Polym. J.*, 2014, **61**, 45–63.

35 T. D. McAllister, L. D. Farrand and S. M. Howdle, *Macromol. Chem. Phys.*, 2016, 1–8.

36 T. Imae, *Curr. Opin. Colloid Interface Sci.*, 2003, **8**, 307–314.

37 S. C. Sharma, D. P. Acharya, M. García-Roman, Y. Itami and H. Kunieda, *Colloids Surfaces A Physicochem. Eng. Asp.*, 2006, **280**, 140–145.

38 H. Shiho and J. M. DeSimone, *Macromolecules*, 2001, **34**, 1198–1203.

39 H. Shiho and J. M. DeSimone, *J. Polym. Sci., Part A Polym. Chem.*, 2000, **38**, 3783–3790.

40 W. Wang, D. J. Irvine and S. P. Armes, *Polymer (Guildf).*, 2003.

41 H. M. Woods, C. Nouvel, P. Licence, D. J. Irvine and S. M. Howdle, *Macromolecules*, 2005, 3271–3282.

42 M. Zong, K. J. Thurecht and S. M. Howdle, *Chem. Commun.*, 2008, 5942–5944.

43 Z. Wang, Y. Jun, Q. Dong, T. Liu and C. Pu, *Polymer (Guildf).*, 2006, **47**, 7670–7679.

44 T. Berger, B. McGhee, U. Scherf and W. Steffen, *Macromolecules*, 2000, **33**, 3505–3507.

45 D. Alaimo, A. Beigbeder, P. Dubois, G. Broze, C. Jérôme and B. Grignard, *Polym. Chem.*, 2014, **5**, 5273.

46 B. Tan, H. M. Woods, P. Licence, S. M. Howdle and A. I. Cooper, *Macromolecules*, 2005, **38**, 1691–1698.

47 P. Licence, M. P. Dellar, R. G. M. Wilson, P. A. Fields, D. Litchfield, H. M. Woods, M. Poliakoff and S. M. Howdle, *Rev. Sci. Instrum.*, 2004, **75**, 3233–3236.

48 D. Alaimo, *Green Strategies Applied to the Synthesis of Polymer Particles for Protein Delivery*, 2015.

49 M. McHugh and V. Krukonis, *Supercrit. Fluid Extr. - Princ. Pract.*, 1994, 99–134.

50 D. A. Canelas and J. M. DeSimone, *Macromolecules*, 1997, **30**, 5673–5682.

Chapter 3

Sulindac encapsulation and release from functional poly(HEMA) microparticles prepared in supercritical carbon dioxide

Rahmet Parilti[a,b], Raphael Riva[a], Yasmine Adriaensen[c], Christine Dupont-Gillain[c], Steven M. Howdle[b], Christine Jerome[a], International Journal of Pharmaceutics, 2017, to be submitted

Abstract

Sulindac loaded poly(HEMA) cross-linked microparticles were synthesized *via* one-pot free-radical dispersion polymerisation in supercritical carbon dioxide ($scCO_2$) in presence of photocleavable diblock stabilisers based on polyethylene oxide (PEO) and poly(heptadecafluorodecyl acrylate) (PFDA) bearing a o-nitrobenzyl photosensitive junction (*hv*) (PEO-*hv*-PFDA) and ethylene glycol dimethacrylate (EGDMA) as cross-linker. Poly(HEMA) cross-linked microparticles either empty or Sulindac loaded were obtained with well-defined spherical morphology with the sizes between 250-350 nm. Additionally, upon UV-photolysis the stabiliser on the surface was cleaved which permits to microparticles to be redispersed in water leading to water swollen microgels about 2.1-3.6 µm. Moreover, the release behaviour from obtained microgels were shown that the sustained release of Sulindac over a period of 8 days. Besides, the surface modification after UV-photolysis was studied and proved that the particles can be functionalised with further chemistries.

1. Introduction

There has been a tremendous growth in the field of designing controlled delivery systems based on polymer carriers, one of them being hydrogel formulations based on (sub)microparticles referred also as micro- or nanogels. These systems combine the characteristics of both hydrogels and particles being a 3D network able to swell in water/ biological fluids and at the same time having a small size and large surface area [1]. Unique features of these networks made them promising candidates to be used in biomedical fields such as tissue engineering, regenerative medicine, diagnostics and many more.[2]

These hydrogel particles can be easily prepared using heterogeneous free radical polymerisation techniques such as dispersion, inverse mini or micro emulsion by introducing a suitable difunctional monomer as cross-linker to the reaction mixture [3]. In dispersion polymerisation by using a proper stabiliser the formed polymers can be dispersed in the continuous phase resulting into spherical particles with sizes ranging between 100 nm to 10 µm with narrow size-distribution [4]. In recent years, an increasing interest was devoted to the use of supercritical carbon dioxide, i.e. a non-toxic and environmental friendly solvent as medium for heterogeneous processes to produce particles [5]. Supercritical carbon dioxide ($scCO_2$) is a non-toxic, non-flammable, inexpensive and environmentally benign solvent with easily achievable critical point, i.e. T_c=31.1°C and P_c=73.8 bar. The aforementioned moderate critical points of CO_2 allow processing conditions compatible with thermo-sensitive drugs. It is also an inert medium which prevents oxidation [6]. Moreover, upon depressurisation, CO_2 goes to gaseous state which offers dry condition at low temperature enabling to handle water, solvent and heat labile substances [7]. Moreover, since the CO_2 can be removed from the media easily, energy consuming solvent removal stage is avoided

which allows us to produce dry powder formulations [8]. Therefore, $scCO_2$ has taken great attention in pharmaceutical applications as a solvent or anti-solvent to either extract or process bioactive agents, most importantly a medium for producing drug loaded polymer particles with enhanced bioavailability [9].

Non-steroidal anti- inflammatory drugs (NSAID)s are frequently used for the treatment of acute and chronic inflammation and related pain. Therefore, they are prescribed in large quantities worldwide for the patients and their use is expected to rise in the future [10]. For instance, aspirin, ibuprofen, diclofenac are some of the well-known and mostly used examples of NSAIDs. NSAIDs can be classified into different groups with respect to their chemical structure and Sulindac falls into the indoleacetic acid group along with indometacin, tolmetin and ketorolac. We are specifically interested in Sulindac since it was reported to have promising anti-proliferative activity towards different cancer types both *in vitro and in vivo*. For instance Sulindac was tested in cell lines of acute myeloid leukemia (AML) and primary cells from bone marrow of the patients [11]. Moreover, it is also found to relieve the pain from arthritis such as osteoarthritis and rheumatoid [12].

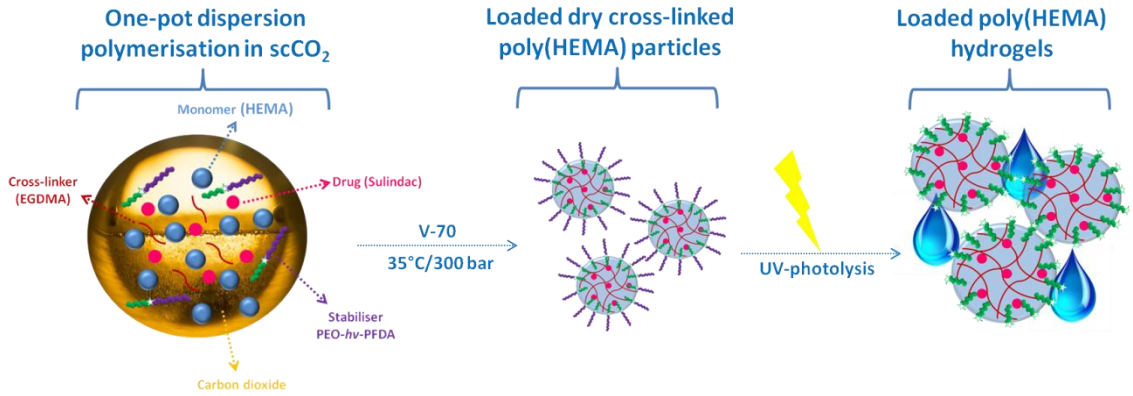
Even though in general NSAIDs are taken orally, they are either practically insoluble or sparingly soluble in aqueous environment; they have low bioavailability and show poor stability which results in storage problems. Also in long-term, they cause gastrointestinal side effects. Therefore to overcome these problems, studies are focused on encapsulation of the NSAIDs into polymeric carriers [13]. Ammar et. al have prepared chitosan and carboxymethyl-β-cyclodextrin (CM-β-CD) cross-linked nanoparticles for the encapsulation of Sulindac.[14] Carmona-Moran *et al.* have encapsulated diclofenac (NSAID) in poly(N-vinylcaprolactam)-co-acrylic acid core-shell nanogels and embedded in the solid hydrogel

matrix for transdermal applications.[15] Choudhary *et al.* encapsulated Sulindac in hydrophobically modified alginate gels. However, in the preparation of these nanogels, extensive purification time (i.e 4 weeks) is required before loading the drug by impregnation or diffusion.[16] In addition to these hydrogels, poly(2-hydroxyethyl methacrylate) (poly(HEMA)) was also investigated previously by Andrade-Vivero *et al.* to be used for the delivery of diclofenac and ibuprofen (NSAID)s.[17]

2-hydroxyethyl methacrylate is a hydrophilic monomer and its homo- or copolymers find well-established biomedical applications [18–20]. The poly(HEMA) hydrogels are widely used to deliver drugs from drug-eluting implants [21,22] in reconstructive materials in dental applications [23], in ocular treatment [24] and also to deliver proteins [25].

The aim of the present paper is to produce well-defined and submicronic poly(HEMA) particles encapsulating Sulindac by dispersion polymerisation in supercritical carbon dioxide. As already reported by Ma *et al.* [26] polyethylene oxide (PEO) block poly(heptadecafluorodecyl acrylate) (PFDA) (PEO-*b*-PFDA) diblock copolymers are efficient stabilisers for the poly(HEMA) particles in supercritical carbon dioxide. In addition, some of us have also reported mild conditions, especially low temperature (35°C) for HEMA dispersion polymerisation in $scCO_2$ giving well-defined and small sized particles (216 nm) [27] (Scheme 1, step 1). In addition, Alaimo et al. have shown that the use of a photocleavable junction between the polyethylene oxide (PEO) and poly(heptadecafluorodecyl acrylate) (PFDA) blocks of the stabiliser (PEO-hv-PFDA) allows to remove the fluorinated block after the particles synthesis and as a consequence allows the poly(HEMA) particles to swell in water (Scheme 1, step 2).[28]

In the present paper, we have studied further such process targeting the one-pot encapsulation of Sulindac, by adding the drug from the beginning of the process. Therefore, the effect of the presence of the drug on the particle size and overall particles properties has been evaluated. The drug encapsulation and release profile in aqueous media are also reported here.



Scheme 1: Synthetic approach to obtain Sulindac loaded poly(HEMA) hydrogels in supercritical carbon dioxide($scCO_2$) using photocleavable stabilisers.

2. Experimental Part

2.1 Materials

All chemicals are purchased from Sigma-Aldrich and used as received unless otherwise it is noted. Sulindac (≥98.0%), fluoresceinamine, isomer I, sodium cyanoborohydride (1.0 M in THF), 2,2'-Azobis(4-methoxy-2,4-dimethylvaleronitrile) (V-70,Wako), 2-hydroxyethyl methacrylate (HEMA, Aldrich, 97%), ethylene glycol dimethacrylate (EGDMA, Aldrich, 98%,), carbon dioxide (I5122,CO2 N27 purity > 99,999%, Air Liquide, Belgium). α,α,α - Trifluorotoluene (TFT, Aldrich, 99+%),. Ultrapure water was produced by MilliQ plus 188 apparatus (Millipore). SpectraPor membrane (cut-off 3.5 kDa and 1kDa). PEO_{45}-hv-$PFDA_{50}$

diblock copolymer bearing a photocleavable junction was synthesized according to previously published procedure.[28]

2.2 Methods

2.2.1 Synthesis of the Sulindac encapsulated poly(HEMA) networks in $scCO_2$

Dispersion polymerisations of 2-hydroxyethyl methacrylate were performed as previously described by Parilti *et al*.[27] The procedure can be described as follows: the high pressure stainless steel cell (82 ml, ToP Industrie) was charged with 8.2 ml of HEMA (10% v/v CO_2), 400 µl of EGDMA (cross-linker, 5% v/v monomer), 0.82 g of stabiliser, 0.187 g V-70 (1% w/v monomer) and 8.79 mg/ 87.9 mg Sulindac (0.1% or 1% with respect to w_{HEMA}). The cell was securely sealed and a small amount of CO_2 was introduced using a syringe pump (ISCO model no. 260D). After the heating mantel was clamped, the stirring rate (400 rpm) and temperature (35°C) were set with the control unit. Temperature and pressure were increased step-wise, the reactor was stabilised at the desired conditions (35°C/300 bar) and the reaction was left for stirring overnight. At the end of the reaction, stirring was stopped and the heating jacket removed allowing the reactor to cool down to ambient temperature. Thereafter, the reactor is depressurized gradually by opening an outlet valve. After total depressurization, the cell was opened and the product was collected as a dry powder. Obtained products were stored in the ambient temperature in a plastic container.

2.2.2 UV photolysis of the particles

The particles were dispersed in TFT with the concentration of 10 mg/ml. The solution was sonicated using horn sonicator for about 3 minutes resulting a milky dispersion. Thereafter solution was subjected to UV under vigorous stirring (700 rpm) using UV lamp (LOT-Oriel Arc Light Source Hg(Xe), power = 500 W, with multichromatic emission showing the

characteristic emission at 300-310 nm for the photocleavage of o-nitrobenzyl groups. The UV exposure times were varied from 30 minutes to 60 minutes.

2.2.3 Release behavior

After fluorine extraction the particles were dispersed with known concentration in water placed into dialysis membranes with a cut off of 1 kDa (SpectraPor membrane). The membrane was placed in a beaker filled with deionized water and left for stirring. Samples were taken from external medium of the membrane in different time intervals, and the water in the beaker was replaced with same volume of fresh water. The membrane was left for stirring for the next measurement. This step was iterated for several days. The withdrawals were measured with UV-vis spectrometer (Shimadzu UV-1800). In order to calculate the amount of released Sulindac the absorbances were taken at 286 nm which then converted to mass (μg) using a calibration curve that was measured previously.

2.2.4 Grafting of Fluoresceinamine on the particles *via* reductive amination

Grafting of the fluoresceinamine was performed according to previously published conditions [29]. The procedure is described as follows. The UV-cleaved particles (100 mg, 1 equivalent of aldehyde groups) were suspended in 50 ml of phosphate buffer solution (500mM, pH: 7.4) and 2 equivalents of fluoresceinamine isomer 1 were added. After 1 hour of stirring, a 10-fold excess sodium cyanaborohydride solution (1.0 M in THF) was added. The mixture was left for stirring for 96 hours and then dialyzed against water for 3 days by changing water for 4 times per day. Particles were recovered by rotary evaporator and freeze-drying.

2.3 Characterisations

All the particles were analyzed with scanning electron microscopy (SEM, JEOL JSM 840-A) to evaluate their morphology. Samples were prepared on SEM stubs and coated with Pt (30 nm). Particles average sizes were calculated from SEM images by random sampling with the aid of VistaMetrix software (version 1.33.0). Coefficient of variance (C_v) is an indicator of size distribution of the particles. It is calculated from the standard deviation (σ) divided by the average diameter size (D_n) that is calculated from the SEM images ($C_v = (\sigma/D_n)*100$) (Eq.1). Transmission electron microscopy (TEM, PHILIPS M100) operating at an accelerating voltage of 100 kV was used to further evaluate the particles size. TEM samples were prepared by placing a drop of diluted dispersion of particles on a TEM grid and left for air drying. The size distribution of particles in suspension in diluted TFT (before UV) and in water (after UV) were estimated by dynamic light scattering (DLS) using a Delsa Nano C Beckman Coulter at 25°C. The intensity of scattered light was detected at 165° to the incident beam and data treated by the cumulant analysis. X-ray photoelectron Spectroscopy (XPS) analyses were performed on a SSX 100/206 spectrometer (Surface Science Instruments - USA) equipped with a monochromatized micro-focused aluminum X-ray source (powered at 20 mA and 10 kV). A flood gun set at 6 eV and a Ni grid placed 3 mm above the sample surface were used for charge stabilisation. The angle between the surface normal and the axis of the analyser lens was 55°; in these conditions, the probed depth was of the order of 5 nm. The molar fractions were calculated from the peak areas normalized on the basis of the acquisition parameters and sensitivity factors provided by the manufacturer. The calculations exclude hydrogen which is not detected by XPS. Carbon and fluorine spectra recorded second time after the analysis in order to validate that the sample was not degraded by X-ray source. The data analysis was performed with the CasaXPS program (Casa Softwares, Teignmouth, UK).

3. Results and discussions

3.1 One-pot sulindac encapsulation by *in-situ* dispersion polymerisation of HEMA

The one-pot encapsulation of Sulindac into cross-linked poly(HEMA) particles has been first studied by following a previously reported supercritical CO_2 process. Indeed, mild reaction conditions (35°C and 300 bar) were reported previously [27] to synthesize well-defined poly(HEMA) particles by dispersion polymerisation in $scCO_2$. Following such process, the monomer, HEMA (10% v/v CO_2), the cross-linker, EGDMA (5% v/v monomer), the photocleavable stabiliser, PEO_{45}-hν-$PFDA_{50}$ (0.82 g) and the initiator, V-70 (1% w/v monomer) were introduced in the high-pressure cell, together with the Sulindac in order to perform its one-pot encapsulation. Two different concentrations of Sulindac 0.1% and 1% with respect to monomer (%,$w_{sulindac}/w_{HEMA}$) have been tested. The overall characteristics of obtained particles in presence of Sulindac are reported in Table 1 and the corresponding SEM and TEM images are reported in Figure 1. They are compared to empty particles prepared in the same conditions but in absence of sulindac (Table 1, Entry 1; Figures 1, 1a and 1b).

Table 1: poly(HEMA) particles characteristics as collected after $scCO_2$ dispersion polymerisation

Entry	Sulindac (%,$w_{sulindac}/w_{HEMA}$)	Encapsulation Efficiency (%)	SEM (nm)	C_v	DLS (nm)
1	0	-----	348	8	256 [a]
2	0.1	81.7	561	6	328[a]
3	1	98.2	336	9	280[a]

a: Measurement taken in trifluorotoluene (TFT).

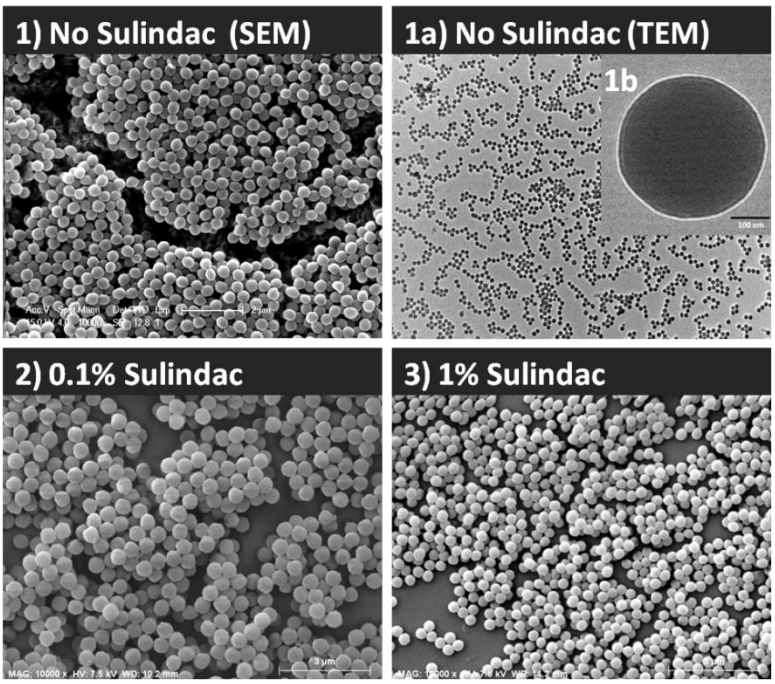


Figure 1: SEM image of the poly(HEMA) particles 1) without Sulindac , 2) with 0.1% Sulindac and 3) with 1% Sulindac; and (1a and 1b) TEM image without Sulindac.

As evidenced by the SEM image of figure 1.1, the empty cross-linked poly(HEMA) particles exhibit a highly uniform spherical shape of small sizes, 348 nm. This was confirmed by TEM image (Figure 1-1a and 1b) giving a size of 230 nm. For TEM measurement particles were suspended in tetrahydrofuran (THF) and a drop was placed on the TEM grid whereas for SEM TFT a good solvent for the stabiliser on the surface was employed. Therefore, difference between SEM size (348 nm) and TEM (230) is resulted from the solvent. As shown on figures 1.2 and 1.3, the addition of sulindac to the reaction medium does not affect the particles formation, shape and dispersity. Table 1 also shows that the particles size, measured by SEM or DLS, is not significantly modified by the presence of 1% of sulindac. Only the particles prepared in presence of 0.1% Sulindac are slightly bigger.

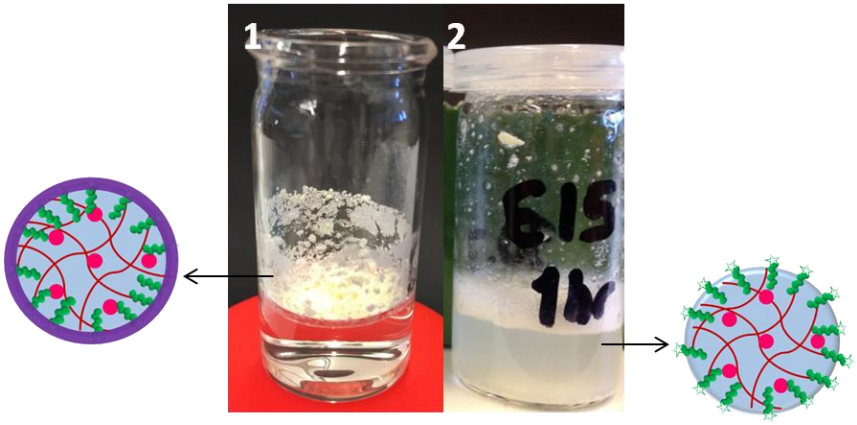
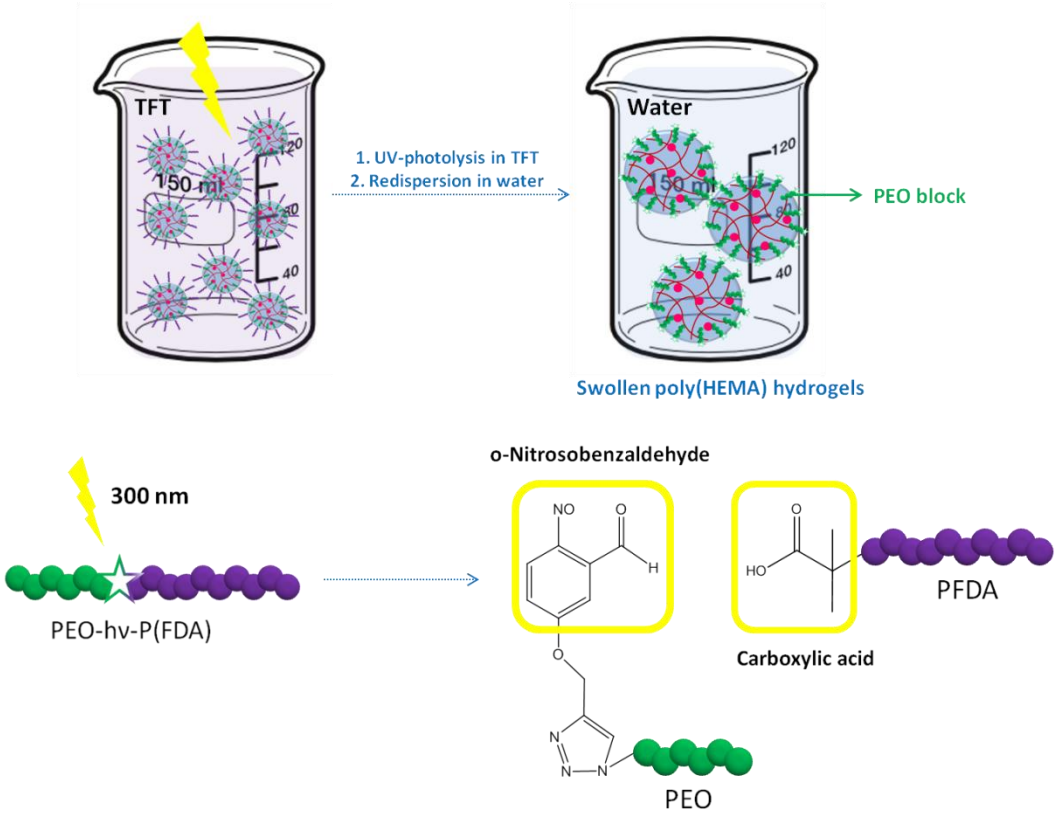


Figure 2: Sulindac loaded poly(HEMA) networks dispersed in water before UV (1), dispersed in water after UV (2).

The dry particles collected after depressurization of the reactor are expected to be composed of a poly(HEMA) network loaded by the sulindac and coated at their surface by the stabiliser as schematized in figure 2. Therefore, these particles cannot be directly dispersed in water due to the hydrophobic PFDA fluorinated block of the stabiliser forming the external corona (Figure 2.1). Therefore, the fluorinated block of the stabiliser was removed thanks to the photocleavable link placed at the junction of both blocks.

For this end, Sulindac encapsulated particles were subjected to UV-photolysis (Scheme 2 in TFT, i.e. a good solvent for the fluorinated block which do not swell the poly(HEMA) network. After 30 minutes or 60 minutes, the irradiation was stopped and the samples were washed with fresh TFT to remove the cleaved fluorinated block and dried under vacuum. As it is evidenced from the SEM images (Figure 3) despite the aggregation of the particles, their shape was preserved after UV and extraction of the fluorinated block (Figure 2-step 1).



Scheme 2: UV-photolysis of the obtained poly(HEMA) particles were performed in TFT. Photocleavage of the stabiliser leads to formation of the o-nitrosobenzaldehyde groups on the particle surface and subsequently fluorinated block is extracted. The photoisomerisation of the stabiliser results in the cleavage of the PEO-*hv*-PFDA stabiliser into first block (PEO) bearing nitrosobenzaldehyde group and carboxylic acid group at the end of second block (PFDA).

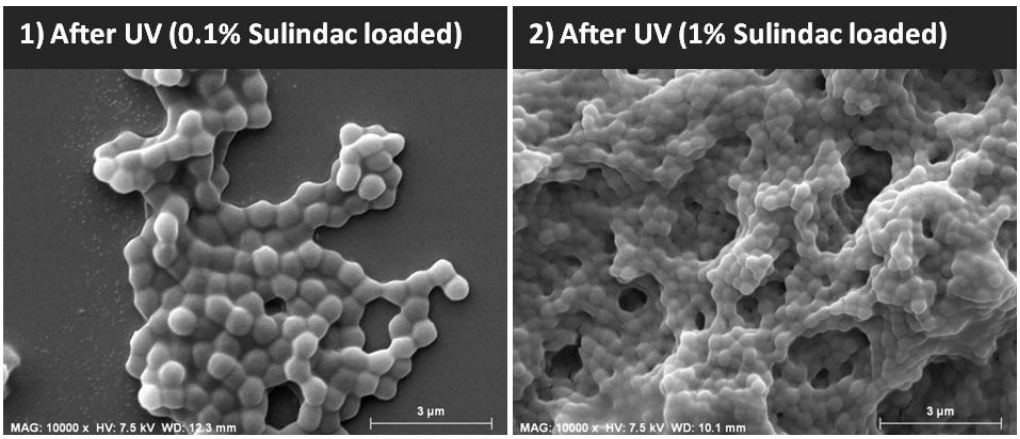


Figure 3: SEM images of the sulindac (0.1% and 1% loaded poly(HEMA) particles after 1 hour UV-photolysis .

For each sample, the efficiency of removal of the fluorinated layer from the particles was determined by X-ray photoelectron spectroscopy (XPS) by comparing the evolution of the total F/C ratios of the particles before and after photolysis of different durations (Table 2).

Table 2: XPS and DLS analyses of Sulindac loaded poly(HEMA) particles for various times of UV-irradiation.

Entry	Sulindac (%,$w_{sulindac}/w_{HEMA}$)	UV-Time (mins)	F/C (tot) (XPS)	Fluorine Extraction (%)	Particle Size (DLS)[a,b]
1	0.1	0	0.89	-----	328nm[a]
2	1	0	0.73	-----	280nm[a]
3	0.1	30	0.52	41.5	2.1 µm[b]
4	0.1	60	0.47	47.1	2.6 µm[b]
5	1	30	0.44	36.7	2.7 µm[b]
6	1	60	0.35	52.0	3.6 µm[b]

a: in trifluorotoluene (TFT) b: in water.

Table 2 clearly evidences that the fluorine content of the particles decreases for increasing UV-irradiation times. In previous work, Alaimo et al.[28] reported on the kinetics of particles photolysis using 0.1 mg particle/ml of TFT (LOT-Oriel UV-lamp was used) and fluorine extraction in TFT. According to the reported results, after 30 minutes of irradiation 72% of fluorine could be extracted.The kinetics of photocleavage reached to a pleateau after 30 minutes and maximum extraction was reached after 6 hours (79% fluorine extraction).

In our case, the photocleavage time was set to relatively short times (30 minutes and 60 minutes) in order to prevent degradation of guest molecules. Moreoever, the concentration of the particle dispersions for photocleavage was increased to 10 mg/ml, to lower the TFT amount. Therefore, direct comparison between these studies cannot be drawn but they are roughly giving similar fluorine extraction efficiency.

In this case, one hour of irradiation leads to the removal of half of the PFDA block from the particles surface. After this treatment, the resulting particles become dispersable in water (Figure 2- 2) and are able to swell thanks to the strong hydrophilicity of poly(HEMA)

(Scheme 2 – step 2). This water swelling was clearly evidenced by DLS. In water, there is a significant increase of the particle size of at least one order of magnitude in each case. This shows that even if some fluorinated chains remain at the particles surface, the cross-linked poly(HEMA) are remarkably able to swell in water (36% of extracted fluorine leads already to a size increase from 271 nm to 2.7 µm). This shows the relatively low impact of the remaining fluorine chains on the particles swelling in water more importantly it does not prevent their water dispersion.

3.2 Determination of the encapsulation efficiency and release behaviour of hydrogel

The encapsulation efficiency of sulindac in the poly(HEMA) particles obtained by the one-pot process of dispersion polymerisation in $scCO_2$ has been first determined before studying the release profile. For this purpose, the dry particles collected from the high-pressure reactor were suspended in water under vigorous stirring to insure their contact with water despite the fluorinated corona. By this way, only the sulindac which is adsorbed at the particles surface or that remains non-encapsulated in the particles would be able to dissolve in water.

The particles before UV treatment were dispersed in water with roughly similar final Sulindac concentrations (1.8 µg Sulindac/ml for 0.1% loaded particles; 1.66 µg Sulindac /ml for 1% loaded particles). The suspensions were mixed under vigorous stirring (app. 750 rpm) for 1 hour. Thereafter, each solution was filtrated by 0.2 µm filter in order to remove the particles. The UV-vis absorptions (286 nm) of the filtrated aqueous solutions were taken and converted to mass using previously recorded calibration curve.[30]

The encapsulation efficiencies were calculated by applying the following formula (Eq.2):

$$EE=(W_{total\ sulindac}- W_{free\ sulindac})/W_{total\ sulindac}*100 \quad \textbf{(Eq.2)}$$

$W_{total\ sulindac}$ is the amount of Sulindac that presents in the solution. In other words, for 0.1% if we take 18 mg particles the total Sulindac amount would be equal to 18 µg and for 1% loaded particles with 16.6 mg of particles the total Sulindac amount would be equal 166 µg. Based on this equation (Eq.2) and UV-VIS data, the EE were found to be 81.7% for 0.1wt% sulindac (Table 1-Entry 2) and 98.2% for 1wt% starting sulindac content (Table 1-Entry 3).

The barrier effect of the fluorinated corona of the particles towards the diffusion of sulindac to water was then investigated. The particles (15 mg) loaded with 1% sulindac (Table 2-Entry 2, 5,6) before photolysis, after 30 minutes or 1 hour exposure to UV light, have been dispersed in mL water and stirred for 24 hours. The amount of released Sulindac was then determined by UV-vis measurements. Figure 4 clearly shows that the particles before UV treatment limit the release of of Sulindac to 2.4 microgram, i.e. 1.5%).

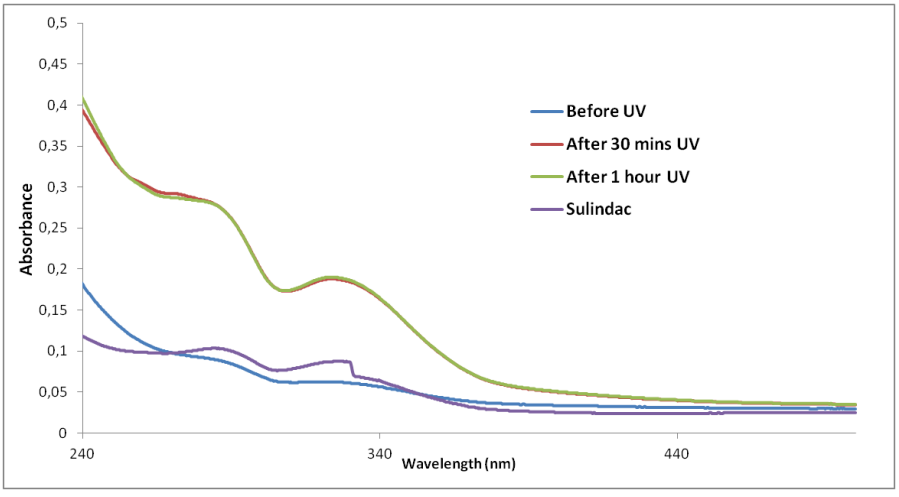


Figure 4: UV-Vis spectra of released Sulindac in water from 1% Sulindac loaded particles (Table 2-Entry 2) Blue: without UV treatment (Table 2-Entry 2); Red: after 30 minutes of UV treatment (Table 2-Entry 5); Green after 1 hour of UV treatment (Table 2- Entry 6); Purple: UV-vis spectrum of a solution of pure Sulindac in water (5µg/ml).

After photolysis and partial removal of the fluorinated corona, the amount of released Sulindac increased to approximately 10 micrograms for both particles subjected to different UV-irradiation times (30 minutes and 1 hour). This shows that the fluorinated corona acts as a barrier towards the Sulindac diffusion however this barrier effect is clearly decreased already after short time of UV irradiation (30 min).

Finally, the release profile of the hydrogels loaded with 1% Sulindac was monitored during one week (Figure 5) for particle after exposure to 1 hour UV for removal of the fluorinated block. The particles were dispersed in water with a known (~ 5 mg/ml) concentration and placed in a membrane with the cut off 1kDa immersed in a beaker filled with 600 ml of deionised water. Samples were withdrawn from the solution outside the membrane in different time intervals after sample removal the membrane was immersed in same amount of fresh deionised water. This procedure was iterated starting from time zero till eight days. The released amount of Sulindac was determined by UV-visible spectrometer following the absorbance of Sulindac at 286 nm.

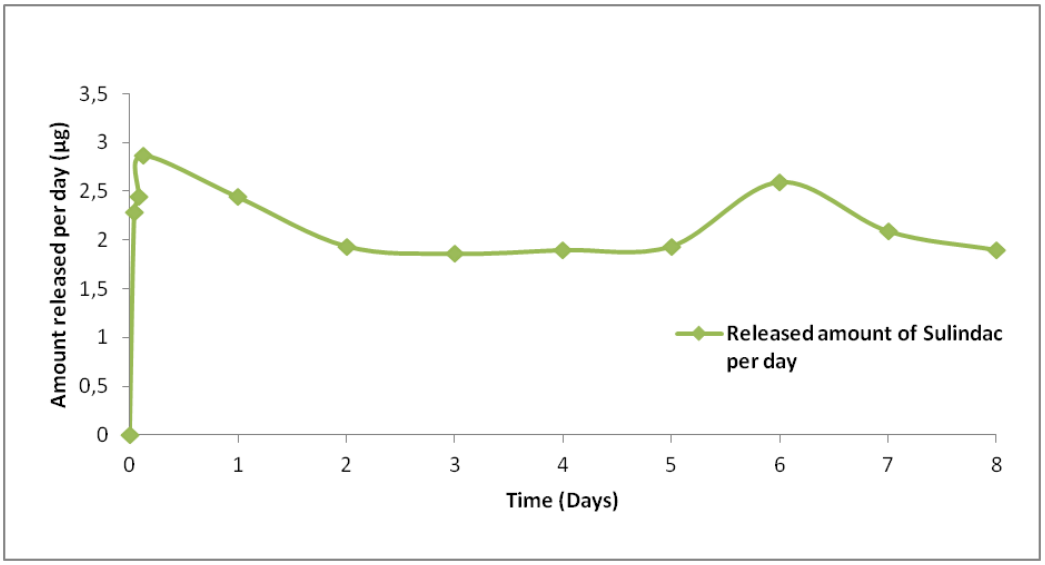


Figure 5: Release profile of Sulindac from the particles having 1% ($w_{sulindac}/w_{HEMA}$) of Sulindac.

Figure 5 shows a Burst effect in the first 24h followed by a controlled release of about 2.0µg per day over the whole period of 8 days. After that period, the total amount of released Sulindac is 24.3µg (Figure 6), i.e. about 17.3 % of the total load (Figure 7).

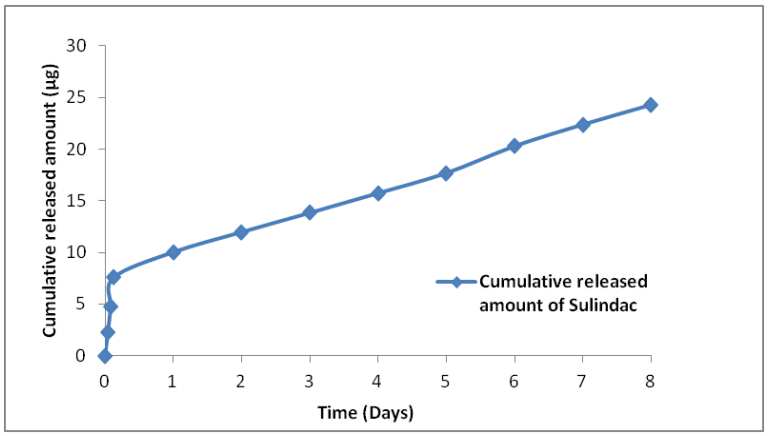


Figure 6: Amount of Sulindac released in total over period of 8 days.

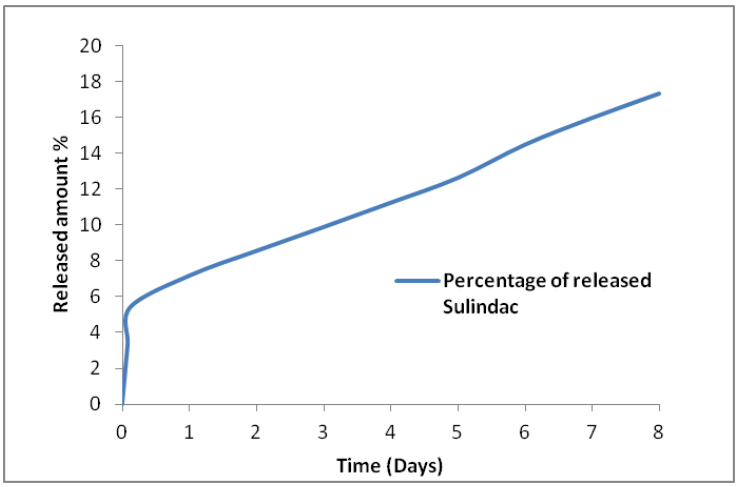


Figure 7: Evolution of the percentage of released amount of Sulindac over a period of 8 days.

3.3 Grafting on the particle surfaces

As discussed above, selecting a stabiliser (PEO-*hv*-PFDA) that exhibit a photocleavable o-nitrobenzyl group at the junction of the blocks of the copolymer allows the removal at least partially of the fluorinated block modifying the release kinetics of Sulindac. Looking closer to

the photoreaction (scheme 2), the light-induced cleavage of o-nitrobenzyl group generates a nitrosobenzaldehyde group at the end of the PEO segment entangled in the poly(HEMA) particles. These aldehyde groups located at the external periphery of the particles could be useful to further functionalisation of the particle surfaces. For instance, different probes for imaging or targeting could be grafted thanks to the aldehyde reactivity.

In the present study, the aldehyde groups have been used for grafting a fluorescent probe, i.e. the fluoresceinamine on the particle surface by using reductive amination. Reported conditions for reductive amination reaction by Freichels *et al.* [29] have been followed as described in details in the experimental part. Extensive washing (i.e 3 days) by dialysis had been carefully performed after grafting. In order to eliminate the excess amount of fluoresceinamine that is not grafted onto the particles

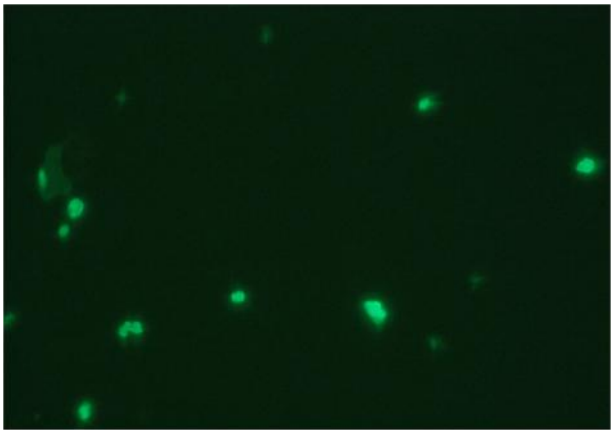


Figure 8: The fluorescence microscopy images of the particles tagged with fluorescent probe.

While before reaction with fluorescein amine, the particles exhibit no fluorescence (not shown), they clearly emit the typical green light of the grafted fluorescein as it can be seen from the fluorescence microscope image (Figure 8). This confirms that the developed process is able not only to provide particles allowing a sustained release of the encapsulated

drug but also that the particles can be tagged with fluorescent probe by taking profit of the reactive groups generated by the photocleavage.

4. Conclusions

One-pot encapsulation of Sulindac in poly(HEMA) networks was successfully performed in supercritical carbon dioxide. The poly(HEMA) networks with or without Sulindac were both produced with monodispersity and well-defined morphology and small size (271nm). The reaction conditions (i.e 35°C) and polymerisation medium ($scCO_2$) leads to sulindac encapsulation with high encapsulation efficiency (98.2%). Moreover, $scCO_2$ can be removed from the reaction media by simple depressurisation which eliminates the reaction work-up step for purification and/or drying and leads after venting to the loaded particles as a dry powder.

In addition, by using a photocleavable stabiliser, part of the fluorinated block can be extracted from the surface allowing the particles to be redispersed and swell in aqueous media. Already after 30min. of UV-photolysis, extensive swelling of the particles is observed when placed in water leading to swollen microgels of about 2.7 µm.

Interestingly, after photocleavage, the generated aldehyde functions on the particle surface enables to perform further chemical functionalization of the particles surface with amine derivatives. As a proof of concept, a fluorescent dye was grafted by using fluoresceinamine leading to particles that can be detected by fluorescence microscope. This reductive amination step performed in aqueous media could be applied to a variety of amino-functional (macro)molecules of use for imaging or targeting. The described process allows thus to produce in few steps, well-defined multifunctional microgels. Thanks to mild

reaction conditions (i.e 35°C) and the non-toxic, inert and environmentally friendly polymerisation medium ($scCO_2$), this process could be extended to heat or solvent-sensitive API and constitute a promising process for advanced formulations.

References

1 M. Hamidi, A. Azadi and P. Rafiei, *Adv. Drug Deliv. Rev.*, 2008, **60**, 1638–49.

2 J.-H. Ryu, R. T. Chacko, S. Jiwpanich, S. Bickerton, R. P. Babu and S. Thayumanavan, *J. Am. Chem. Soc.*, 2010, **132**, 17227–35.

3 R. T. Chacko, J. Ventura, J. Zhuang and S. Thayumanavan, *Adv. Drug Deliv. Rev.*, 2012, **64**, 836–51.

4 L. Cao, L. Chen, X. Chen, L. Zuo and Z. Li, *Polymer (Guildf).*, 2006, **47**, 4588–4595.

5 J. Jennings, M. Beija, J. T. Kennon, H. Willcock, R. K. O. Reilly, S. Rimmer and S. M. Howdle, *Macromolecules*, 2013, **46**, 6843–6851.

6 M. J. Cocero, Á. Martín, F. Mattea and S. Varona, *J. Supercrit. Fluids*, 2009, 47, 546–555.

7 O. R. Davies, A. L. Lewis, M. J. Whitaker, H. Tai, K. M. Shakesheff and S. M. Howdle, *Adv. Drug Deliv. Rev.*, 2008, **60**, 373–387.

8 Y. Miyazaki, N. Aruga, K. Kadota, Y. Tozuka and H. Takeuchi, *Int. J. Pharm.*, 2017, **528**, 118–126.

9 O. Nuchuchua, M. R. Nejadnik, S. C. Goulooze, N. J. Lješković, H. A. Every and W. Jiskoot, *J. Supercrit. Fluids*, 2017, **128**, 244–262.

10 N. S. Gerstein, W. H. Gerstein, M. C. Carey, N. C. K. Lam, H. Ram, N. R. Spassil and P. M. Schulman, *J. Cardiothorac. Vasc. Anesth.*, 2014, **28**, 369–378.

11 R. Singh, R.-P. Cadeddu, J. Fröbel, C. M. Wilk, I. Bruns, L. F. Zerbini, T. Prenzel, S. Hartwig, D. Brünnert, T. Schroeder, S. Lehr, R. Haas and A. Czibere, *Apoptosis*, 2011, **16**, 889–901.

12 J. K. Lee, M. F. Paine and K. L. R. Brouwer, *J. Pharmacol. Exp. Ther.*, 2010, **334**, 410–8.

13 W. Badri, K. Miladi, Q. A. Nazari, H. Greige-Gerges, H. Fessi and A. Elaissari, *Int. J. Pharm.*, 2016, **515**, 757–773.

14 H. O. Ammar, S. A. El-Nahhas, M. M. Ghorab and A. H. Salama, *J. Incl. Phenom. Macrocycl. Chem.*, 2012, **72**, 127–136.

15 C. A. Carmona-Moran, O. Zavgorodnya, A. D. Penman, E. Kharlampieva, S. L. Bridges, R. W. Hergenrother, J. A. Singh and T. M. Wick, *Int. J. Pharm.*, 2016, **509**, 465–476.

16 S. Choudhary, J. M. Reck, A. J. Carr and S. R. Bhatia, *Polym. Adv. Technol.*, 2017, 1–7.

17 P. Andrade-vivero, E. Fernandez-gabriel, C. Alvarez-lorenzo and A. Concheiro, *J. Pharm. Sci.*,

2007, **96**, 802–813.

18 S. Abraham, S. Brahim, K. Ishihara and A. Guiseppi-Elie, *Biomaterials*, 2005, **26**, 4767–4778.

19 A. J. Cadotte and T. B. Demarse, *J. Neural Eng.*, 2005, **2**, 114–122.

20 C. González-Chomón, M. E. M. Braga, H. C. De Sousa, A. Concheiro and C. Alvarez-Lorenzo, *Eur. J. Pharm. Biopharm.*, 2012, **82**, 383–391.

21 T. J. Long, C. C. Sprenger, S. R. Plymate and B. D. Ratner, *Biomaterials*, 2014, **35**, 8164–8174.

22 H. Macková, Z. Plichta, H. Hlídková, O. Sedláček, R. Konefal, Z. Sadakbayeva, M. Dušková-Smrčková, D. Horák and Š. Kubinová, *ACS Appl. Mater. Interfaces*, 2017, **9**, 10544–10553.

23 H. Kitagawa, K. Takeda, R. Kitagawa, N. Izutani, S. Miki, N. Hirose, M. Hayashi and S. Imazato, *Acta Biomater.*, 2014, **10**, 4285–4295.

24 E. Garcia-Millan, S. Koprivnik and F. J. Otero-Espinar, *Int. J. Pharm.*, 2015, **487**, 260–269.

25 E. V. Hackl, V. V. Khutoryanskiy and I. Ermolina, *J. Appl. Polym. Sci.*, 2017, **134**, 1–13.

26 Z. Ma and P. Lacroix-desmazes, *Polym. J.*, 2004, **45**, 6789–6797.

27 R. Parilti, D. Alaimo, B. Grignard, F. Boury, S. M. Howdle and C. Jérôme, *J. Mater. Chem. B*, 2017, **5**, 5806–5815.

28 D. Alaimo, B. Grignard, C. Kuppan, Y. Adriaensen, M. J. Genet, C. Dupont-Gillain, J.-F. Gohy, C.-A. Fustin, C. Detrembleur and C. Jérôme, *Polym. Chem.*, 2017, **8**, 581–591.

29 H. Freichels, D. Alaimo, R. Auzély-Velty and C. Jérôme, *Bioconjug. Chem.*, 2012, **23**, 1740–1752.

30 R. B. Guerra, D. A. Gálico, B. B. C. Holanda and G. Bannach, *J. Therm. Anal. Calorim.*, 2016, **123**, 2523–2530.

Chapter 4

Encapsulation of antimicrobial peptides in poly(HEMA) networks in supercritical carbon dioxide

Rahmet Parilti, Jeremie Caprasse, Raphael Riva, Michael Alexandre, Steve Howdle, Christine Jerome, Colloids and Surfaces B: Biointerfaces, 2017, to be submitted.

Abstract

Antimicrobial peptide (AMP) loaded poly(2-hydroxyethyl methacrylate) (poly(HEMA)) particles were synthesized in supercritical carbon dioxide *via* one-pot free-radical dispersion polymerisation of 2-hydroxyethyl methacrylate (HEMA) and a cross-linker. For that purpose, a CO_2-philic stabiliser, i.e. a diblock copolymer based on polyethylene oxide (PEO) and poly(heptadecafluorodecyl acrylate) (PFDA) and bearing a o-nitrobenzyl photosensitive moiety at the block junction (*hv*) (PEO-*hv*-PFDA) has been designed. By adjusting the molecular weight and the concentration of the stabiliser added to the dispersion polymerisation medium, the size and morphology of the resulting poly(HEMA) particles can be controlled. The stabilizer of shortest length was proved to stabilise the dispersion at the lowest concentration (5wt%). Even in the presence of the AMP in the reaction mixture, discrete particles with a well-defined morphology and a diameter as low as 450 nm have been obtained in one pot. The encapsulation and release of the AMP was confirmed by antimicrobial tests that demonstrated for the first time a sustained release of AMP from poly(HEMA) microgels prepared by one pot dispersion in $scCO_2$.

1. Introduction

Nowadays, an increasing number of therapeutic peptides and proteins are approved by FDA, and many others are being developed at various stages including pre-clinical or clinical trials.[1] Historically, importance of the proteins for human beings was highlighted by the human genome studies; most of genes were found to be responsible for protein encoding.[2] Having said the importance of proteins for human body, it was also revealed that they can be used as therapeutics to treat different kinds of diseases for instance genetic and degenerative disorders, protein malfunction and enzyme deficiencies. When the peptide/protein based drugs are compared to conventional drugs, they can be more active, may exhibit lower toxicity and weaker drug-drug interactions.[3] As an example, protein-based drugs offer momentary actions which make them safer than existing therapies such as gene therapy where random or permanent genetic alterations occurs.[4] Considering all the advantages of proteins, a vast number of studies turned to formulate active pharmaceutical ingredients based on peptides or proteins. However, peptides and proteins exhibit some drawbacks such as a rapid degradation or inactivation, a low bioavailability and a low permeability towards biological membranes.[5] Therefore, researches are focused on the idea of encapsulating them to increase their bioavailability, protect them from harsh environmental conditions and more importantly insure their controlled release over a course of time.[6]

Among the valuable available peptides, one emerging family is the antimicrobial peptides (AMPs) developed to circumvent the global increase of antibiotic resistance and address the major infectious public health problems.[7] Roughly all types of *Staphylococcus aureus* species show resistance towards the conventional antibiotics such as penicillin and methicilin.[8]

Therefore, to find solutions against the resistant bacteria holds a great importance in the research area. Studies focussing on the development of alternative antibiotic agents such as gene-coded antimicrobial peptides (AMPs) are thus numerous.[9] Among them, temporins are short AMPs having up to 14 aminoacids which are derived from amphibians and showed high bactericidal efficiency. This group was named from the frog called *Rana temporaria* from which the AMP was initially extracted. Temporin A (TA) and Temporin L (TL) are active against Gram-positive bacteria, *Candida* species, fungi and with the ability to bind and permeate both artificial and biological membranes. TAs and TLs differ in the range of their antimicrobial activity as well as their toxicity. TLs were found to possess the strongest activity against fungi, Gram-positive and Gram-negative bacteria in comparison to other temporins. However, it was found that TLs were able to bind and permeate the membrane of mammalian cells (erythrocytes and cancer cells).[10] TLs are toxic on human erythrocytes thus necessitate for the synthesis of analogues. The amino acid sequence of the TL and its analogue Pro^3TL is given below. Replacement of the Glutamine (Gln) residue in the third position with Proline (Pro) showed superior antimicrobial activity and lower haemolytic activity compared to native TLs.[11]

TL: H-Phe^1-Val^2-Gln^3-Trp^4-Phe^5-Ser^6-Lys^7-Phe8-Leu^9-Gly^{10}-Arg^{11}-Ile^{12}-Leu^{13}-NH_2

Pro^3-TL: H-Phe^1-Val^2-Pro^3-Trp^4-Phe^5-Ser^6-Lys^7-Phe8-Leu^9-Gly^{10}-Arg^{11}-Ile^{12}-Leu^{13}-NH_2

Nevertheless, there is a need to encapsulate such AMP in order to control their release and time of action. Polymer network particles that have nano/micro scale size prepared by either physical or chemical cross-linking are referred as nano/microgels. These hydrogels were proven to be very promising candidates as drug carriers owing to their high loading capacity and stability.[12] Moreover, nano- or microgels hold a great promise due to their

combinatorial properties between nanoparticles and hydrogels. They are highly hydrophilic and able to swell, whereas they have small size and large surface area as particles. Nano/microgels for protein/peptide delivery systems can be composed of either homo- or copolymers. 2-hydroxyethyl methacrylate (HEMA), ethylene glycol dimethacrylate (EGDMA), N-isopropyl acrylamide (NIPAAM), acrylic acid (AA) and methacrylic acid (MA) monomers are extensively used to form 3D polymer matrices. The polymer matrix will define the affinity for water whereas the cross-linking degree modulates the swelling of the network, therefore have an impact on the release behaviour of the encapsulated molecules.[3] Hydrogels of poly(HEMA) present excellent biocompatibility and can act as potential carriers in drug delivery, dental, ophthalmic, and neural tissue engineering applications.[13,14] Poly(HEMA) networks can be produced by free radical dispersion polymerization of HEMA monomer in the presence of a cross-linker and appropriate stabilizer. As previously mentioned, peptides and proteins have a sensitive structure which can be degraded easily by temperature and upon exposure to solvents leading to the loss of their activity. [4,15] In order to encapsulate them efficiently without altering their activity, a variety of production methods have been studied [16,17] including supercritical carbon dioxide processes. [18] Supercritical carbon dioxide ($scCO_2$) is a green alternative for the conventional solvents. It is non-toxic, non-flammable and has low critical point (31.1°C and 73.8 bar).[19] More interestingly, $scCO_2$ goes to gaseous state upon depressurisation which enables to produce formulations as dry powders offering better stability in comparison to liquid formulations. [18]

Some of us have previously demonstrated the successful synthesis of cross-linked poly(HEMA) particles in supercritical carbon dioxide ($scCO_2$) using mild conditions (35°C/300 bar) [20] and on their further dispersion and swelling in water[21]. This work relies on the

synthesis and use of a fluorinated photocleavable stabilizer, i.e. poly(ethylene oxide) (PEO)-hν-poly(heptadecafluorodecyl acrylate) (PFDA) (PEO-*h*ν-PFDA) block copolymer where hν stands for a photosensitive moiety designed to perform dispersion polymerization in $scCO_2$ leading to nanoparticles of poly(HEMA) that can swell in water after photolysis and removal of the fluorinated block.[21]

The aim of this present work is to apply this process to the one-pot encapsulation of AMPs in cross-linked poly(HEMA) particles and to demonstrate the possible controlled release behaviour of the antibacterial peptide from the resulting nanogels.

2. Experimental

2.1 Materials

All chemicals are purchased from Sigma-Aldrich and used as received unless otherwise it is noted. 2,2'-Azobis(4-methoxy-2,4-dimethylvaleronitrile) (V-70,Wako), 2-hydroxyethyl methacrylate (HEMA, Aldrich, 97%), Ethylene glycol dimethacrylate (EGDMA, Aldrich, 98%,), Carbon dioxide (I5122,CO_2 N27 purity > 99,999%, Air Liquide, Belgium). Ultrapure water was produced by MilliQ plus 188 apparatus (Millipore). Bradykinin, Pro^3TL and S. Aureus were kindly provided by the Symbiose Biomaterials. The photocleavable diblock copolymers used as stabilisers, PEO_{45}-*hv*-$PFDA_{40}$ and PEO_{45}-*hv*-$PFDA_{82,}$ were synthesized according to the previously published method by Alaimo *et.al.*[21] Their structure is given in Scheme 1A and hv signifies the photocleavable junction.

2.2 Methods

2.2.1 Synthesis of the poly(HEMA) networks in $scCO_2$

Dispersion polymerisations of 2-hydroxyethyl methacrylate were performed as previously described by Parilti *et al.*[20] The procedure can be described as follows: the high pressure stainless steel cell (82 ml, ToP Industrie) was charged with 8.2 ml of HEMA (10% v/v CO_2), 82 µl of EGDMA (cross-linker, 1% v/v monomer), 0.82 g of stabiliser (10% $w_{stabiliser}/V_{monomer}$), 0.187 g V-70 (1% w/v monomer) and 8.79 mg peptide (0.1% $w_{Bradykinin}$ or w_{Pro3TI}/w_{HEMA}). The amounts were adjusted for desired reactions. The cell was securely sealed and a small amount of CO_2 was introduced using syringe pump (ISCO model no. 260D). After the heating mantel was clamped, the stirring rate (400 rpm) and temperature (35°C) were set with the control unit. Temperature and pressure were increased step-wise, and the reactor was stabilised at the desired conditions (35°C/300 bar) and reaction was left for stirring overnight. At the end of the reaction, for the depressurization, initially stirring was stopped and the heating jacket removed and the reactor is allowed to cool down to ambient temperature. Thereafter, the reactor is depressurized gradually by opening an outlet valve. After total depressurization, the cell was opened and the product was collected as a dry powder.

2.2.2 UV photolysis of the particles

The particles were dispersed in TFT with the concentration of 10 mg/ml. The solution was sonicated using horn sonicator for about 3 minutes resulting into a milky dispersion. Thereafter the solution was subjected to UV under vigorous stirring (700 rpm) using UV lamp (LOT-Oriel Arc Light Source Hg(Xe), power = 500 W, with multichromatic emission. Power around 310 nm = 400 W. Particles were subjected 10 or 30 minutes of irradiation,

after they are washed in TFT and then analysed by XPS to confirm the at least partial removal of the fluorinated block.

2.2.3 Antibacterial Test

For the quantification of the biocidal activity of the particles the following multiple step protocol has been applied as follows:

1. A *S. aureus* preculture has been prepared by taking a few bacteria spread on a Luria-Bertani agar gel (LBA), and placed in 10 mL of Luria-Bertani culture medium (LB) then incubated at 37 ° C overnight under agitation. Then, 2 ml of this solution was placed in 10 ml of fresh LB at 37° C under stirring until the optical density at 600 nm is equal to about 0.5;
2. The samples to be tested (i.e. the free AMP, or 5 ml of the aqueous dispersion of loaded or empty particles), were added with 4.5 mL of water and 0.5 mL of the bacterial solution;
3. Then at each time t, 10 µL of solution was picked out and placed in a tube containing 10 ml of LB culture medium; these tubes were placed on ice and then used for the drop plate method in order to count the colonies of viable bacteria. For this test, 3x 10µl were placed on an LBA gel putting the plates vertically so that the drops go down thanks to gravity. Once they were almost down, the plate was turned horizontally and incubated at 37°C for 20 hours and then the bacteria colonies visible to the naked eye were enumerated.

   For these experiments, the LB solution was composed of 10g/L of Bactotryptone, 10g/L of NaCl and 5g/L of yeast extract. For the LBA solution, the composition was the same as for LB except that 15g/L of agar was added.

2.2.4 Grafting of targeting peptide *via* reductive amination

Grafting of two different targeting peptides on the particles was performed according to the procedure as follows: Under an inert atmosphere 1.1 equivalance of targeting peptide was added onto 1 eq. of aldehyde of the particles in 10 ml of THF and stirred for 10 min. 1.5 eq. of sodium triacetoborohydride was then added to the solution still under an inert atmosphere and the mixture was left for stirring for 48h. After the completion of reaction, 10 mL of NaOH (3M) is added to the solution. The supernatant was removed by centrifugation for 10 min at 3000 rpm. Subsequently, particles were collected and washed with 15 mL of deionized water for 5 times. (**Peptide 1:** *S. Aureus* without spacer (MM = 1230.1 g / mol), Sequence: H-Val-Pro-His-Asn-Pro-Gly-Leu-Ile-Ser-Leu-Gln-Gly-NH_2 **Peptide 2:** *S. Aureus* with spacer (MM = 1343.57 g / mol), Sequence: Ahx-Val-Pro-His-Asn-Pro-Gly-Leu-Ile-Ser-Leu-Gln-Gly-NH_2 (Ahx = aminohexanoic acid)).

2.3 Characterisations

All the particles were analyzed with scanning electron microscopy (SEM, JEOL JSM 840-A) to evaluate their morphology. Samples were prepared on SEM stubs and coated with Pt (30 nm). The size distribution of particles in suspension in diluted TFT (before UV) and in water (after UV) were estimated by dynamic light scattering (DLS) using a Delsa Nano C, Particle Analyzer, Beckman Coulter at 25°C. The intensity of scattered light was detected at 165° to an incident beam and data treated by the cumulant analysis. X-ray photoelectron Spectroscopy (XPS) analyses were performed on a SSX 100/206 spectrometer (Surface Science Instruments - USA) equipped with a monochromatized micro-focused aluminium X-ray source (powered at 20 mA and 10 kV). A flood gun set at 6 eV and a Ni grid placed 3 mm above the sample surface were used for charge stabilisation. The angle between the surface

normal and the axis of the analyser lens was 55°; in these conditions, the probed depth was of the order of 5 nm. The molar fractions were calculated from the peak areas normalized on the basis of the acquisition parameters and sensitivity factors provided by the manufacturer. The calculations exclude hydrogen which is not detected by XPS. Carbon and fluorine spectra recorded second time after the analysis in order to validate that the sample was not degraded by X-ray source. The data analysis was performed with the CasaXPS program (Casa Softwares, Teignmouth, UK).

3. Results and discussion

3.1 Synthesis of the photocleavable stabiliser

PEO-*hv*-PFDA diblock copolymer used as stabiliser was synthesized according to the previously published paper by our group. [21] The composition of the diblock copolymer was varied in order to study the impact on the size of poly(HEMA) particles . For that purpose, a macroCTA composed of PEO bearing a photosensitive nitrobenzyl group and a trithiocarbonate (PEO-*hv*-CTA) was specifically designed and used for the RAFT polymerisation of the fluorinated acrylate block with various lengths (FDA) (Scheme 1-A). Two different stabilisers have been targeted and successfully obtained bearing a PEO block with a DP of 45 and perfluorinated block of either 40 or 82 units as confirmed by ^{1}H-NMR analysis.

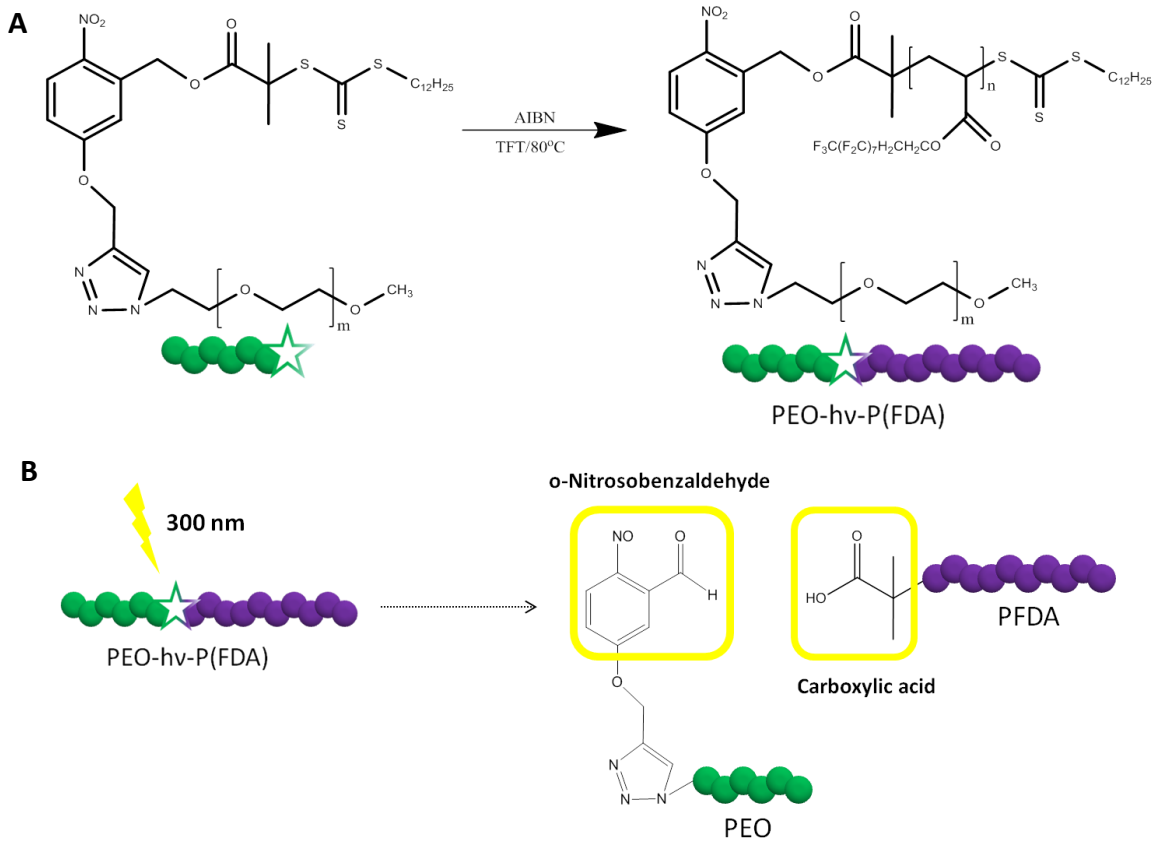


Figure 1: Synthetic approach for the CO_2-philic diblock copolymer bearing photosensitive junction represented by *hv* (A)and photocleavage reaction of this diblock copolymer upon UV irradiation (B).

3.2 Poly(HEMA) networks in supercritical carbon dioxide ($scCO_2$)

Cross-linked poly(HEMA) nanoparticles were prepared by dispersion polymerisation of HEMA and a cross-linker (EGDMA) in $scCO_2$ in mild conditions (35°C, 300bar) with the aid of the different of stabilisers (Figure 2). For the one-pot encapsulation of the antimicrobial peptide, Bradykinin or Pro^3TL, was introduced to the original reaction mixtures in different experiments.

The SEM micrographs and the characteristics of the obtained particles corresponding to the different stabiliser compositions, stabiliser amounts, cross-linking degrees, and the particles synthesized in presence of peptide are reported in the Figure 3 and Table 1 respectively.

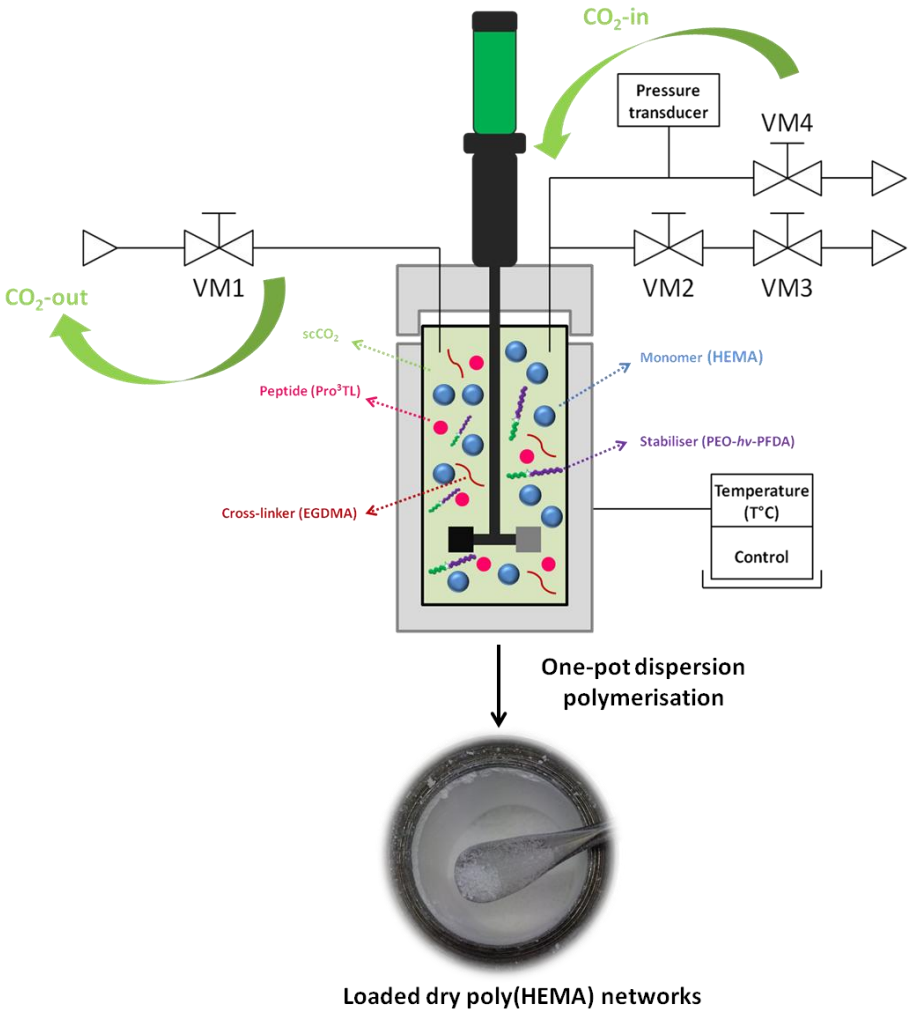


Figure 2: Schematic description of the one-pot dispersion polymerisation of poly(HEMA) networks in the presence of the antimicrobial peptide (AMP) to be encapsulated. Up: Scheme of the high-pressure stainless steel cell which is charged with HEMA (monomer), EGDMA (cross-linker), PEO-*hv*-PFDA (stabiliser), initiator and Pro^3TL (AMP) and then pressurized with CO_2. Down: A picture of the dry powder obtained after complete depressurization of the cell.

As evidenced by the SEM images (Figure 3), in each condition, spherical particles are obtained successfully which indicates the versatility of the method.

At 10% wt. stabiliser concentration, PEO_{45}-hv-$PFDA_{40}$ led to monodisperse particles having a mean particle diameter of 279 nm (Table 1: Entry 1, Figure 3: Entry 1). Variation in the block copolymer molecular weight of PFDA block was observed to have an effect on particle

morphology. Whilst keeping the same stabiliser concentration (10%wt), increase of the fluorinated block length of the stabiliser (Entry2: PEO_{45}-*hv*-$PFDA_{82}$) led to increase in particles diameter to 877 nm.

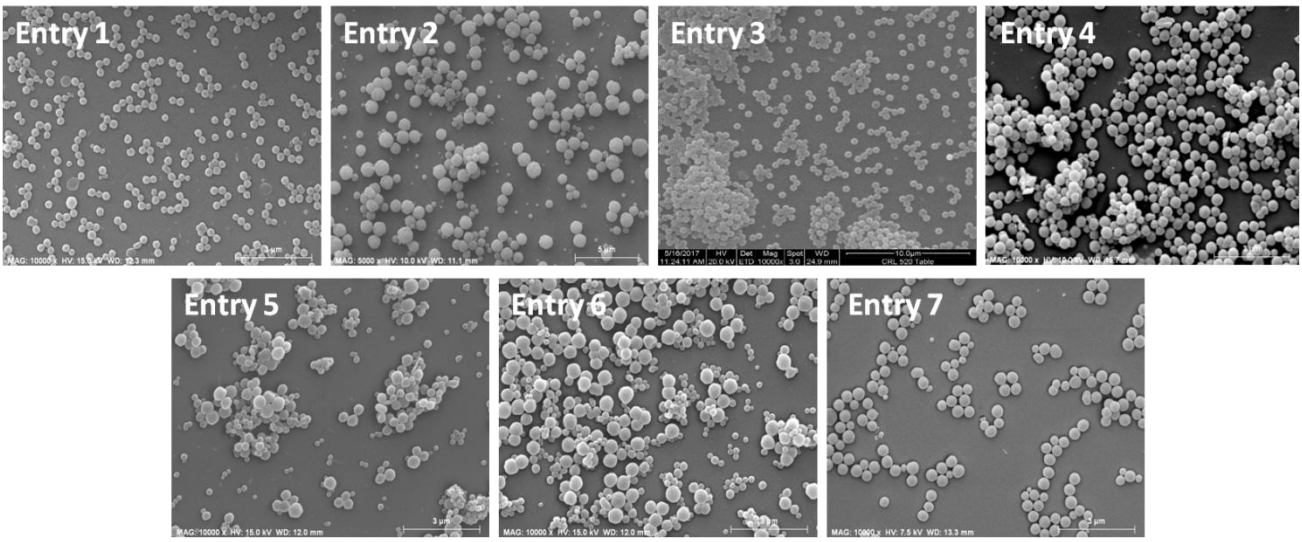


Figure 3: SEM images of the obtained poly(HEMA) cross-linked nanoparticles in supercritical carbon dioxide ($scCO_2$). Entries 5-7 were synthesized in the presence of peptide to be encapsulated. For the polymerisations initial monomer, initiator contents and reaction conditions (35°C/300 bar) were kept constant whereas cross-linker and amount of stabiliser were altered (see Table 1) in order to probe the effect on the particle.

The CO_2-philicity (solubility in $scCO_2$) was expected to increase by increasing the fluorinated block length of the stabiliser (PFDA), i.e. the molar mass of the stabiliser. Since the weight concentration was kept constant between both experiments the increase in particle size might be explained by the decreased molar ratio of the high molar mass stabiliser. This was also evidenced by the higher coefficient of variance number. (Table 1: Entry 2, Figure 3: Entry 2). Therefore, the PEO_{45}-hv-$PFDA_{82}$ stabiliser concentration was raised to 20% to keep the same molar ratio (i.e. $3.86*10^{-5}$ mol/L). In that case, more monodisperse particles having a mean diameter of 534 nm are obtained (Table 1: Entry 3, Figure 3: Entry 3), showing that still PEO_{45}-*hv*-$PFDA_{40}$ was much more efficient stabiliser.

In light of these findings, we repeated the experiment lowering the concentration of the PEO_{45}-*hv*-$PFDA_{40}$ stabiliser (5wt% with respect to monomer, i.e. a $2*10^{-5}$ mol/L) which mimics the conditions reported for Entry 2. The particles were obtained with narrow dispersity and well-defined shape having size of 404 nm (Table 1: Entry 4, Figure 3: Entry 4).

Table 1: Characteristics of synthesized poly(HEMA) networks

Entry	$M_{n\ (PFDA)}$	Stabiliser	EGDMA	Bradykinin	Pro^3TL	D_n	C_v[a]	Size DLS		UV	Fluorine extraction
	(kg/mol)	(%,wt)	(%, v)	(%, w_t)		SEM		Before UV[c]	After UV[d]	Time Min.	%[e]
1	20.5	10	1			279	9	461 nm	4.1 µm	30	57.6
2	42.5	10	1			877	21[b]	1.27 µm	5.3 µm	10	38
3	42.5	20	1			534	7	975[b] nm	2.4 µm	30	--
4	20.5	5	1			404	12	1.10 µm	4.4 µm	10	--
5	20.5	10	1	0.1		316	43[b]	771 nm	3.2 µm	30	--
6	20.5	10	2.5	0.1		436	34[b]	639 nm	3.0 µm	30	--
7	20.5	5	2.5		0.1	432	8	700 nm	3.8 µm	10	41

Monomer 2-hydroxyethyl methacrylate (8.2 ml, 10% v/v CO_2) and initiator V-70 (0.187 g, 1% w/v monomer) concentration and reaction conditions (35°C/300 bar) were kept constant. a: C_v stands for the coefficient of variance which is calculated according to the equation (Standard Deviation/D_n)*100 applied to SEM data, b: Bimodal distribution.c: DLS recorded in trifluorotoluene d: DLS recorded in water e: Amount of extracted fluorine as calculated from XPS measurements performed on the particles before UV and after UV treatment.

Expectedly, decreasing the content of the stabiliser resulted into an increase of the particles size. Interestingly, for a similar molar content of stabiliser, decreasing the length of the CO_2-philic block leads to a decrease of the particles size (Table 1: Entry 2 vs. Entry 4, Figure 3:Entry 2 vs. Entry 4).

The PEO_{45}-*hv*-$PFDA_{40}$ stabiliser appears thus the most efficient to stabilise small particles even at low concentrations (5% wt). Therefore, it was selected to repeat the particles synthesis in the presence of the peptide to be encapsulated. With the purpose to evaluate the impact of the presence of the peptide on the dispersion polymerisation reaction in

$scCO_2$ Bradykinin a model peptide readily available and presenting no bactericidal activity has been firstly used, then Pro^3TL, an active antibacterial peptide was introduced to the reaction mixture for encapsulation.

Initially, Bradykinin loaded particles were synthesized with two cross-linker concentrations (1% and 2.5 %) using 10% wt stabiliser. Although particles were obtained with well-defined morphology, they had a bimodal distribution which was clearly evidenced by SEM images (Figure 3: Entry 5, 6) and confirmed by very high C_v number. Bradykinin was found to have a low solubility in HEMA, therefore some phase separations could explain this large dispersity. On the other hand, the one-pot encapsulation of Pro^3TL was carried out in the presence of 5% wt. of the PEO_{45}-*hv*-$PFDA_{40}$ stabiliser. At the end of polymerisation, monodisperse spherical particles with 432 nm diameter were harvested as a dry fine powder (Table 1: Entry 7, Figure 3: Entry 7). The presence of the peptide in the medium did not appear to affect the particles formation and size (Table 1: Entry 7, Figure 3: entry 7). In that case, the cross-linker content was also set to 2.5% in order to get a denser network to sufficiently trap the peptide inside the particles and insure a controlled release.

In order to remove the fluorinated block from the particles surface, they were dispersed in TFT and irradiated by UV for 10 or 30min. UV-photolysis of the nitrobenzyl group at the blocks junction leads to the release of the hydrophobic block (PFDA) of the stabiliser in the TFT solution as previously reported. [21] The percentage of the extracted PFDA was probed by XPS measurements. Between 35-57% of PFDA could be extracted from the particles (Table 1, Fluorine extraction). This partial removal of PFDA was sufficient to allow the particles dispersion and swelling in water. Indeed, as demonstrated by DLS measurements performed in water (Table 1, after UV), all the particles showed a significant size increase upon swelling

in water as compared to the dry state (Table 1, SEM) or to TFT, a non-solvent of poly(HEMA) (Table 1, before UV) resulting in hydrogel particles of 3-4µm.

3.3 Antibacterial test

3.3.1 Free Bradykinin and Pro^3-TL

Initially free Pro^3-TL solutions were tested in order to identify the minimum concentration of peptide needed for to have a bactericidal effect. Determining this concentration would allow us to choose particle concentration to assess the antibacterial activity of the peptide loaded particles over an extended period of time. The results are reported in Table 2 and clearly indicate the strong (no bacterial colonies) and rapid (<10 min.) antibacterial activity of the free Pro^{3}TL. The same test performed with bradykinin confirms the expected inactivity of this negative reference peptide against *S. aureus*.

Table 2: Biocidal activity of peptides against S. Aureus (UC stands for uncountable colonies = large number of remaining colonies due to no bactericidal effect)

Time	Water	Free Bradykinin (µg/ml)		Free Pro^{3}TL (µg/ml)	
		6.25	12.5	6.25	12.5
<10	UC	UC	UC	2 0 2	0
10	UC	UC	UC	0	0
20	UC	UC	UC	0	0
40	UC	UC	UC	0	0
1 hr	UC	UC	UC	0	0
2 hrs	UC	UC	UC	0	0
3 hrs	UC	UC	UC	0	0
4 hrs	UC	UC	UC	0	0
5 hrs	UC	UC	UC	0	0
6 hrs	UC	UC	UC	0	0
24 hrs	UC	UC	UC	0	0

3.3.2 Antibacterial tests on empty and loaded particles

In order to determine the potential of this encapsulation strategy, the bactericidal behaviour of the particles loaded with Pro^3TL have been evaluated against *Staphylococcus Aureus* and compared to the behaviour of empty particles. Some preliminary tests have been performed on the particles obtained from Table 1 entries 1, 5, 6 and 7 after removal of the fluorinated block by irradiation of the particles in TFT for 30 minutes. The first assays for antibacterial tests were performed right after the irradiation and removal of the fluorinated segments. For that purpose, a selected amount (either 56 mg or 112 mg according to the minimum concentration of peptide) of the particles were incubated with *S. aureus* solutions. A reference sample in water was also performed, i.e. i.e. incubation of the bacteria in water without particles as negative reference. The numbers of remaining viable bacterial colonies was counted at regular time intervals and are reported in Table 3.

The analysis of Table 3 firstly confirms that the bacterial strains are able to multiply as shown by the test in aqueous medium in which the number of bacterial colonies is very large (Uncountable colonies (UC)). The empty particles (Table 1: Entry 1) at both concentrations did not present any bactericidal behaviour for 24 hours meaning that there is no residual monomer nor other contamination from the synthesis that is interfering with the bactericidal response. The test performed with bradykinin, the peptide of similar molar mass to Pro^3-TL that has no bactericidal effect on *S. aureus* also confirms that when the synthesis of the particles is performed in presence of a peptide, the process is not perturbed by the peptide so that it would lead to remaining unreacted bactericidal compounds. Indeed, regardless of the concentration, Bradykinin loaded particles (Table 1: Entry 5 and 6) showed similar behaviour as empty particles which did not present any bactericidal effect

for 24 hours. This first set of tests evidenced that the encapsulation carrier as produced by the scCO2 process does not exhibit any effect on the bacteria growth and proliferation. Therefore, in a second set of tests, the particles prepared in presence of the AMP were then used for the two similar concentrations, i.e. 56mg and 112mg of particles loaded with ~0.1% of Pro^3-TL.

When a low concentration of the particles loaded with Pro^3-TL (Table 1: Entry 7) (56 mg of particles, thus ~5,6 µg/mL of AMP) is incubated with the bacteria, no bactericidal effect is observed after 24h in strong contrast to free Pro^3-TL than immediately kills the bacteria already at a concentration of 6.25 µg/mL. This evidences that the main part of the AMP is well encapsulated in the particles at the term of the process and is released slowly during the first 24h so that no bactericidal concentration is reached for this period. A deactivation of the peptide could also account for this loss of activity but doubling the concentration of particles to 11,2 mg/ml (~11,2 µg/mL of AMP) against the same amounts of bacteria led to a clear recovery of the bactericidal effect after 1 hour which becomes significant after 4 hours of release evidencing the gradual release of the active peptide from the nanogel particles. The incubation time was extended till 24 hours leading to further release of the peptide and allowed the complete killing of the bacteria after 5h. This proves that the encapsulated peptide is still active, and able to diffuse slowly out of the particles to reach a minimal concentration in solution leading to the bactericidal effect. These data show for the first time that the developed process allows an efficient encapsulation of the peptide while keeping its bactericidal activity, and its sustained release from the particles.

Table 3: Number of remaining bacterial colonies corresponding to various incubation times. A solution of *Staphylococcus Aureus* incubated with AMP loaded poly(HEMA) particles having 2.5% of cross-linking agent EGDMA. (UC stands for uncountable colonies = large number of remaining colonies due to no bactericidal effect): Test 1

Time	Water	Empty Particles 1% EGDMA mg/ml		Brad. loaded particles 1% EGDMA mg/ml		Brad. loaded particles 2.5 % EGDMA mg/ml		Pro^3TL loaded particles 2.5 % EGDMA mg/ml		
		5,6	11,2	5,6	11,2	5,6	11,2	5,6	11,2	
<10	UC	UC	UC	UC	UC	UC	UC	UC	UC	
10	UC	UC	UC	UC	UC	UC	UC	UC	UC	
20	UC	UC	UC	UC	UC	UC	UC	UC	UC	
40	UC	UC	UC	UC	UC	UC	UC	UC	UC	
1 hr	UC	UC	UC	UC	UC	UC	UC	UC	107	116	112
2 hrs	UC	UC	UC	UC	UC	UC	UC	UC	79	93	73
3 hrs	UC	UC	UC	UC	UC	UC	UC	UC	92	88	94
4 hrs	UC	UC	UC	UC	UC	UC	UC	UC	22	33	33
5 hrs	UC	UC	UC	UC	UC	UC	UC	UC	0	0	0
6 hrs	UC	UC	UC	UC	UC	UC	UC	UC	0	0	0
24 hrs	UC	UC	UC	UC	UC	UC	UC	UC	0	0	0

A second run of assays was performed after storing the dry particles at room temperature for 10 days after UV treatment (Table 4). In this test, the quantity of particles has been increased from 112 mg to 225 mg to accelerate the biocidal effect (Table 4). According to the results reported in Table 4, this second test further confirmed the gradual release of the encapsulated Pro^3-TL from the nanogels matrix for both concentrations (11,2 mg/ml and 22,5 mg/ml). As the concentration of the particles increases (from 11,2 mg/ml to 22,5 mg/ml),the amount of released peptide in the same period of time is increased and leads to faster bactericidal effect.

Table 4: Number of remaining bacterial colonies corresponding to various incubation times. A solution of *Staphylococcus Aureus* incubated with AMP loaded poly(HEMA) particles having 2.5% of cross-linking agent EGDMA. (UC stands for uncountable colonies = large number of remaining colonies due to no bactericidal effect): Test 2 at higher concentration of particles after 10 days of storage.

Time	Water	Pro^3-TL loaded particles 11,2 mg/ml	Pro^3-TL loaded particles 22,5 mg/ml
10'	UC	UC	UC
20'	UC	UC	UC
40'	UC	UC	UC
1h	UC	UC	UC
2h	UC	UC	82 73 51
3h	UC	UC	89 75 88
4h	UC	UC	39 39 31
5h	UC	UC	17 22 14
6h	UC	UC	0
24h	UC	1 0 1	0

Complete killing of the bacteria is observed between 5 to 6 hours of incubation time for the highest concentration (22,5 mg/ml, ~22,5 µg/mL of AMP) while 24h of incubation are required for the lower concentration (11,2 mg/ml, ~11,2 µg/mL of AMP). The photographs of figure 5 illustrate the decrease in the number of bacterial colonies as a function of the contact time between *S. Aureus* and the nanogels suspension.

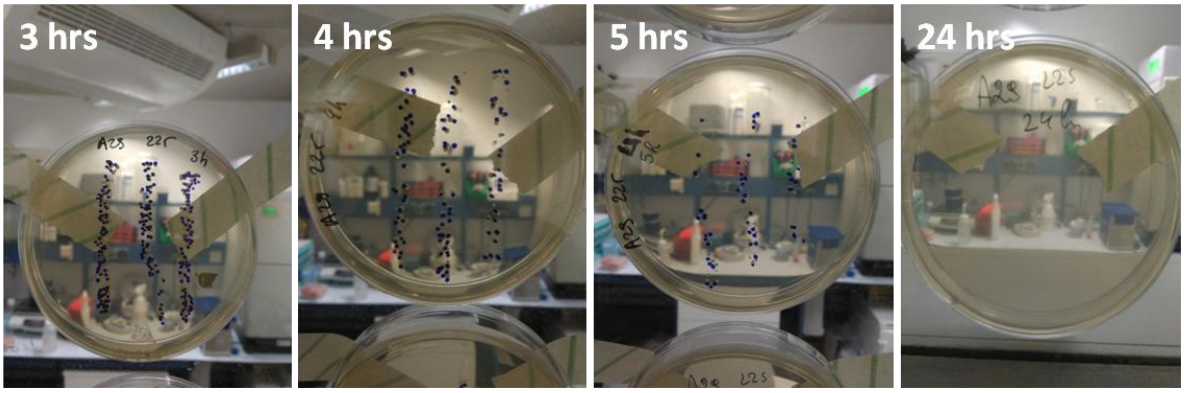


Figure 5: Illustration of the decay of bacterial colonies as a function of the release time (3 hours, 4 hours, 5 hours, 24 hours) for a concentration of particles of 22,5 mg/ml which equals to ~22,5 µg/ml of AMP.

In the case of the smaller number of particles (112 mg, ~11,2 µg/mL of AMP), the effect of the release appears after 6 hours of contact and the number of bacterial population, after 24 hours of release, is zero. Clearly, with the same number of particles, the kinetics of release appears slower than in the previous test (Table 3). Therefore, a third test was performed in triplicates (Table 5).

Table 5: Number of remaining bacterial colonies corresponding to various incubation times. A solution of *Staphylococcus Aureus* incubated with AMP loaded poly(HEMA) particles having 2.5% of cross-linking agent EGDMA. (UC stands for uncountable colonies = large number of remaining colonies due to no bactericidal effect): third test performed after 2 months of particles storage.

Time	**Water**	**Pro^3-TL loaded particles 11,2 mg/ml**			**Pro^3-TL loaded particles 22,5mg/ml**								
		1st	**2nd**	**3rd**	**1st**			**2nd**			**3rd**		
20'	UC	UC	UC	UC	UC			UC			UC		
40'	UC	UC	UC	UC	UC			UC			UC		
1h	UC	UC	UC	UC	UC			UC			UC		
2h	UC	UC	UC	UC	UC			UC			UC		
3h	UC	UC	UC	UC	UC			UC			UC		
4h	UC	UC	UC	UC	UC			UC			UC		
5h	UC	UC	UC	UC	77	74	79	80	81	75	72	80	101
6h	UC	UC	UC	UC	64	65	70	66	58	61	61	81	78
7h	UC	UC	UC	UC	42	/	46	49	55	41	51	47	52
24h	UC	UC	UC	UC	0	0	0	0	0	0	0	0	0

This antibacterial test was performed with the same batch of particles treated with UV and then stored for 2 months in the dry state in glass vial at room temperature. These results reported in table 5 indicate that the bacteria are still proliferating after 24h for the lowest concentration (11,2mg/ml particles, ~11,2 µg/mL of AMP), and that the kinetic tests performed simultaneously are reproducible, regardless of the quantity of microgels. In the case where a larger amount of microgels is used (22,5mg/ml, ~22,5 µg/mL of AMP), the decrease in the number of bacterial colonies is progressive with a population number equals to zero after 24 hours of release. Nevertheless, once again, the bactericidal effect appears

after a longer time period than in the previous tests reported in Tables 3 and 4 performed with the same batch of particles but at early stages after their preparation. From these measurements, we can conclude that the peptide is well encapsulated in the particles which control its release. Nevertheless, it appears that the peptide stability and/or its release rate is affected by the prolonged storage of the particles. Further studies will have to be done to clarify the origin of this phenomenon. Nevertheless, the complete killing of the bacteria is still observed for 24h of release for a storage time of 2 months showing the sustained release of the AMP thanks to the developed encapsulation process.

3.4 Surface Functionalisation

As it was depicted in the Scheme 1 upon UV-photolysis aldehyde groups will be generated on the surface of the particles. As already demonstrated in the previous work (Chapter 3), these aldehydes can be further used for functionalisation of the surface *via* reductive amination to graft targeting/imaging agents.

We took advantage of the presence of these reactive groups at the particles surface in order to graft a peptide with and without spacer able to target *Staphylococcus Aureus* bacteria. The spacer was used in order to reduce possible steric hindrances at the particle surface thus diminishing the particle recognition by the bacteria.

As evidenced by the images (Figure 6), when the particles do not bear the targeting peptide, the particles remain aggregated and *S. Aureus* are mainly adsorbed at the surface of these aggregates whereas when the targeting peptide is grafted, a larger number of the particles are individually surrounded by the bacteria. This is especially visible on the Image 2 of Figure 6, corresponding to the peptide grafted without the spacer.

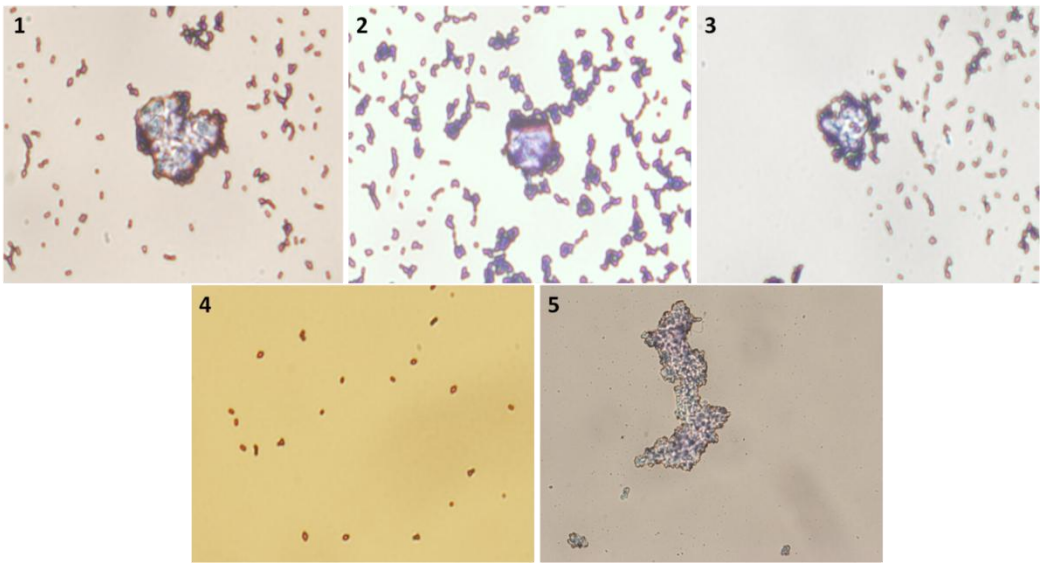


Figure 6: Optical microscope images after Gram staining of *Staphylococcus Aureus* with 1. Non-functionalised particles 2. Peptide grafted particle 3. Peptide-spacer grafted particle. For sake of comparison 4. *S. Aureus* alone and 5. Particles alone.

4. Conclusions

In this work, we have developed a novel process for the encapsulation of peptide in well-defined spherical poly(HEMA) cross-linked particles *via* one-pot free radical dispersion polymerisation in $scCO_2$ with the aid of photocleavable stabiliser. By varying the stabiliser molecular weight and concentration, the particle size could be easily tuned, opening the door to the optimization of the operational conditions in regards of the particles size required by the application. Stabiliser with lower chain length (i.e molecular weight) at even low concentration resulted into discrete monodisperse peptide loaded poly(HEMA) particles.

After UV treatment of 30 min. allowing the extraction of the fluorinated block of the stabiliser, particles dispersible in water as micron-size hydrogels have been easily achieved as confirmed by DLS measurements. The antibacterial tests indicated the sustained release

of the AMP from these poly(HEMA) microgels. In contrast to free AMP, the antibacterial effect was delayed which confirmed the encapsulation of the AMP thus proved the robustness of the developed one-pot encapsulation method even if a slight decrease of the bactericidal efficiency was observed for prolonged storage time. However concrete hypothesis could not be drawn with respect to data in hand and would require further investigations beyond the scope of this first study which opens a pathway to encapsulate the active pharmaceutical ingredients, especially such as peptides in mild conditions using a green polymerisation medium.

References

1 A. J. Almeida and E. Souto, *Adv. Drug Deliv. Rev.*, 2007, **59**, 478–490.
2 M. L. Tan, P. F. M. Choong and C. R. Dass, *Peptides*, 2010, **31**, 184–193.
3 J. Renukuntla, A. D. Vadlapudi, A. Patel, S. H. S. Boddu and A. K. Mitra, *Int. J. Pharm.*, 2013, 447.
4 Z. Gu, A. Biswas, M. Zhao and Y. Tang, *Chem. Soc. Rev.*, 2011, **40**, 3638–55.
5 J. H. Hamman, G. M. Enslin and A. F. Kotz, *Biodrugs*, 2005, **19**, 165–177.
6 L. M. Sanders and R. W. Hendren., *Protein Delivery Physical Systems*, Kluwer Academic Publishers, 2002.
7 A. M. Carmona-Ribeiro and L. D. de M. Carrasco, *Int. J. Mol. Sci.*, 2014, **15**, 18040–18083.
8 R. Wright, *Am. J. Med.*, 1995, **98**, 599–600.
9 M. L. Mangoni, A. Carotenuto, L. Auriemma, M. R. Saviello, P. Campiglia, I. Gomez-monterrey, S. Mal, L. Marcellini, D. Barra, E. Novellino and P. Grieco, *J. Med. Chem.*, 2011, 1298–1307.
10 A. Carotenuto, S. Malfi, M. R. Saviello, P. Campiglia, I. Gomez-monterrey, M. L. Mangoni, L. Marcellini, H. Gaddi, E. Novellino and P. Grieco, *J. Med. Chem.*, 2008, **51**, 2354–2362.
11 M. R. Saviello, S. Malfi, P. Campiglia, A. Cavalli, A. Carotenuto, P. Grieco and E. Novellino, *Biochemistry*, 2010, **49**, 1477–1485.
12 A. V. Kabanov and S. V. Vinogradov, *Angew. Chemie - Int. Ed.*, 2009, **48**, 5418–5429.
13 A. J. Cadotte and T. B. Demarse, *J. Neural Eng.*, 2005, **2**, 114–122.
14 S. Abraham, S. Brahim, K. Ishihara and A. Guiseppi-Elie, *Biomaterials*, 2005, **26**, 4767–4778.
15 M. J. Whitaker, J. Hao, O. R. Davies, G. Serhatkulu, S. Stolnik-Trenkic, S. M. Howdle and K. M. Shakesheff, in *Journal of Controlled Release*, 2005, vol. 101, pp. 85–92.
16 D. M. Cook, B. M. K. Biller, M. L. Vance, a. R. Hoffman, L. S. Phillips, K. M. Ford, D. P. Benziger, a. Illeperuma, S. L. Blethen, K. M. Attie, L. N. Dao, J. D. Reimann and P. J. Fielder, *J. Clin. Endocrinol. Metab.*, 2002, **87**, 4508–4514.
17 W. S. Choi, G. G. Murthy, D. a Edwards, R. Langer and a M. Klibanov, *Proc. Natl. Acad. Sci. U. S. A.*, 2001, **98**, 11103–11107.
18 S. P. Cape, J. A. Villa, E. T. S. Huang, T. Yang, J. F. Carpenter and R. E. Sievers, *Pharm. Res.*, 2008, **25**.
19 H. Tai, V. K. Popov, K. M. Shakesheff and S. M. Howdle, *Biochem. Soc. Trans.*, 2007, **35**, 516–

521.
20 R. Parilti, D. Alaimo, B. Grignard, F. Boury, S. M. Howdle and C. Jérôme, *J. Mater. Chem. B*, 2017, **5**, 5806–5815.
21 D. Alaimo, B. Grignard, C. Kuppan, Y. Adriaensen, M. J. Genet, C. Dupont-Gillain, J.-F. Gohy, C.-A. Fustin, C. Detrembleur and C. Jérôme, *Polym. Chem.*, 2017, **8**, 581–591.

Chapter 5

Hydrocarbon based stabilisers for the synthesis of poly(HEMA) cross-linked particles in supercritical carbon dioxide

Rahmet Parilti, Alba Castañon, Christine Jerome, Steven M. Howdle, Polymer Chemistry, 2017, to be submitted

Abstract

An environmentally-friendly process to prepare well-defined particles of poly(2-hydroxyethyl methacrylate) networks has been investigated. The dispersion polymerisation of HEMA with a cross-linker ethylene glycol dimethacrylate (EGDMA) was performed in supercritical carbon dioxide ($scCO_2$) using stabilisers based only on vinyl acetate (VAc) and vinyl pivalate (VPi) copolymers; thus avoiding the use of silicone or fluorine based stabilisers which are normally required in $scCO_2$. The effect of molecular weight and composition of the PVAc-*s*-PVPi stabilisers on the shape and size of the product microparticles was investigated. A copolymer stabiliser with 55:45 (VAc:VPi) composition (M_n 12.8 kg/mol) was found to be the most efficient, resulting in well-defined spherical cross-linked poly(HEMA) particles (1.2 μm diameter). This particular stabiliser was found to provide good steric stabilisation in the presence of a range of cross-linker ratios and upon addition of a co-monomer such as N-vinylpyrrolidone (N-VP) allowing tuning of the properties of the microparticulate products. Finally, partial hydrolysis of the ester groups of the stabiliser located on the surface of the microparticles leads to more hydrophilic alcohol moieties and allows formation of microparticles that can easily be dispersed into water leading to valuable microgels.

1. Introduction

Green chemistry is defined as the design of products and processes that eliminate either use or generation of hazardous substances.[1] Green chemistry is described by 12 principles and worldwide research groups are trying to design synthetic methods that utilise these principles; for example to replace volatile organic conventional solvents.[2] In that framework, supercritical carbon dioxide ($scCO_2$) is an excellent candidate with accessible critical temperature (31.1°C) and pressure (73.8 bar), gas-like diffusivity and liquid-like densities. Moreover $scCO_2$ is a naturally highly abundant, non-toxic, non-flammable solvent which makes it a good candidate for VOC replacement. Most importantly, $scCO_2$ can be removed by simple depressurisation, this can also help significantly in removing unreacted monomer and hence eliminating post-reaction purification processes.[3] The use of $scCO_2$ as a solvent has witnessed tremendous growth[4] in many areas; from commercialized extractions in the food industry[5] to intricate pharmaceutical formulations for drug delivery[6] or as a solvent or anti-solvent to produce polymer particles with controlled size and shape.[7] One of the most versatile routes to polymer particles is heterogeneous free-radical polymerisation. Most common monomers are soluble, but their corresponding high molecular weight polymers are usually insoluble making $scCO_2$ an ideal candidate for dispersion polymerisation.[8]

A key factor for the successful dispersion polymerisation and control of the particle size is the selection of a relevant stabiliser. Stabilisers can either adsorb or chemically graft onto the growing polymer microparticles limiting growth and preventing aggregation by steric stabilisation.[9] Efficient stabilisers for dispersion polymerisation in $scCO_2$ require macromolecules exhibiting a "CO_2-philic" part to ensure solubility in CO_2 and provide steric

stabilisation to prevent particle aggregation. [10] Up till now only fluorinated and silicone based polymers have shown sufficient CO_2 solubility. However, these are expensive and this might limit large scale application.[11] Consequently, an area of focus has been the synthesis of alternative hydrocarbon based stabilisers. Kazarian *et al.* have shown that polymers containing electron donating functional groups such as carbonyls, interact with CO_2 molecules via Lewis acid-base type interactions.[12] Sarbu *et al.* proposed that a CO_2-philic block could be a combination of a monomer (A) which gives flexibility and free volume to polymer chain and enhances the entropy of mixing, and a co-monomer (B) containing Lewis base group, such as carbonyl, to facilitate interaction with CO_2. Poly(ether carbonate)s (PEC)s were reported to be $scCO_2$ soluble at reasonable temperature and pressure.[13] Similarly, Tan *et al.* reported facile synthesis of $scCO_2$ soluble poly(ether carbonate)s and poly(ether ester)s by step-growth polymerisation method. [14] In addition they showed that polymers composed of poly(ethylene glycol) (PEG) and oligovinyl acetate(OVAc), PEG-*b*-OVAc diblock and OVAc-*b*-PEG-*b*-OVAc triblock copolymers could be efficient emulsifiers for water in $scCO_2$. These diblock and triblock copolymers were able to emulsify up to 97% v/v CO_2 in water and polymerisation in this medium resulted in highly porous poly(acrylamide) (PAM) networks.[15] The porosity of the PAM networks were found to be higher than those synthesized with a perfluoropolyether (PFPE) showing that OVAc based block copolymers might advantageously replace fluorinated materials in $scCO_2$.[15,16] Poly(vinyl acetate-alt-dibutyl maleate) (PVAc-alt-PDBM) copolymers also showed good CO_2 solubility [17] Cloud point measurements demonstrated that copolymers of PVAc-*s*-PVBu (50:50 composition) have higher solubility than PVAc and PVBu homopolymers. These materials then were exploited to perform the first successful dispersion polymerisations in $scCO_2$ using hydrocarbon based stabilisers. The dispersion polymerisation of *N*-vinylpyrrolidone (N-VP)

led to poly(vinylpyrrolidone) (PVP) monodisperse microparticles.[18] This work was then extended to creating stabilisers from copolymers of vinyl pivalate (VPi) and vinyl acetate (VAc). PVAc-*s*-PVPi copolymers were synthesized and the stabiliser efficiency was tested by dispersion of N-VP in $scCO_2$. Again, micron sized spherical PVP particles were produced successfully.[19] Park *et al.* extended this study to the synthesis of copolymers based on vinyl acetate (VAc), vinyl butyrate (VBu) and vinyl octanoate (VOc). Their cloud point data indicate that the solubility of the stabiliser (PVAc-s-PVBu) was increased with increasing VBu monomer in the copolymer; as well as leading to better stabilisation of N-VP, while in the case of PVAc-s-PVOc stabilisers the opposite behaviour was observed.[20] Girard *et.*al reported on the synthesis of poly (N,N-dimethyl acrylamide)-b-poly(vinyl acetate) (PDMA-b-PVAc) diblock copolymers and showed that their solubility in $scCO_2$ was decreased at higher PDMA content.[3]

Cross-linked poly(HEMA) microparticles have shown utility as drug carriers [21], in dental, ophthalmic and in tissue engineering applications.[22] A key challenge is to find routes to their synthesis that are clean, but do not require perfluorinated or silicone based stabilisers. Moreover, the materials produced should be able to be easily dispersed in water. Hence, in this paper we focus on the dispersion polymerisation of 2-hydroxyethyl methacrylate (HEMA) in the presence of ethylene glycol dimethacrylate (EGDMA) as a cross-linker using PVAc-*s*-PVPi copolymer stabilisers to obtain microparticulate poly(HEMA) networks directly from $scCO_2$. If successful, PVAc-*s*-PVPi stabiliser will be present on the microparticle surfaces and, by hydrolysis, could provide a facile route to hydrophilic poly(vinyl alcohol) units to allow dispersion of the microparticles into water.

2. Experimental

2.1 Materials

The chemicals that are purchased are used as received unless otherwise noted. 2,2'-Azobis(2-methylpropionitrile) (AIBN, 98%), ethylene glycol dimethacrylate (EGDMA, 98%), 2-hydroxyethyl methacrylate (HEMA, ≥99%), potassium ethyl xanthogenate (96%) and vinyl pivalate with hydroquinone as inhibitor 5-30 ppm (VPi, 99%) were purchased from Sigma Aldrich. Dichloromethane (DCM, AnalaR NORMAPUR® ACS,Reag. Ph. Eur. analytical reagent), ethanol (EtOH, ≥99.9%), methanol (MeOH) were purchased from VWR. N-Vinyl pyrrolidone (N-VP, 98%, Merck Millipore), 2,2'-azobis(4-methoxy-2,4-dimethylvaleronitrile) (V-70) were purchased from Wako Chemicals. Vinyl acetate (VAc, 99%, stab. with 8-12ppm hydroquinone) was purchased from Alfa Aesar. Carbon dioxide (CO_2, 99.99%) was purchased from BOC, UK. Methyl methacrylate was kindly provided by Kaneka Belgium NV.

2.2 Methods

2.2.1 Synthesis of O-ethyl-S-(1-methoxycarbonyl) ethyl dithiocarbonate

Methyl bromoacetate (16g, 104.6 Mmol) was dissolved in methanol (75mL) in a 250 mL round bottom flask with a stirring bar and in an ice bath. Potassium ethyl xanthogenate (19.515g, 121.7 mmol) was dissolved in ethanol (100mL) in a beaker for 30 minutes and added dropwise to the flask using an addition funnel. The mixture was stirred at room temperature for 24h and filtered to remove KBr salts. The filtrate was evaporated under reduced pressure, dissolved in dichloromethane (50 mL) and washed with water (3x15 mL). The organic phase was dried with magnesium sulfate and dried under vacuum to yield a yellow liquid. Yield= 79%. ^{1}H NMR ($CDCl_3$): δ= 4.5 ppm (q, 2 H), 3.8 ppm (s, 2H), 3.6 ppm (s, 3H), 1.3 ppm (t, 3H).

2.2.2 Synthesis of PVAc-s-PVPi copolymers

Typical copolymer synthesis in bulk: Vinyl acetate (17.99g, 209 mmol), vinyl pivalate (2.97 g, 23.23 mmol), *O*-ethyl-*S*-(1-methoxycarbonyl) ethyl dithiocarbonate (0.684 g, 3.6 mmol) and AIBN (0.06 g, 0.36 mmol) were placed in a sealed round bottom flask with a stirring bar and degassed with argon for 30 minutes in an ice bath. The mixture was stirred at 60°C for 5 hours to a conversion of around 60% as determined by NMR. The polymer product was precipitated in a mixture of ice cold methanol: water (4:1) and dried under vacuum for 24 h to remove both the solvent and unreacted monomer. ^{1}H NMR ($CDCl_3$): δ= 6.4-6.7 ppm (m, 0.5 H), 4.7-5 ppm (m, 52 H), 4.5-4.7 ppm (m, 2 H), 3.6 ppm (s, 3H), 2.25-2.35 ppm, 1.5-2.1 ppm (m, 228 H), 1.3-1.4 ppm, 1.1-1.3 ppm (m, 161 H), M_n(NMR)= 12800 g/mol, VAc:VPi = 55:45, M_n(SEC)= 13000 g/mol, $Đ$= 1.05.

2.2.3 Dispersion polymerisation in $scCO_2$

Dispersion polymerisations were performed in a 60 ml high pressure autoclave. Prior to use, the autoclave was leak tested with a high pressure of CO_2 and all the fittings were tested by using leak detector lubricant Snoop® purchased from Swagelok. A typical one-pot procedure was followed for the free radical dispersion polymerisation of 2-hydroxyethyl methacrylate (HEMA) and/or copolymerisation with methyl methacrylate (MMA) and 1-vinyl-2-pyrrolidone (N-VP) monomers in $scCO_2$ unless otherwise noted.

The autoclave body was charged with 6ml of monomer (10% $v_{monomer}/v_{CO2}$), 0.1368g of V-70 (1% $w_{V\text{-}70}/w_{monomer}$), 60 µl EGDMA (1% $v_{cross\text{-}linker}/v_{monomer}$), and 0.6 g (10% $w_{stabiliser}/v_{CO2}$) of stabiliser. Initially the autoclave was filled with 800 psi (55bar) then stirring was started at 200 rpm. The cell was heated up to 35 °C. As the final temperature is reached and stabilised for a few minutes, the cell was taken up progressively to 3500 psi (240bar) or desired final

pressure. The reaction was left stirring overnight at 35°C and 3500 psi. To stop the reaction the heating was switched off and the heating jacket disconnected. The cell was allowed to cool down to room temperature and depressurized very slowly by the outlet tab into the fume hood. Stirring was left on at all times until low pressure (700-600 psi) was reached. The autoclave was opened once atmospheric pressure was reached (14-18 psi). Polymer products were then collected for analysis.

2.2.4 Hydrolysis of the stabiliser and stabilized particles

Two conditions have been tested to hydrolyse the PVAc-s-PVPi copolymer into PVOH based on previously reported conditions for PVAc homopolymer (condition 1) and for PVPi homopolymer (condition 2) by Bernard *et al*.[23] The following procedures were applied first on the stabiliser only and then on the poly(HEMA) stabilized particles.

Condition 1 called "PVAc conditions": 100 mg of statistical copolymer was dissolved (or 100mg of particles were suspended) in 10 ml of methanol and a solution of 200 mg KOH in 10 ml methanol was added. The mixture was left stirring for 24 hours at room temperature. Then the mixture was dialysed against methanol for 24 hours. The solvent was evaporated by rotary evaporator (particles were freeze-dried in order to eliminate the small amount of residual solvent).

Condition 2 called "PVPi conditions": 90 mg of statistical copolymer was dissolved in 1 ml ethanol (or 90 mg of particles were suspended) and a 1ml solution of NaOH (1wt% in methanol) was added on the mixture. The mixture was left for stirring for 24 hours at 60°C. The reaction was dialysed against methanol for 24 hours and the solvent was evaporated by rotary evaporator (particles were freeze-dried in order to eliminate the small amount of residual solvent).

2.3 Characterisations

The solubility of the statistical copolymers in $scCO_2$ indicates their potential to be used as stabiliser for dispersion polymerisation in this solvent/media. Cloud point measurements were recorded for the range copolymers of different compositions and molecular weights. The cloud point in $scCO_2$ can be defined as the pressure at which the polymer starts to precipitate out from the solution at a fixed temperature.[14] The cloud points of synthesised statistical copolymers that have been described in the previous section were determined in the CO_2/monomer mixture by using a high pressure variable volume view cell.[24]

For a typical cloud point measurement 3g (15% wt monomer/ CO_2) of HEMA, 150 mg of stabiliser (5%wt stabiliser/HEMA) and 20 g of CO_2 were used. The stabiliser was dissolved in a given amount of HEMA and injected into the view cell. CO_2 was then transferred to the view cell by using a small stainless steel CO_2 bomb. The weight of the bomb was recorded before and after addition to calculate the exact amount of CO_2 in the cell. The cell was heated up to the desired temperature and allowed to stabilise. Thereafter, the hydraulic piston was slowly moved forward to increase the pressure in the cell until a single phase was observed through the sapphire window. At this pressure, the light placed at the end of the view cell will be visible. The piston was moved back again slowly to decrease the pressure in a controlled manner to observe the pressure at which the solution is no longer a single phase. A cloudy mixture is observed due to precipitation of the polymer from the solution mixture and the point at which light at the back of the view cell is no longer visible anymore is taken as the cloud point. Measurements were repeated in triplicate. Cloud points were taken at 35, 45, 55, 65 and 75 °C and each point was repeated 3 times. The cloud points are reported as an average value of these three repetitions.[19] Dynamic

mechanical analysis enables us to investigate material properties such as stiffness, viscosity, elasticity at various temperatures. Glass transition temperatures (T_g) of the samples can therefore be obtained. The collected particles were analysed by using a Triton Technology TT DMA using powder pockets which allows analysis of samples in powder form. The analysis pocket was filled with the particles as collected from the high pressure reactor. DMA was performed in single cantilever bending mode with a ramp rate 5°C/min starting from room temperature to 120°C or 150°C. ^{1}H NMR was used throughout this work to determine structure, molar ratios, conversion and molecular weights of the polymers. We used a Bruker AV3400 spectrometer equipped with a 400 MHz magnet and deuterated chloroform ($CDCl_3$) as solvent. Analysis of end groups was carried out at 256 scans and relaxation times of 1 second. All data were processed using MestRe-Nova software. An Agilent 1260 Infinity system equipped with 2 polystyrene columns of 8x300 mm and Wyatt OptilabrEX refractive index detector was used. THF was used as eluent at 0.5 mL min^1 flow rate. PMMA standards were used for calibration. The morphology of the obtained polymer particles was analysed by JEOL 6490LV SEM and JEOL JSM 840-A in secondary electron image (SEI) mode under high vacuum (HV). Samples were prepared on aluminium stubs supplied by Agar. Two-sided carbon discs were placed on the aluminium stub and sufficient amounts of samples were spread on the discs. Thereafter samples were coated with Platinum (Pt) sputter coater for 120 seconds with uniform thickness. In order to improve the quality of the images and depth of analysis, some of the particles were dispersed in a proper solvent using high speed sonicator. In that case, glass substrate was placed on the carbon disc and few drops of the samples were placed on the substrate. Solvent was evaporated during night under high vacuum oven at proper temperature. The sample was then coated with Pt before observation. The samples are not dispersed unless otherwise

noted. Hydrodynamic diameters of polymer particles in diluted solutions were recorded using DelsaNano C by Beckman Coulter. The size distribution of the diluted water dispersions was estimated by Photon Correlation Spectroscopy (PCS) using a particle-size analyser at 25°C. The intensity of the scattered light was detected at 165° to the incident beam.

3. Results and discussions

3.1 Synthesis of the stabilisers *via* RAFT polymerisation

Statistical copolymers of VAc and VPi of varying targeted molecular weights and compositions were synthesized via RAFT/MADIX polymerisation (Figure 1) because of its ease of implementation and good control over the polymerisation of vinyl ester monomers.[25,26]

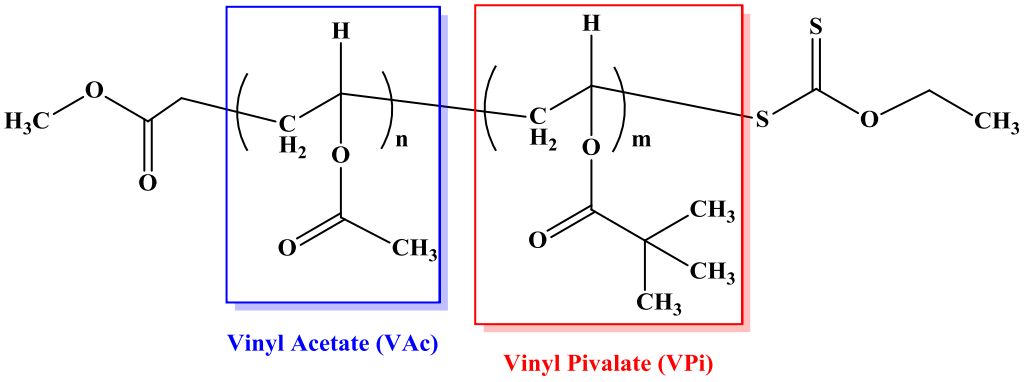


Figure 1: Structure of PVAc-*s*-PVPi copolymers bearing Xanthate end-group.

Stabilisers of different composition and molecular weight were obtained by varying the co-monomer and monomer:RAFT ratios. Conversions around 60% were achieved after 5 h in all cases. Reactions were typically stopped at 60% conversion to minimise undesired side reactions. The macromolecular characteristics of the obtained copolymers were determined

by ^{1}H-NMR and SEC after purification and all results are summarized in Table 1. A representative ^{1}H-NMR spectrum is shown in Figure 2.

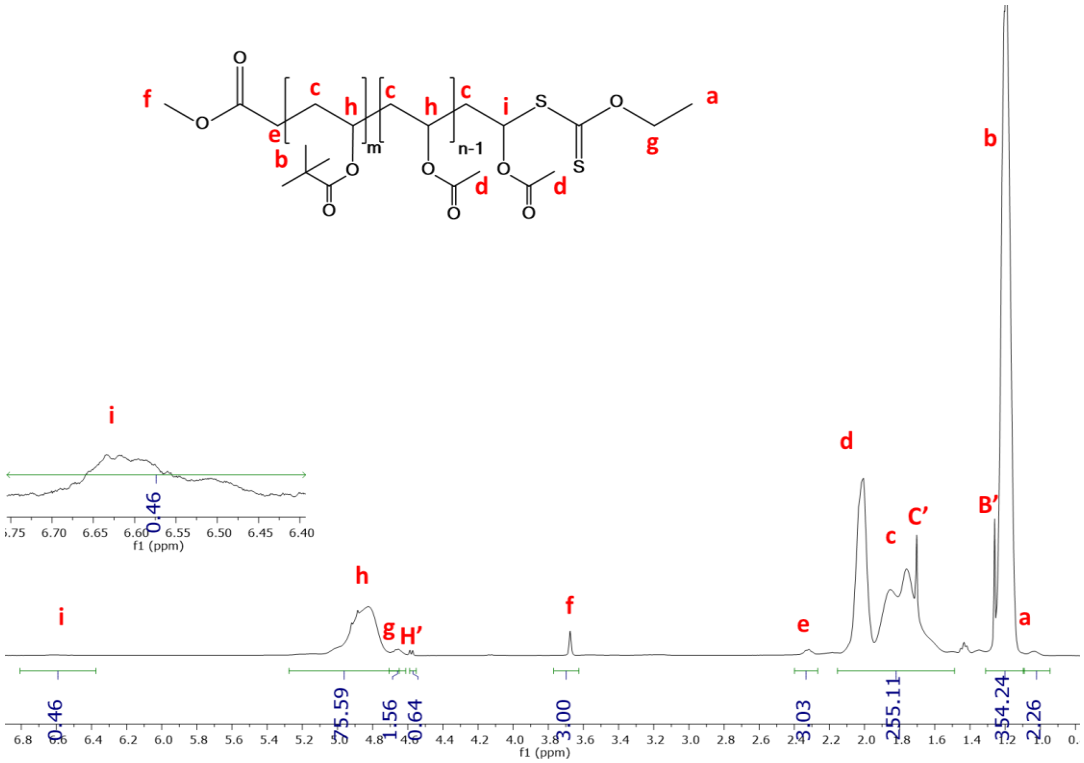


Figure 2. : ^{1}H-NMR spectrum for a standard PVAc-*s*-PVPi copolymer.

The VAc:VPi ratios were calculated by comparison of the peaks b (VPi, 9H from ^{t}Bu), c and d [5VAc (3H from CH_3 + 2H from CH_2)+ 2VPi (2H from CH_2)]. From these values we can compute the number of VAc and VPi units. Thus, by applying the equation given below the percentage of either VAc/VPi units in the resultant copolymer can be calculated:

$$\% \text{ VAc} = [\text{VAc} / (\text{VAc} + \text{VPi})]\text{x}100 \quad \textbf{(Eq. 1)}$$

Molecular weight was calculated from the degree of polymerisation obtained from the integration of the peaks h and i divided by peak of alpha chain-end (peak f), leading to a molar mass of 8200 g/mol. Signals B', C' and H' correspond to residual VPi that could not be fully removed. The amount of residual VPi can be calculated comparing integrals H' and H and was in all cases lower than 1% compared to the polymer so it has no negative impact on

the quality of the material. The signal at 6.60 ppm (i) corresponds to the proton of the last vinyl acetate or vinyl pivalate unit that is attached to the sulfur atom of the xanthate end and therefore has a much higher chemical shift. Signals a and g being not accurate, the integral of this signal (i) can be used to determine the percentage of the polymer chains that retain the RAFT end, in this case for the given NMR is 46%. For the other 54% of the chains that are not RAFT functional, the last vinyl acetate or pivalate unit will have the same chemical shift as the rest of the units and will therefore be included in signal h.

Table 1: Macromolecular characteristics of the synthesized stabilisers and the size and size distribution of the poly(HEMA) particles obtained using those stabilisers in dispersion polymerisation in $scCO_2$.

Entry	Composition ([VAc:VPi], ^{1}H-NMR)	$M_{n\ (stabiliser)}$ (kg/mol, ^{1}H-NMR)	Đ (SEC)	RAFT-end (%-^{1}H-NMR)	Particle Size (µm,SEM)[a]	C_v[b]
1	9:91	4.6	1.22	89	3.7	11.2
2	12:88	7.5	1.42	77	2.3	8.3
3	17:83	9.8	1.49	---	4.4	9.6
4	23:77	9.8	1.42	65	Porous	
5	29:71	10.6	1.20	98	Aggregate	
6	36:64	7.8	1.02	100	1.2*	10.8
7	36:64	9.9	1.08	88	2.1	11.6
8	42:58	10.3	1.20	85	Aggregate	
9	44:56	10.7	1.08	89	2.3	10.5
10	47:53	6.6	1.13	100	Irregular shaped	
11	50:50	12.0	1.47	62	1.9	9.0
12	49:51	14.5	1.50	51	Aggregate	
13	50:50	22.0	1.42	52	0.9*	12.5
14	56:44	8.6	1.05	92	2.2	7.5
15	55:45	12.8	1.07	91	1.3	13.2
16	75:25	9.5	1.38	66	Porous	

a: The average size of the particles determined from individual SEM images (D_n), b: Cv= (σ/D_n)*100 where σ indicates the standard deviation. *: In these samples a particle size is reported for individual particles but there is also significant aggregation observed. For entry 3 the RAFT ends could not be determined.

The data provided in the table show that PVAc-*s*-PVPi with M_n between 4.6 and 12.8 kg/mol and VAc:VPi 29:71 to 75:25 were successfully synthesised in a controlled manner as confirmed by the low dispersity values (<1.5) in all cases.

3.1.1 Cloud point measurements

The cloud point in $scCO_2$ is defined as the pressure where the polymer starts to precipitate out from the medium at a given temperature and is measured at the point where the LED lights in the system are no longer visible. Therefore, by measuring cloud points one is able to estimate the reaction conditions for the copolymer to be used efficiently as a stabiliser in dispersion polymerisation in $scCO_2$.

In this study, cloud point measurements were carried out in a high pressure variable volume view cell as described in detail in the experimental part. Cloud points of the two synthesized PVAc-*s*-PVPi copolymers were performed within a mixture of dispersing medium ($scCO_2$) and HEMA monomer which also mimics the initial phase of dispersion polymerisation. Moreover, in this mixture the monomer also behaves as a co-solvent enhancing the solubility of the copolymers in $scCO_2$. Photographic images (Figure 3) were taken at discrete phase changes during cloud point measurements which represent the different stages of a cloud point experiment.

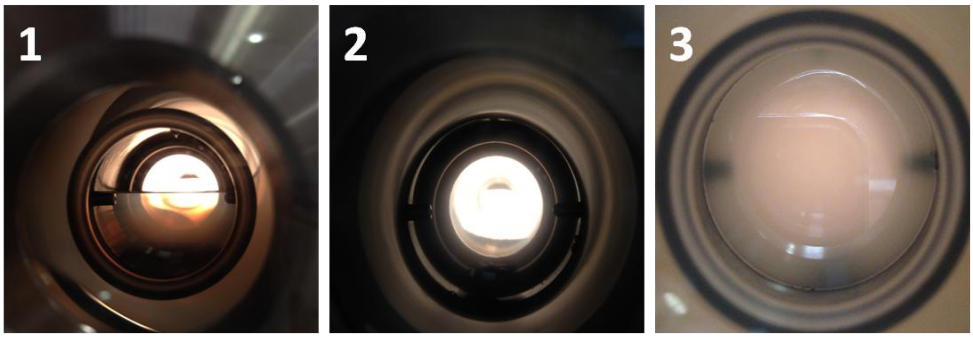


Figure 3: Illustrative pictures of the cloud point measurements for the typical PVAc-*co*-PVPi stabiliser. **1:** Initial mixture of monomer (3g, HEMA monomer), stabiliser (150 mg) and carbon dioxide (20 g) at initial pressure (around 50 bar) and room temperature; **2:** the view cell is heated to the desired temperature (i.e. 35°C) and pressure is increased until there is complete dissolution of the copolymer in the monomer and carbon dioxide mixture; **3:** Keeping the temperature constant the rear sapphire piston is withdrawn to lower the pressure (and density) and the copolymer starts to precipitate out from the mixture forming the cloud and obscuring the LED back-lights.

Initially the view cell was charged with a known amount of monomer, copolymer and CO_2 (Figure 3-1). This non-homogeneous mixture was stirred and the view cell was heated to the desired temperature. The pressure was increased until a single phase transparent solution was observed and the back light could be seen clearly (Figure 3-2).

After complete dissolution of the components, the piston was then slowly moved backwards decreasing the pressure until the stabiliser precipitated out from the solution and the back light was not visible anymore (Figure 3-3). That pressure was taken as the cloud point. The results of these measurements are reported in Table 2.

Table 2: Cloud points of two representative copolymers in HEMA/CO_2.

Entry	**Copolymer**				**Cloud Points [T (°C) vs. P(bar)]**				
	[PVAc: PVPi] (^{1}H-NMR)	**M_n total** (kg/mol,^{1}H-NMR)	**Đ** (SEC)	**T_g** (°C,DSC)	**35°C**	**45°C**	**55°C**	**65°C**	**75°C**
1	47:53	7.8	1.13	51.5	174,6	207,8	237,8	263,9	286,6
2	57:43	9.3	1.02	48.3	175,8	217,6	250,4	278,6	305,2

A clear trend is seen, increase in temperature (35°C to 75°C) led to higher cloud point pressures for both samples. This behaviour is strongly related to the lower CO_2 density at higher temperatures which necessitates increase in the pressure in order to have same solvent strength. Nevertheless, the copolymers show quite similar cloud points at 35°C (175 bar) the conditions under which our dispersion polymerisations in scCO_2 will operate.

Moreover, the cloud point of a stabiliser with roughly similar molecular characteristics (VAc:VPi 44:56/M_n 9.4 kgmol^{-1}/Đ:1.5/ T_g: 47.4 °C) was measured in scCO_2 in the presence of a different monomer N-VP. The data showed very similar values to the HEMA system 160 bar (2236 psi) thus indicating that perhaps the syntheses of HEMA may proceed effectively, as has previously been demonstrated for N-VP. [19]

In light of these measurements, all the synthesized stabilisers were expected to be soluble within the selected conditions for the HEMA dispersion polymerisation (35°C and 240 bar).

3.2 Dispersion polymerisation of HEMA in $scCO_2$

Dispersion polymerisation of HEMA was performed in $scCO_2$ according to the procedure described in the experimental section. Synthesis conditions and feed ratios for producing cross-linked poly(HEMA) particles have been selected on the basis of cloud point measurements along with our previous work using fluorinated stabilisers[9], i.e. 35°C and 240 bar which are above the critical conditions for CO_2.

In all of the dispersion polymerisations in $scCO_2$ we observed an increase of the final pressure of around 14 bar (200 psi). This phenomenon was also reported by other researchers for polymerisation of styrene (Sty)[27] , methyl methacrylate (MMA)[28] and 2-hydroxyethyl methacrylate (HEMA)[29] in $scCO_2$ and is attributed to the thermodynamics of mixing leading to expulsion of both CO_2 and monomer from the polymer phase.

After overnight polymerisation at 35°C and 240 bar the heating was turned off and the autoclave was left to cool down to room temperature and remaining CO_2 was slowly vented. After complete depressurisation, the polymer was collected from within the autoclave as either a free-flowing powder or as a brittle disc from the bottom of the reactor (Figure 4).

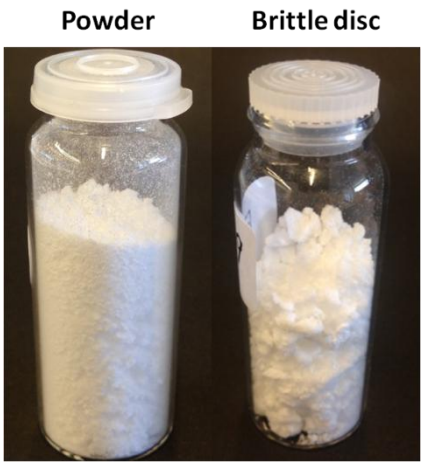


Figure 4: Representative product photos taken straight after depressurisation of the autoclave. Left hand-side the product photo obtained as free flowing powder, right hand-side brittle disc that was chiselled out from the reactor.

Further inspection of the polymer disc by SEM (Figure 5) showed that aggregated polymer product formed by coalescence of well-defined spherical particles.

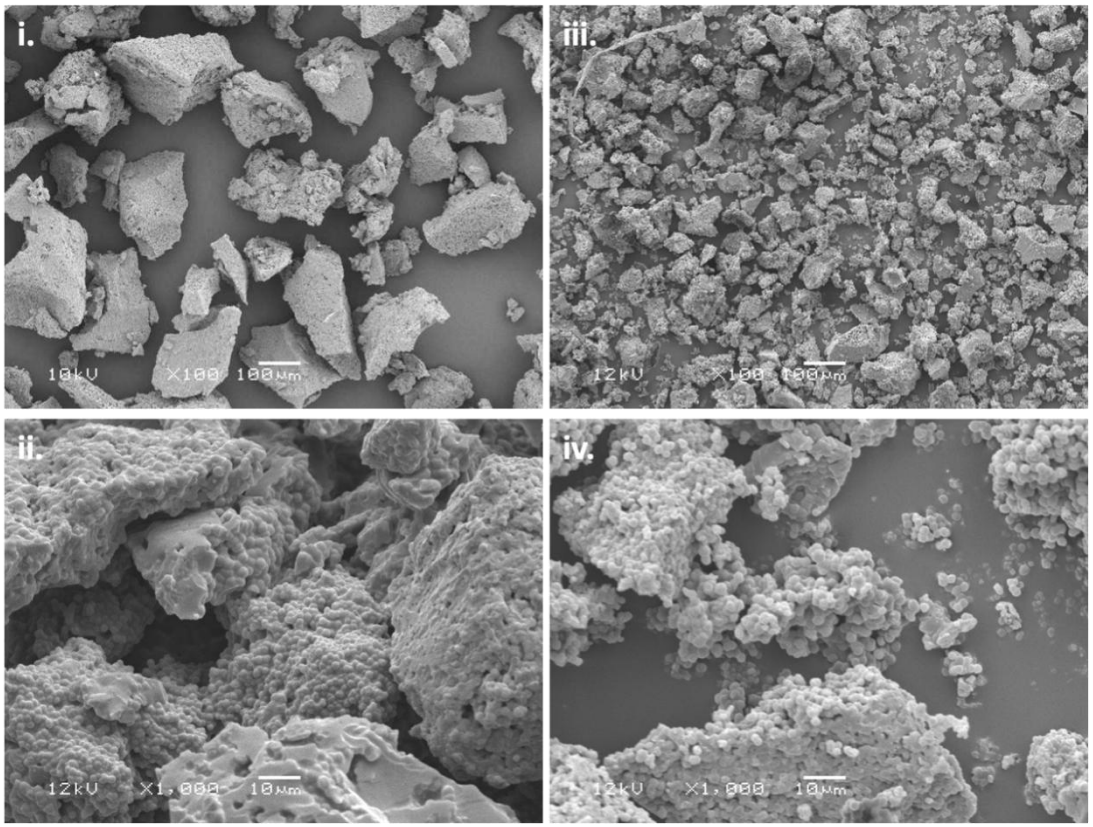


Figure 5: Representative SEM images of the solid disc polymer product (figure 4 right) obtained by dispersion polymerisation in $scCO_2$; (Example 1) i.100X magnification ii. 1000X magnification; (Example 2) iii. 100X magnification iv. 1000X magnification.

Similarly, large aggregates of poly(styrene) particles were also observed by Canelas *et.*al using poly(styrene-*b*-dimethylsiloxane) block copolymers as stabiliser.[27] They explained the formation of poly(styrene) aggregates by collapsing of PDMS chains during venting process.

3.2.1 Effect of stabiliser composition and molecular weight

i. Composition

A series of PVAc-*s*-PVPi polymers having roughly similar molecular weights (~10 kg/mol) with different compositions were tested to find the most suitable VAc:VPi ratio for stabilising HEMA in $scCO_2$. The initial feed ratios were kept constant for all the reactants; HEMA (monomer, 10% v/v_{CO2}), EGDMA (cross-linker, 1% $v/v_{monomer}$), stabiliser (10% $w/v_{monomer}$) and low temperature initiator (V-70, 1% $w/v_{monomer}$). After overnight polymerisation for all copolymer stabilisers, high HEMA conversions were achieved. However, depending on the molecular characteristics of the stabilisers, different polymer product morphologies were observed by SEM (Figure 6). Stabilisers and their corresponding particle characteristics details are listed in Table 1.

The copolymer composition was shown to have a major impact on particle stabilisation, morphology and size. It was observed that the best defined and smallest particles were obtained when the copolymer compositions were close to 50:50 (especially VAc:VPi 55:45). Higher VAc content in the copolymers resulted in better stabilisation of the poly(HEMA) cross-linked particles affording diameters around 2 microns. This behaviour of the PVAc-s-PVPi copolymer was in line with already reported observations for the dispersion polymerisation of N-VP in $scCO_2$[19].

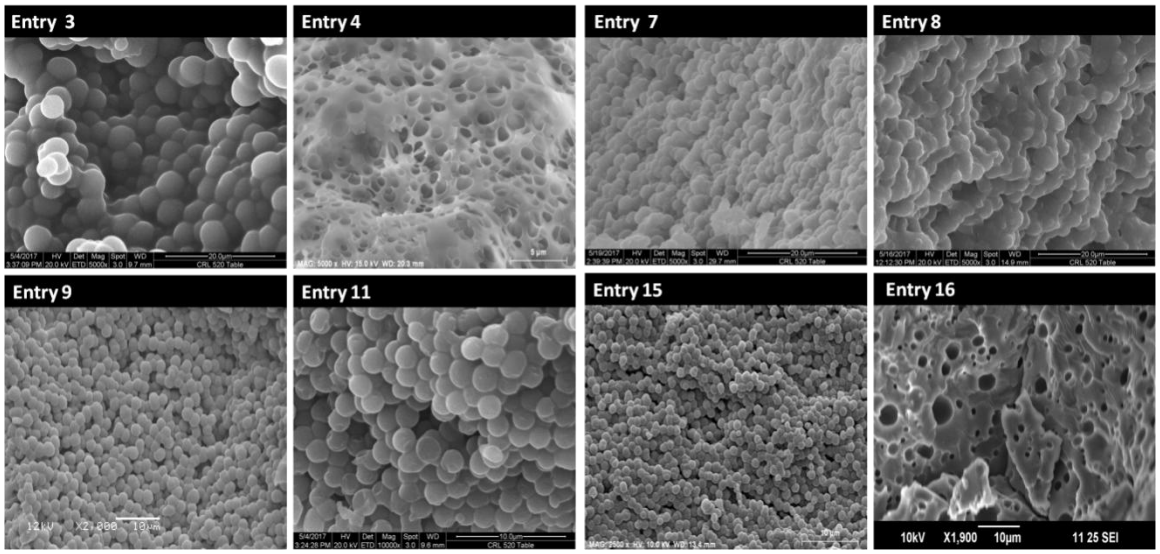


Figure 6: SEM images of the particles obtained after dispersion polymerisation of HEMA (10% v/v CO_2) and EGDMA (cross-linker, 1% v/v monomer) with stabiliser (10% $w/v_{monomer}$) of different compositions (see table 1) and initiator (V-70, 1% w/v monomer).

There appears to be a morphology change of the poly(HEMA) product for stabiliser compositions that were clearly rich in one of the co-monomers (23:77 and 75:25 VAc/VPi ratio). These copolymers led to formation of porous poly(HEMA) monoliths instead of particles (Figure 6, Entry 4 and 16) . For these extreme compositions the copolymers were not able to stabilize the growing HEMA particles, but the breakdown of steric stabilisation leads to a porous polymer poly(HEMA) network.

Notably, some of the stabilisers were still end-capped by the RAFT agent with a percentage was determined by ^{1}H-NMR and reported in Table 1. By comparing the results collected in Table 1 (Entry 4,11,16), the stabilisation efficiency does not seem to be guided by the chain end functionality (Figure 6: Image 4/11/16). Therefore, the origin of stabilisation appears to be mainly by adsorption of the stabiliser on the particle surface and imparting long-range repulsion rather than anchoring to the particles *via* RAFT end-groups[18].

ii. Molecular weight

Different molecular weight stabilisers (PVAc-*s*-PVPi) were tested for their effect on particle formation, morphology and size. Surprisingly, quite well-defined particles are formed for stabilisers with very low VAc content and low molecular weights (Figure7- Entry 1/2/3). This is attributed to the higher solubility of these lower molecular weight stabilisers. However, the particles produced do remain quite large in diameter (Table 1-Entry 1/2/3). Further increasing the composition (Figure 7: 5/6/7) ill-defined particles were observed. At 50:50 (VAc:VPi) stabiliser composition, the molecular weight effect was clearly evidenced by SEM (Figure 7: 10/11/12/13). At this composition, there seems to be a specific molecular weight (M_n: 12 kg/mol) to achieve good stabilisation (Figure 7: 11).

The best-defined and smallest particles are produced with a composition of VAc:VPi 55:45 (Figure 7, Image-14,15). In general, the composition appears to the dominant parameter for efficient stabilisation of the particles. At this composition (VAc:VPi 55:45) an increase of molar mass from 8.6 kg/mol to 12.8 kg/mol shows a significant and controllable decrease of the particles size from 2.2μm to 1.3 μm, although the size distribution was slightly broadened.

In previous work we produced poly(HEMA) nanoparticles in $scCO_2$ aided by a perfluorinated diblock stabiliser based on polyethylene oxide (PEO) and poly(heptadecafluorodecyl acrylate) (PFDA)(PEO-*b*-PFDA). The particles were obtained with diameter as small as 200 nm[9]. Others have shown that dispersion in $scCO_2$ using a silicone based stabiliser can yield controlled particle sizes from 300 nm to 7 μm for PMMA.[30] Although the particles obtained in this work (Figure 7- Entry 15) had larger sizes (diameters in micrometre range) they are still very well-defined and of practical interest. In conclusion, the most efficient stabiliser

was found to be the copolymer with VAc:VPi 55:45 composition and 12.8 kg/mol and was therefore selected for further investigation.

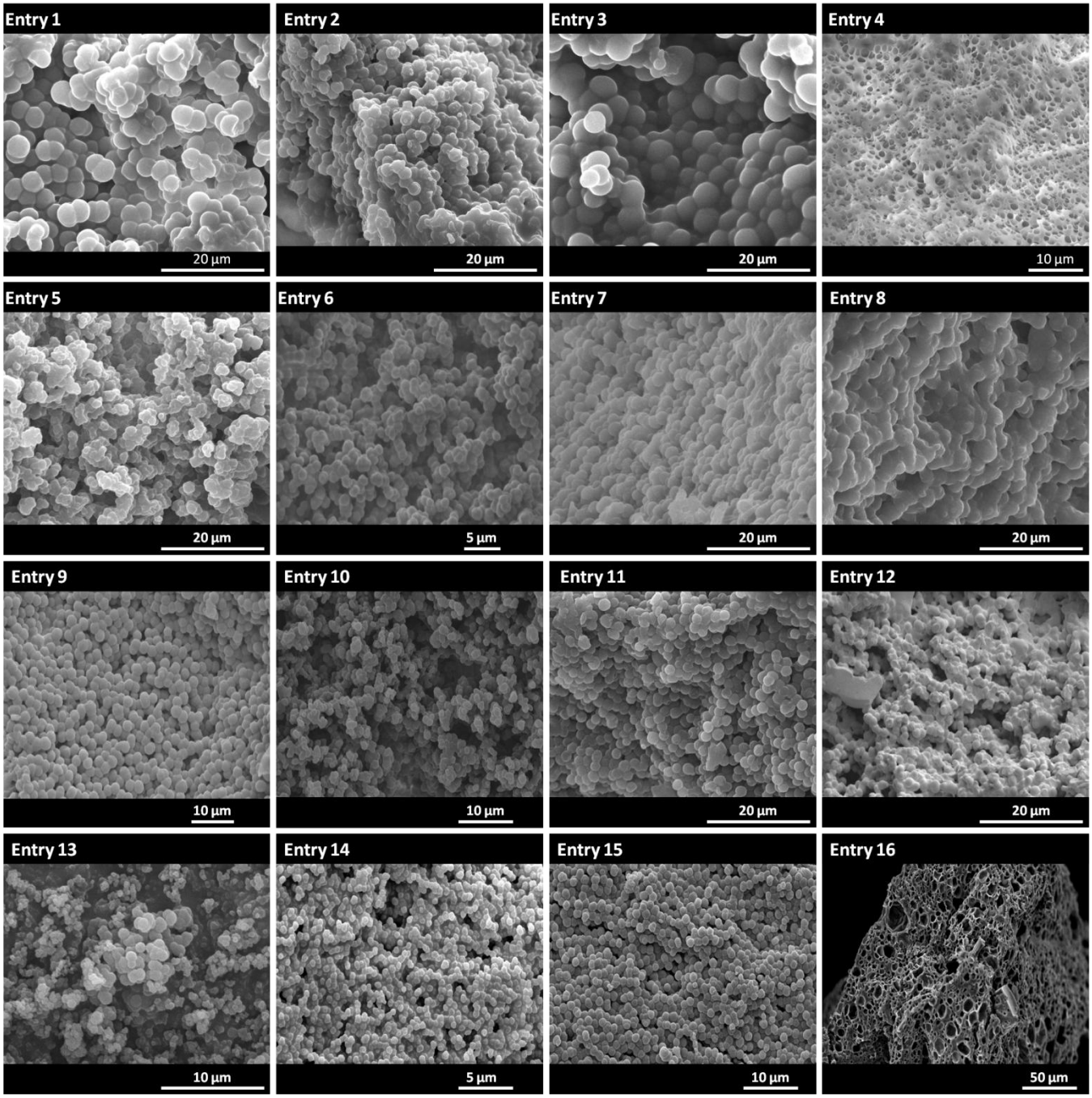


Figure 7: SEM images of the particles obtained after dispersion polymerisation of HEMA (10% v/v CO_2) and EGDMA (cross-linker, 1% v/v monomer) with stabiliser (10% w/$v_{monomer}$) of different compositions (see entry of table 1) and initiator (V-70, 1% w/$v_{monomer}$).

3.2.2. Effect of cross-linker content

It has been reported that mechanical properties such as stiffness and surface hardness of bulk or particle hydrogel networks can be tuned by tailoring the composition of the network by incorporating co-monomers or varying cross-linking density. [31,32]

Thus, dispersion polymerisation of HEMA was carried out with three different initial concentrations of EGDMA whilst keeping the other parameters constant (i.e stabiliser composition, ratio). The effect of initial cross-linking content on the particle size and morphology were demonstrated by SEM images (Figure 8). Surprisingly we found that in our control epxeriments with no added EGDMA the poly(HEMA) particles were found to be slightly cross-linked. However, this can be explained by the fact that small levels of EGDMA are present as an impurity in the monomer.[33] A clear trend (Figure 8) is seen as the cross-linking initial concentration increases (0 to 3% wt); more uniform and discrete particles were formed.

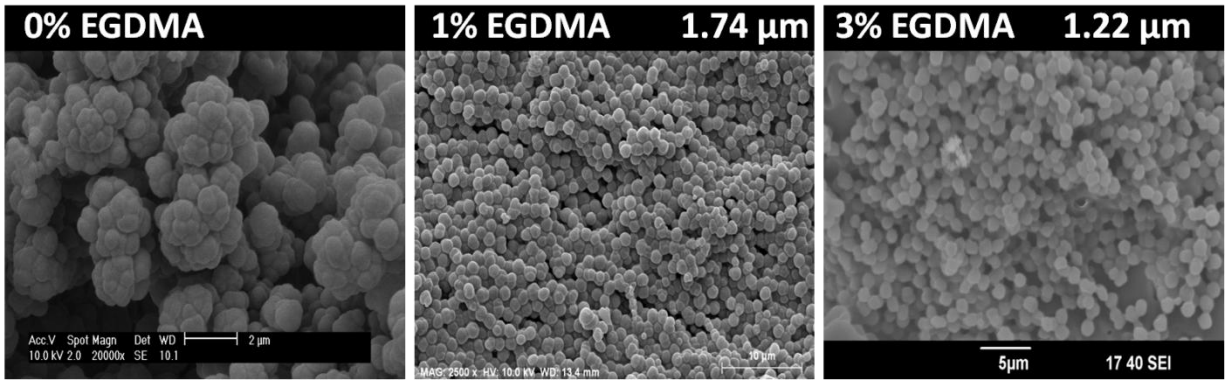


Figure 8: Effect of cross-linker concentration on particle morphology A: 0% EGDMA, B: 1% EGDMA, C: 3% EGDMA added. Stabiliser characteristics are listed at Table 1- Entry 15.

The likely reason for the apparently better stabilisation is that the particle surfaces have become rigid because of the action of the cross-linker and this helps in preventing coalescence of the particles when they collide in the dispersion process or after

depressurisation.[34] In addition to better stabilisation, the particle size also decreased from 1.74 to 1.22 µm as cross-linker EGDMA was increased from 1% wt to 3% wt.

Dynamic mechanical analysis (DMA) was conducted in order to see the effect of the cross-linking density on the particle properties. DMA plots (Figure 9) indicate two distinctive peaks. The first peak in the DMA curves is ascribed to the stabiliser present on the particle surfaces a conclusion drawn from comparison with DSC analyses of the stabiliser alone which gives a peak at around 50°C. The second peak is clearly assigned to the poly(HEMA) network (Figure 9) based on literature data[35] and this peak increases with cross linker density.

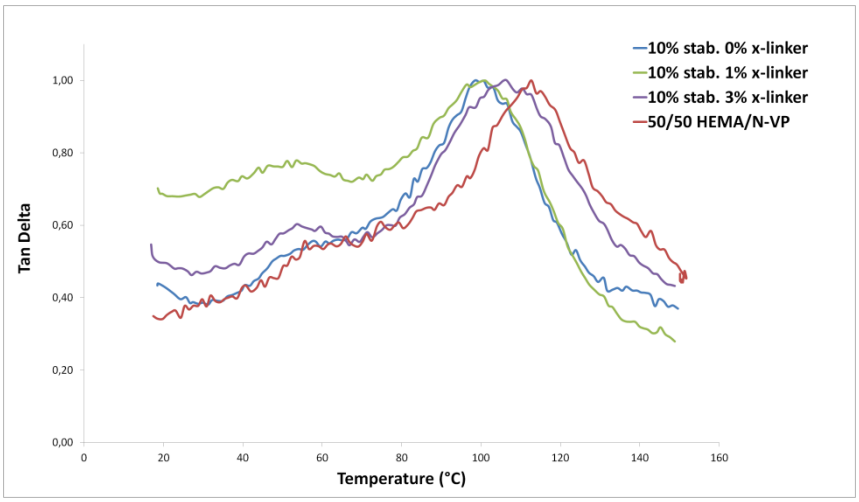


Figure 9: Dynamic mechanical analysis of the poly(HEMA) particles obtained with various cross-linker concentrations as well as copolymerisation of HEMA with N-VP using 1% cross-linker.

A clear trend is seen, with high concentration of crosslinker leading to higher T_gs and indicating that higher cross-linking density was achieved in the resultant networks (Table 3-Entry 3). Thus, by this process, the cross-linking density can be adjusted simply by tuning the

amount of cross-linking agent concentrations (EGDMA) to reach the desired properties required in the function of the targeted application.

Table 3: DMA results of the poly(HEMA) particles

Entry	Stabiliser %	Cross-linker %	Peak 1 (°C)	Peak 2 (°C)
1	10	0	57.5	98.5
2	10	1	53.5	101
3	10	3	53.6	106.5

3.2.3 Copolymerisation with MMA and N-VP

As mentioned earlier, another approach to vary the properties of the poly(HEMA) particles is copolymerisation with either a hydrophobic or a hydrophilic co-monomer. Therefore, copolymerisations of HEMA with methyl methacrylate (MMA) or N-vinylpyrrolidone (N-VP) have been performed using 50% v/v monomer initial feed ratios.

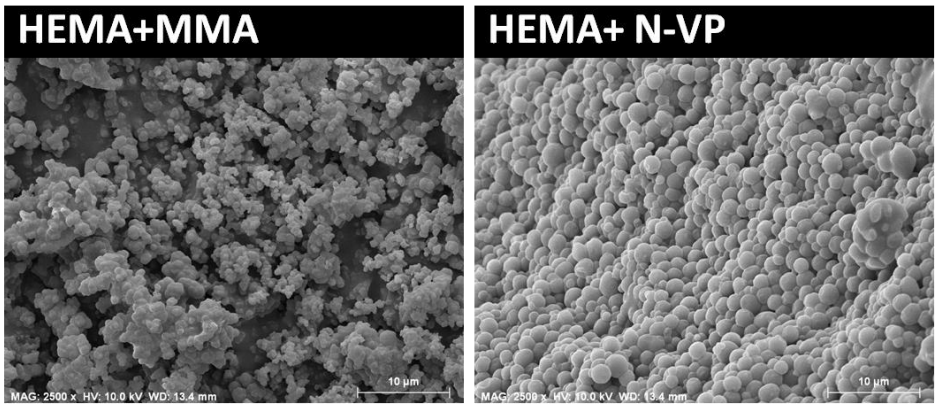


Figure 10: Copolymerisation with 50% v/v MMA/N-VP with respect to HEMA. The feed ratios for stabiliser (10% w/$v_{monomer}$), cross-linker (EGDMA, 1% v/v monomer), (55/45, 12.8k, Table 2- Entry 7), and initiator (1% $w_{V\text{-}70}/w_{monomer}$), kept constant as well as the reaction conditions (35°C and 240 bar).

As shown by the SEM images (Figure 10), the addition of MMA to the reaction mixture alters the stabilisation of the system and ill-defined particles were produced. By contrast, the copolymerisation of HEMA with N-VP results in largely spherical particles with a small amount of aggregation. A previous work on this PVAc-*s*-PVPi hydrocarbon based stabiliser

has already reported the successful stabilisation of PVP particles thanks to the polymerisation of VP from the macroRAFT stabiliser. [19] Nevertheless, the lower reactivity of methacrylic radicals prevents the particles formation of PMMA by the same process. Therefore, a better stabilisation of the poly(HEMA) particles is expected when it is copolymerised with N-VP rather than with MMA. Poly(HEMA-*co*-NVP) particles were obtained with a size of 1.8 µm which essentially the same as that obtained for poly(HEMA) particles (1.74 µm) with the same stabiliser (Table 1-Entry 15)

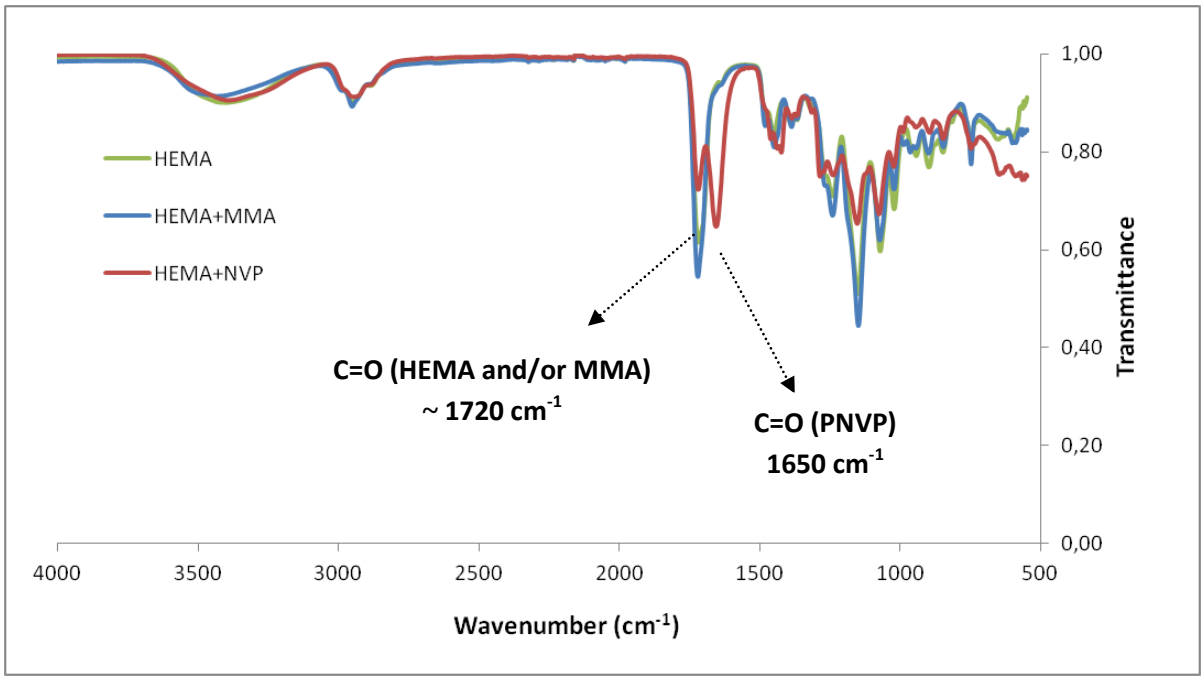


Figure 11: ATR FTIR spectra for poly(HEMA-*co*-MMA) and poly(HEMA-*co*-NVP)

The incorporation of MMA and N-VP as co-monomers was evidenced using ATR-IR (Figure 11). Successful copolymerisation of HEMA with N-VP was confirmed by the appearance of the characteristic peak of a carbonyl group (C=O) assigned to the N-VP moieties at 1650 cm^{-1}. The introduction of N-VP units in the poly(HEMA) network impacts the properties of the particles (Figure 9). DMA measurements demonstrate that the Tg of the network containing N-VP is shifted from 101°C to 113° as would be expected.

All of these data clearly show that we have developed a robust and fluorine-free dispersion process in $scCO_2$ that allows production of well-defined hydrophilic networks of poly(HEMA) and N-VP with both adjustable Tg and variable cross-link density; both of which could be used to potentially modulate their swelling in water. But there is a problem, these surfactants are hydrophobic, thus it is unlikely that the materials will disperse in water. For this reason we began to look closely at the possibility of hydrolysing the particle surface located surfactant molecules.

3.3 Hydrolysis of the stabiliser towards hydrogel microparticles

In order to create water dispersible particles, the stabiliser adsorbed on the particle surface must be hydrolysed. The statistical copolymer of PVAc-*s*-PVPi could be converted into the water soluble poly(vinyl alcohol) (P(VOH)) by hydrolysis of the ester groups. Bit could this occur successfully on the microparticle surfaces. Two different hydrolysis procedures were tested and the resultant particles were first interrogated by FTIR-ATR results (Figure 12). These clearly demonstrate that hydrolysis occurs since broad –OH peaks have clearly appeared at around 3500 cm^{-1}.

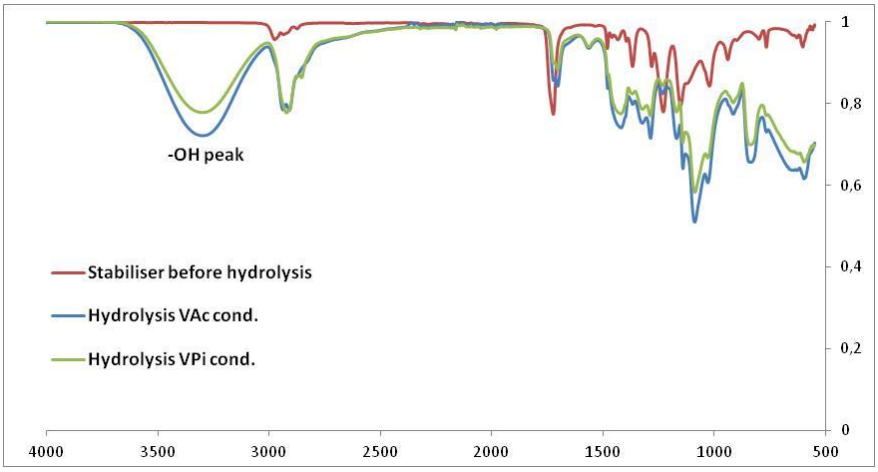


Figure 12: FTIR-ATR spectra of the P(VAc-co-VPi) stabiliser before (red) and after hydrolysis under two different sets of hydrolysis conditions (see the experimental section)

As expected, the carbonyl peak at around 1700cm^{-1} decreases, but it does not completely disappear. Most importantly, this very simple hydrolysis system provides sufficient hydrolysis of the surface located stabiliser molecules to allow the microparticles to become dispersible in water. A significant breakthrough that shows that we can overcome the previous issues found with the fluorinated systems to create a clean and facile route to readily water dispersible microparticulate gel systems.

Having established the hydrolysis parameters, we repeated these experiments on poly(HEMA) particles prepared with the selected PVAc-*s*-PVPi stabiliser in presence of 1% or 3% cross-linker. Hydrolysed particles were harvested from the hydrolysis process by rotary evaporation and subsequent freeze-drying. Particle morphologies were further inspected by SEM and compared to the non-treated particles. SEM images (Figure 13-left) clearly show that hydrolysis was non-destructive for the poly(HEMA) particle morphology, especially for the 3% cross-linker content.

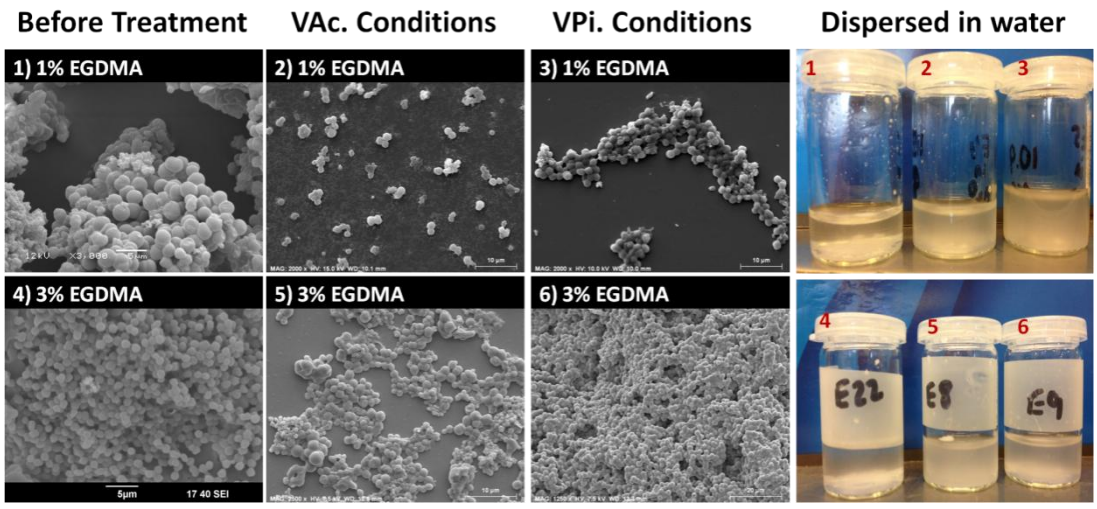


Figure 13: Left: SEM images for poly(HEMA) particles obtained with either 1% (Samples 1 to 3) or 3% crosslinker (samples 4 to 6), before and after hydrolysis Right: pictures of the same particles redispersed in water clearly showing that the hydrolysed samples (2 & 3) are redispersed in water.

The hydrolysed particles were redispersed in water at a concentration of 5mg/ml and sonicated for 2 minutes using a horn sonicator at high amplitude and frequency. The solution behaviour (Figure 13-right) clearly demonstrates that hydrolysis enables dispersion in water. Before hydrolysis, most of the particles settle to the bottom of the vial (Figure 13-Vial 1 and 4,) whereas after hydrolysis a much larger portion of the particles are clearly dispersed in water (Figure 13-Vial-2, 3, 5 and 6,) a clear result of the increased hydrophilicity of the microparticle surfaces through hydrolysis of the ester groups of the stabiliser.

For sake of comparison, these hydrolysis parameters have been applied to previously synthesised poly(HEMA) cross-linked particles obtained in the presence of a perfluorinated stabiliser, i.e. PEO-*b*-PFDA diblock copolymer.[9] The photos (Figure 14) before and after hydrolysis clearly evidences the slight improvement in the dispersion of the particles in aqueous media.

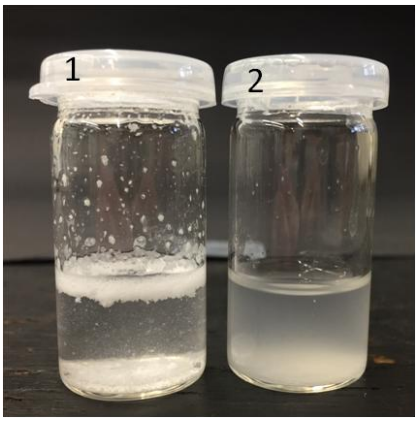


Figure 14: poly(HEMA) particles synthesized in the presence of PEO-*b*-PFDA before hydrolysis (1) and after hydrolysis (2). Images are taken just after dispersion in water with a concentration of 5 mg/ml. Some improvement is clearly seen for PEO-*b*-PFDA stabiliser but it is perhaps attributable to hydrolysis of RAFT-end groups leading to an improvement of the water dispersability. More importantly, the stability of this dispersion is lower compared to the other hydrolysed particles. Less than 15 minutes the particles starts to phase separate and we see a clear water phase. By contrast those from PVAc-*s*-PVPi persist for 48 minutes.

This could be explained by the minor effect of the hydrolysis procedure on the particle surface (i.e hydrolysis of the RAFT agent and/or superficial ester groups).In comparison to former particles, reprecipitation of the PEO-*b*-PFDA stabilised particles was found to be rapid (<15 minutes). In contrast, the hydrolysis procedure proved to be strongly enhancing the redispersion of the particles synthesised in the presence of the PVAc-*s*-PVPi stabiliser (still stable after 45 minutes).

3.3.1 Swelling of the homo/copolymer networks in water

Since poly(HEMA) is highly hydrophilic, the swelling of the networks after hydrolysis can be gauged by DLS. The size of the particles was measured by DLS directly after suspension in water. DLS measurements were done in triplicates and the values are reported as an average in Table 4. The values obtained from DLS measurements were compared to the size measured in the dry state from SEM micrographs. It is clear that all the particles exhibit a significant size increase in water compared to the dry state confirming their quick swelling capability.

Table 4: DLS size distributions for the homo- and copolymer networks.

Entry	Monomer(s)	Cross-linker	SEM size	DLS[a] size (µm)	
		(%, v/v monomer)	(Dry,µm)	Peak 1	Peak 2
1	HEMA	1	1,74	348 nm	3.74
2	HEMA	3	1,22	3.05	
3	HEMA+N-VP	1	1,80	4.81	

a: DLS measurements were done in water.

In case of lightly cross-linked poly(HEMA) with 1% cross-linker, a bimodal distribution is observed by DLS indicated by appearance of two peaks first peak average around 350 nm

and second one around 3,7 micrometre. This bimodal distribution was the evidence that all the particles were not evenly cross-linked leading to size differences throughout the sample.

This was further confirmed by the monomodal distribution observed for poly(HEMA) particles with higher cross-linker content (3%) underwent a size increase from dry state 1.22µm to 3.05 µm in water. As it was anticipated higher cross-linked particles size increased less than the In poly(HEMA)with 1% cross-linking content. This behaviour is observed for cross-linked particles where increase in cross-linking degree leads to lower swelling ratio. I n the case of the poly(HEMA-co-NVP) particles showed a rapid swelling from 1.8 µm to 4.8 µm. Compared to the homopolymer particles, the poly(HEMA-co-NVP) particles have shown a higher swelling due to increased hydrophilicity of the network owing to lactam group in N-VP co-monomer.[31] Therefore, DMA and DLS analyses have demonstrated that the mechanical and swelling properties of the resultant polymer network can be altered either by copolymerisation or by varying the cross-linking density. More importantly, the swelling behaviour of the homo/copolymer networks in the aqueous suspensions provides a clean route to poly(HEMA) microgels that is highly versatile and can be adjusted with several parameters to obtain particles of interest.

4. Conclusions

Poly(HEMA) particles were successfully obtained in $scCO_2$ using a fluorine-free stabiliser system composed of VAc and VPi. After studying various stabilisers of different molecular weight and composition, the optimised stabiliser was based upon PVAc-*s*-PVPi with a molar mass of 12.8 kg/mol and a composition of 55:45 and is the most efficient for the dispersion copolymerisation of HEMA and EGDMA in $scCO_2$, leading to well-defined particles having

size of 1.22 µm. This green process was also found to be robust enough to be applied to HEMA copolymerisation with various amounts of cross-linker and with addition of other monomers, i.e. MMA and N-VP allowing control of physico-mechanical properties of the obtained particles. An increase in the glass transition temperature (Tg) of the networks was observed in both cases.

In addition, the PVAc-*s*-PVPi adsorbed stabiliser on the surface of the particles could be hydrolysed to PVOH to facilitate their redispersion in water leading to hydrogel particles of a few micron-size depending on the cross-linker or co-monomer content. This facile and green route to poly(HEMA) based microgels opens a pathway to a wide range of formulations for biomedical applications such as *in-situ* encapsulation of solvent and temperature sensitive bioactive ingredients especially protein/peptide based drugs.

References

1 P. T. Anastas, Lauren G. Heine and Tracy C. Williamson, in *Green Chemical Syntheses and Processes*, 2000, vol. 767, pp. 1–6.
2 P. T. Anastas and M. M. Kirchhoff, *Acc. Chem. Res.*, 2002, **35**, 686–694.
3 E. Girard, T. Tassaing, J.-D. Marty and M. Destarac, *Polym. Chem.*, 2011, **2**, 2222–2230.
4 E. J. Beckman, *J. Supercrit. Fluids*, 2004, **28**, 121–191.
5 M. Sihvonen, E. Järvenpää, V. Hietaniemi and R. Huopalahti, *Trends food Sci. Technol.*, 1999, **10**, 217–222.
6 O. R. Davies, A. L. Lewis, M. J. Whitaker, H. Tai, K. M. Shakesheff and S. M. Howdle, *Adv. Drug Deliv. Rev.*, 2008, **60**, 373–387.
7 S. P. Nalawade, F. Picchioni and L. P. B. M. Janssen, *Prog. Polym. Sci.*, 2006, **31**, 19–43.
8 A. I. Cooper, *J. Mater. Chem.*, 2000, **10**, 207–234.
9 R. Parilti, D. Alaimo, B. Grignard, F. Boury, S. M. Howdle and C. Jérôme, *J. Mater. Chem. B*, 2017, **5**, 5806–5815.
10 J. M. DeSimone and J. S. Keiper, *Curr. Opin. Solid State Mater. Sci.*, 2001, **5**, 333–341.
11 P. Raveendran and S. L. Wallen, *J. Am. Chem. Soc.*, 2002, **124**, 12590–12599.
12 S. G. Kazarian, M. F. Vincent, F. V Bright, C. L. Liotta and C. A. Eckert, *J. Am. Chem. Soc.*, 1996, **118**, 1729–1736.
13 T. Sarbu, T. Styranec and E. J. Beckman, *Lett. to Nat.*, 2000, **405**, 165–168.
14 B. Tan, H. M. Woods, P. Licence, S. M. Howdle and A. I. Cooper, *Macromolecules*, 2005, **38**, 1691–1698.
15 B. Tan and A. I. Cooper, *J. Am. Chem. Soc.*, 2005, **127**, 8938–8939.

16 K. Chen, N. Grant, L. Liang, H. Zhang and B. Tan, *Macromolecules*, 2010, **43**, 9355–9364.
17 H. Lee, J. W. Pack, W. Wang, K. J. Thurecht and S. M. Howdle, *Macromolecules*, 2010, **43**, 2276–2282.
18 H. Lee, E. Terry, M. Zong, N. Arrowsmith, S. Perrier, K. J. Thurecht and S. M. Howdle, *J. Am. Chem. Soc.*, 2008, **130**, 12242–3.
19 N. A. Birkin, N. J. Arrowsmith, E. J. Park, A. P. Richez and S. M. Howdle, *Polym. Chem.*, 2011, **2**, 1293.
20 E. J. Park, A. P. Richez, N. a. Birkin, H. Lee, N. Arrowsmith, K. J. Thurecht and S. M. Howdle, *Polymer (Guildf).*, 2011, **52**, 5403–5409.
21 A. J. Cadotte and T. B. Demarse, *J. Neural Eng.*, 2005, **2**, 114–122.
22 H. S. Ganapathy, H. S. Hwang, M. Y. Lee, Y. T. Jeong, Y. S. Gal and K. T. Lim, *J. Mater. Sci.*, 2008, **43**, 2300–2306.
23 J. Bernard, A. Favier, L. Zhang, A. Nilasaroya, T. P. Davis, C. Barner-Kowollik and M. H. Stenzel, *Macromolecules*, 2005, **38**, 5475–5484.
24 P. Licence, M. P. Dellar, R. G. M. Wilson, P. A. Fields, D. Litchfield, H. M. Woods, M. Poliakoff and S. M. Howdle, *Rev. Sci. Instrum.*, 2004, **75**, 3233–3236.
25 S. Perrier and P. Takolpuckdee, *J. Polym. Sci. Part A Polym. Chem.*, 2005, **43**, 5347–5393.
26 C. E. Lipscomb and M. K. Mahanthappa, *Macromolecules*, 2009, **42**, 4571–4579.
27 D. A. Canelas and J. M. DeSimone, *Macromolecules*, 1997, **30**, 5673–5682.
28 Y.-L. Hsiao, E. E. Maury, J. M. DeSimone, S. Mawson and K. P. Johnston, *Macromolecules*, 1995, **28**, 8159–8166.
29 H. Shiho and J. M. DeSimone, *Macromolecules*, 2000, **33**, 1565–1569.
30 T. D. McAllister, L. D. Farrand and S. M. Howdle, *Macromol. Chem. Phys.*, 2016, 1–8.
31 E. Seo, S. Kumar, J. Lee, J. Jang, J. H. Park, M. C. Chang, I. Kwon, J.-S. Lee and Y. Huh, *Macromol. Res.*, 2017, **25**, 704–711.
32 W. Hou, Y. Shen, H. Liu, A. Zhang and S. Dai, *React. Funct. Polym.*, 2014, **74**, 101–106.
33 Z. Ma and P. Lacroix-desmazes, *Polym. J.*, 2004, **45**, 6789–6797.
34 S. P. Bassett, N. A. Birkin, J. Jennings, E. Chapman, R. K. O. Reilly, M. Howdle and H. Willcock, *Polym. Chem.*, 2017, **8**, 4557–4564.
35 J. Kopecek, *J. Polym. Sci. Part A Polym. Chem.*, 2008, **49**, 487–488.

Chapter 6

General conclusions and perspectives

General conclusions and perspectives

Drug delivery systems for hydrophobic drugs have been widely investigated for their controlled and targeted delivery to the intended organ, tissue or intercellular applications. However, there are still some obstacles to overcome the delivery of more complex drugs such as peptides and proteins. As it was mentioned in the first chapter, we have witnessed the plethora of works to design and synthesize peptide/protein based drugs. Peptide/protein drugs had taken great attention due to their specific activity and properties. Therefore, in comparison to small hydrophobic drugs, they offer much efficient therapies. Owing to these facts, great deal of studies is devoted to design hydrophilic drug delivery systems which would enable to encapsulate efficiently therapeutic protein and deliver them in controlled and targeted manner. Considering that, hydrophilic 3D polymer networks (hydrogels) has been extensively studied in biomedical application for delivery of hydrophilic drugs either in bulk form such as scaffolds for tissue engineering or in particle of sub(micronic) sizes as nano-/microgels which are able to carry drugs in their core. As it was mentioned in the Chapter 1 the nano-/microgels have withdrawn a great attention due to their unique features making them ideal candidates for delivery of the protein based drugs. Therefore, we focused on designing a protein delivery system based on cross-linked polymer particles of 2-hydroxyethyl methacrylate (HEMA). As it was highlighted in the first chapter homo/copolymer of HEMA have been employed in numerous drug delivery applications. Therefore, we have chosen poly(HEMA) as our polymer particle matrix. Further on this topic, we also wanted to tackle the use of organic solvents in synthesis of the polymers for biomedical applications. Hence, we have chosen supercritical carbon dioxide ($scCO_2$) as polymerisation medium which confers environmentally benign properties to particle

production system i.e dispersion polymerisation. In addition to that, this non-toxic FDA approved solvent enable to produce particles without solvent residues, as well as enabling handling heat labile active pharmaceutical ingredients (APIs).

For this purpose, in the second chapter, we have probed the effect of stabiliser architecture, molecular weight, temperature and pressure on poly(HEMA) particle size and morphology in $scCO_2$. Using a diblock stabiliser based on PEO and PFDA and with the aid of mild conditions (35°C/300 bar) we have achieved highly monodisperse well-defined spherical poly(HEMA) particles having size around 200 nm.

Even though, PEO-*b*-PFDA stabiliser results in excellent poly(HEMA) particles, it limits is redispersion in water due to its high hydrophobicity. Thus, based on our previous expertise, we have synthesized a photocleavable stabiliser which hydrophobic part (PFDA) can be extracted with UV after successful dispersion in $scCO_2$. In more details, the photosensitive moiety is photocleaved into corresponding aldehyde groups on the surface and carboxylic acid groups on the PFDA chain to be removed. Therefore, allowing us to perform surface modifications employing these generated aldehyde groups. Having established these mild conditions for obtaining cross-liked particles in $scCO_2$, we investigated forming particles in the presence of drug to be encapsulated employing this novel photocleavable stabiliser PEO-*hv*-PFDA. This one-pot encapsulation of a drug in sCO_2 was studied in following chapter (Chapter 3) using a NSAID Sulindac as a model drug. The results indicated that the one-pot encapsulation of Sulindac into poly(HEMA) networks was achieved with high encapsulation efficiency. Thereafter, upon UV-photolysis, the hydrophobic block of the stabiliser can be removed and enabled to disperse the Sulindac loaded poly(HEMA) cross-linked particles in water and leading to swollen microgels. The release behaviour of these swollen microgels

was studied and indicated that the Sulindac diffused from the poly(HEMA) matrix with a controlled manner. For surface modifications, a flurorescent probe was successfully grafted as demonstrated by fluorescent microscope images.

This work could be improved by using different cross-linking content to probe the effect on particle size and release behaviour. As well as, it would be beneficial to study higher drug feed ratios to gauge the limits of the one-pot encapsulation. Moreover, it would be interesting to graft different agents on the surface as targeting or imaging to establish both therapeutic and diagnostic (theranostic) applications. Moreover, release behaviour also could be studied after grafting of different agents to see the effect on the Sulindac diffusion. Even so, this study opened a promising pathway to study the one-pot encapsulation of protein/peptide based drugs. Additionally, we addressed some of these studies in the following chapter.

As we have emphasized our aim is to encapsulate protein/peptide based hydrophilic drugs. Hence, we applied the same method to encapsulate an antimicrobial peptide (AMP) in the poly(HEMA) particles. We have chosen AMP for well-founded reason which is to address the global antibiotic resistance. In this chapter (Chapter 4) PEO-*hv*-PFDA stabiliser was further investigated using different molecular characteristics, concentration to see the effect on the particle stabilisation and morphology. The AMP for S. Aureus was encapsulated successfully and the sustained release of the AMP from the microgels was confirmed by *in vitro* antibacterial activity. Having established the antibacterial activity of the particles, we further investigated the surface functionalisation of these particle surfaces grafting a targeting peptide for S. Aureus. These results showed that the particles could be targeted to the S. Aureus bacteria. Besides, we had some preliminary results on the selective S. Aureus

targeting of the particles with/without targeting peptide on the surface in the mixture of several types of bacteria colonies. Even though initial results hold a promise thus it needs to be improved. Therefore, these results were not incorporated in the thesis.

A common drawback of the studies of Chapter 3 and Chapter 4 is the use of an organic solvent (TFT) for the photolysis and the extraction of the fluorinated block of the stabiliser from the particle surfaces. in. A previous study[1] showed that both the photocleavage and extraction of the fluorinated block could be successfully performed in $scCO_2$. However, photocleavage in $scCO_2$ necessitates special high-pressure equipment with proper sapphire windows allowing efficient irradiation. If this strategy is followed in future, special attention should be given not to extract the guest molecules from the particles..

Finally, as an alternative to expensive fluorinated stabilisers for the dispersion polymerisation, a hydrocarbon stabiliser based on statistical copolymer of vinyl acetate (VAc) and vinyl pivalate (VPi) was used. In this chapter (Chapter 5) PVAc-*s*-PVPi copolymers with different molecular characteristics having different VAc and VPi ratio, molecular weights were tested along with different cross-linking degrees. In this chapter, we have shown that by a careful design of hydrocarbon based stabiliser well-defined poly(HEMA) particle can be produced in $scCO_2$ in micrometre range. In addition to that, by using this stabiliser, we can also introduce an alternative for UV treatment step that was required for fluorinated stabilisers. Thanks to simple hydrolysis reaction, we can convert the ester groups of the stabiliser into corresponding P(VOH) alcohol moieties. This enabled us to disperse the particles in water leading to poly(HEMA) microgels.

To best of our knowledge, so far hydrocarbon based stabiliser was not used for the synthesis of poly(HEMA) particles in $scCO_2$. Therefore, we strongly believe that this initial work

constitutes a platform to synthesize this highly biocompatible polymer using non-toxic environmentally benign solvent and that will be very beneficial for both manufacturing and medical point of view. Nevertheless, one-pot encapsulation and release behaviour from these particles should be carefully studied.

As conclusive remarks, supercritical carbon dioxide has been extensively used as a solvent or anti-solvent to produce drug loaded particles. However, co-precipitation, impregnation methods suffer from the solubility of either polymer or drug in this medium. Therefore, one-pot encapsulation using heterogeneous polymerisation techniques hold a great promise. Although this area of research is still in its infancy, we believe that in the near future the applications will be broadened.

1. D. Alaimo, B. Grignard, C. Kuppan, Y. Adriaensen, M. J. Genet, C. Dupont-Gillain, J.-F. Gohy, C.-A. Fustin, C. Detrembleur and C. Jérôme, *Polym. Chem.*, 2017, **8**, 581–591.

Annex

High pressure equipments

Abstract

Supercritical carbon dioxide necessitates utilisation of special high pressure equipment set-ups and procedures. Therefore, compared to conventional atmospheric processes, it is more challenging to perform experiments (such as sampling, stirring, heating, cleaning, etc.). Consequently, an annex is devoted to explain the technical aspects/challenges of the high-pressure equipments utilised in this project. Annex includes the high-pressure reactors description and mode of utilisation. Moreover, special cleaning procedure was also described for the ToP Industrie equipment.

1. ToP Industrie High pressure reactor (University of Liege)

Dispersion polymerisations of 2-hydroxyethyl methacrylate (HEMA) for Chapter 2, 3, 4 were carried out in a high pressure stainless-steel cell (82 ml, ToP Industrie) equipped with mechanical stirrer, a pressure transducer, a rupture disc, an internal thermocouple (Figure 1).

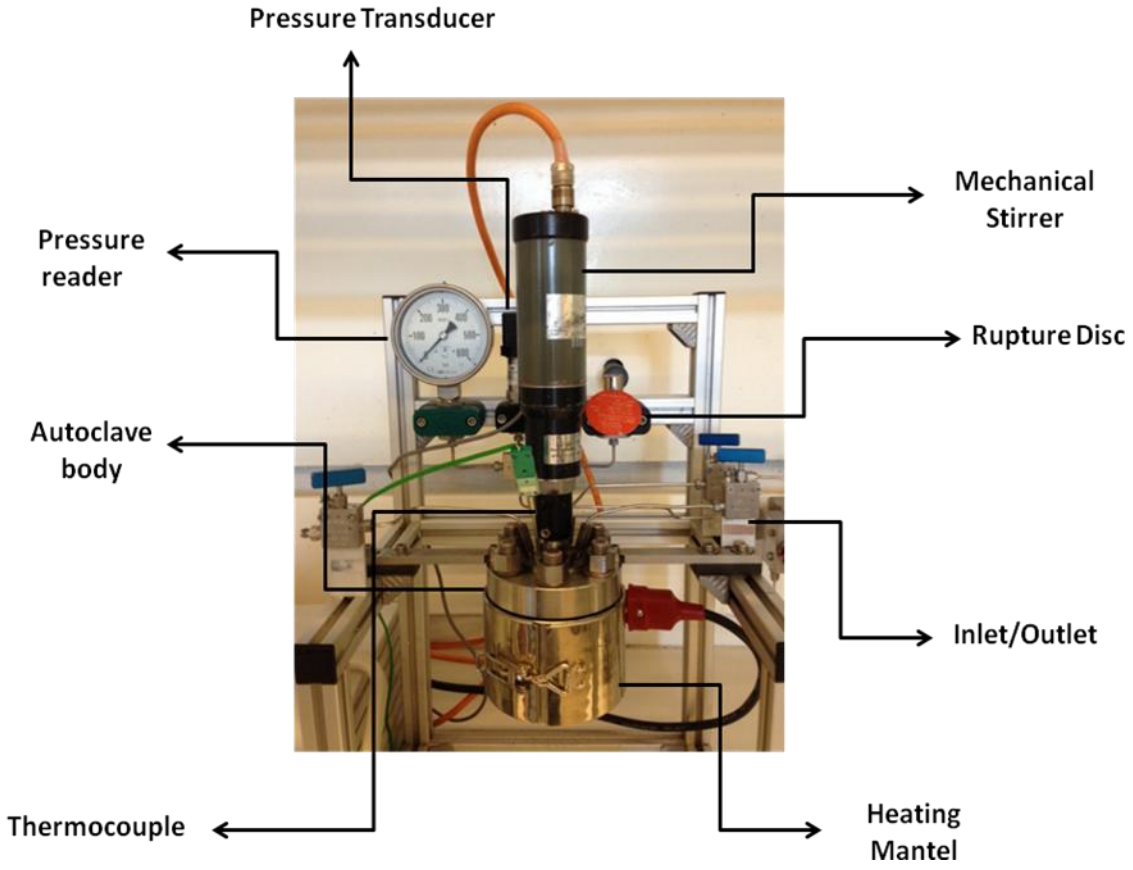


Figure 1: High pressure stainless steel cell (ToP Industrie)

As it can be seen from the photo there are 3 different valves interchangeable as inlet or outlet. The body of autoclave is bolted to the head of the reactor with 6 housings. And a key is used to securely tighten the bolts.

Internal parameters (temperature, pressure and stirring rate) are monitored by temperature control box containing an Auto-Adaptive PID controller. The electronic control unit can be seen in details in the figure below (Figure 2).



Figure 2: ToP Industrie® electronic control unitTouch-screen electronic unit allows adjusting internal parameters and also instant monitoring of internal parameters. Stirring and heating can be started after setting up the parameters on the screen simply pushing start/stop button.

Carbon dioxide (I5122, CO_2 N27/N48, Air Liquide, Belgium) is transferred to cell via ISCO 260D model syringe pump (Figure 3-Left) which is designed to handle and transferring supercritical fluids for research purposes. The pump has 266 ml of CO_2 capacity and can go up to pressures to 7500 psi (571 bar). As well as flow rate of the CO_2 can be adjusted in a wide range allowing constant desired flow of CO_2. The syringe is controlled by an LCD monitor (Figure 3-Right) attached to it. Syringe is connected and filled with CO_2 directly from the CO_2 tank with proper piping. The initial pressure on the syringe screen is equal to CO_2 bottle which is usually around 55 bar. Thereafter CO_2 pressurised by the cylinder present in the pump to the working pressures.



Figure 3: ISCO 260D® pump with one cylinder and LCD control unit.

1.1 Cleaning of the high-pressure reactor

Another challenging issue is the cleaning of the high-pressure equipment for further experiments. After polymerisations, the cell was opened and the products were collected as fine powders as described in the experimental chapters. Since cross-linked particles are obtained as fine powder during the experiment and depressurisation, they penetrate to the cavities of the reactor mostly to the mechanical stirrer. Therefore, the whole reactor has to be disassembled. The reactor parts are soaked in dimethylformamide (DMF) to swell the cross-linked particles (30 minutes to1 hour). Swollen particles are washed away till little or no particle is left. Thereafter, the reactor is assembled again and half-filled with DMF. The reactor is heated to 40°C and pressurized up to 200 bar. The reactor is left for stirring for an hour for the first washing. After, the reactor is stopped and opened. DMF is removed and the reactor body is dried with acetone. Following the drying step, the reactor is once again pressurized till 200 bars with CO_2 to ensure that there is no solvent left. After this second washing with CO_2, the reactor is ready for further use.

2. High pressure equipments (University of Nottingham)

2.1 MKIII clamp-seal autoclave

All dispersion polymerisations of HEMA that are reported in Chapter 5 are performed in 60 ml stainless steel autoclave (Figure 5) that is designed and produced by University of Nottingham. The autoclave is consisted of stainless steel head **(c)** and body **(d)**, safety clamp **(h)**, safety key **(**needle**, f)** and a stirrer **(e)**.

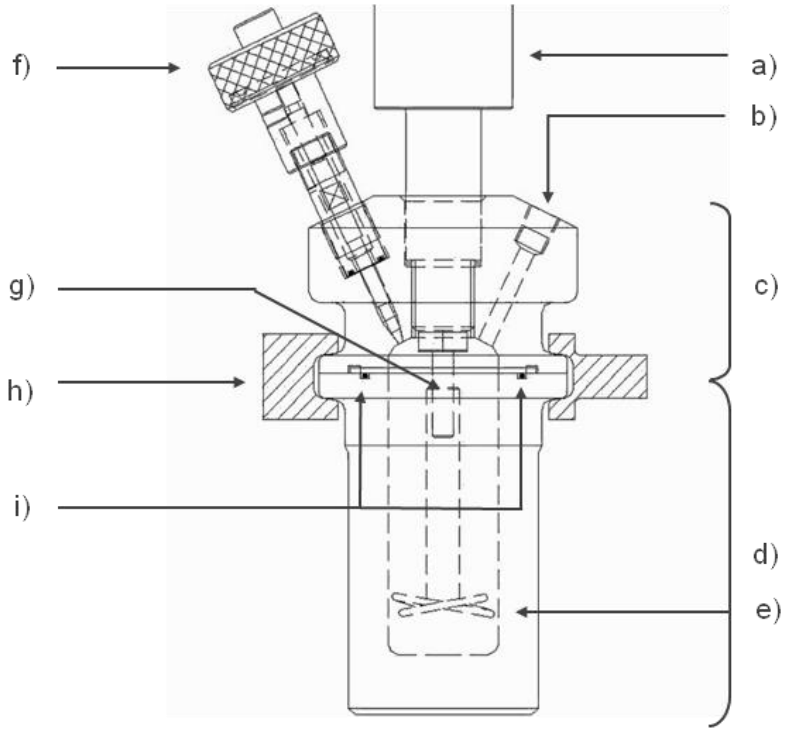


Figure 4: Scheme of 60 ml clamp-seal stainless steel autoclave.

In order to ensure the secure sealing of autoclave head **(c)** to the body **(d)** an EPDM O-ring **(i)** is placed in between. Additionally a clamp **(h)** is placed around these sections and

screwed with the unique key **(f)** for the autoclave. By this two-step sealing system the autoclave can hold pressures up to 4350 psi (300 bar). It can be seen from the Figure 4 a conventional autoclave head bears 5 housings **(b)** for inlet, outlet, thermocouple, safety valve and housing for additional feature such as connecting a high performance liquid chromatography (HPLC) pump for adding reagents under pressure to the reaction mixture.

As the name implies inlet tab is connected to the high pressure pump system which allows transferring CO_2 into the cell whereas the outlet tab is used for depressurizing the reactor. All the individual autoclaves are connected to the general pickel pump line which allows compressed CO_2 delivery.

The set-up for the general CO_2 flow can be seen in the diagram below. CO_2 bottle is connected to the pickel pump (Figure 5) which is equipped with a condenser to liquefy the CO_2 gas and then fed to the refrigerated pump. Liquefied CO_2 is then compressed to high pressures with the aid of compressor.

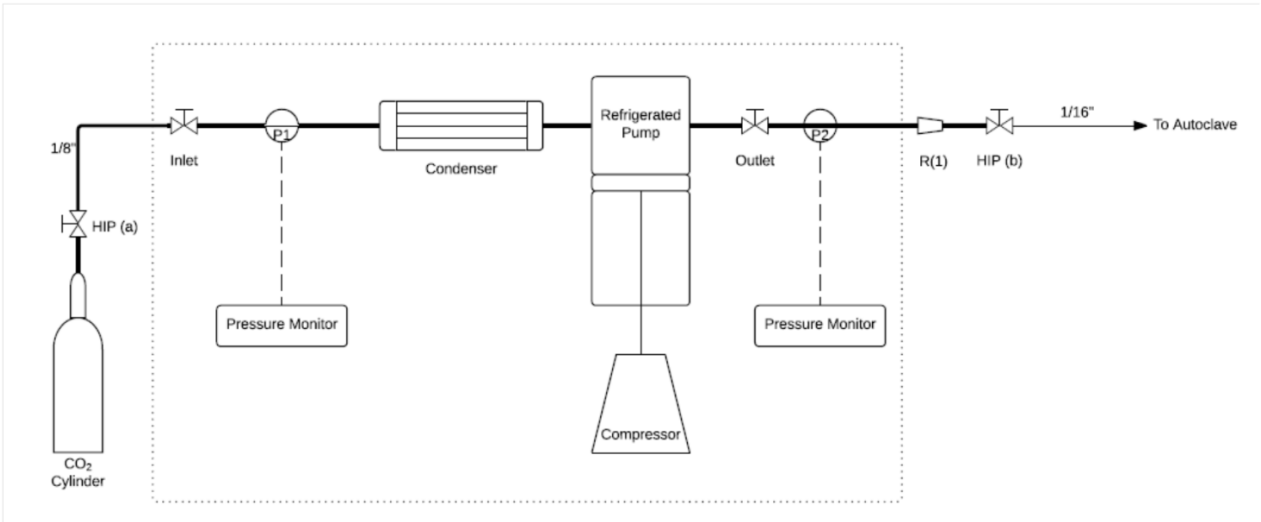


Figure 5: Schematic diagram of high pressure CO_2 pump line to individual autoclaves.

Normally inlet pressure is around 55 bar. However, to ensure the constant flow of CO_2 to numerous autoclaves pickel pump is employed where it allows to CO_2 transferring to many autoclaves at the same time with desired pressure. The outlet pressure of the pump is set to 300 bar and it is controlled by the air inlet. It can be also regulated by using the knob which is placed in front of the pump.

After successful transfer of CO_2 to the autoclaves internal pressure is monitored by the piezoelectric pressure transducer that is connected to electronic monitor. The high pressure autoclave (Figure 6) is heated with an electrical jacket. Heating jacket can be calibrated over a range of temperatures to allow controlled heating rate and stabilisation of the final reaction temperatures.

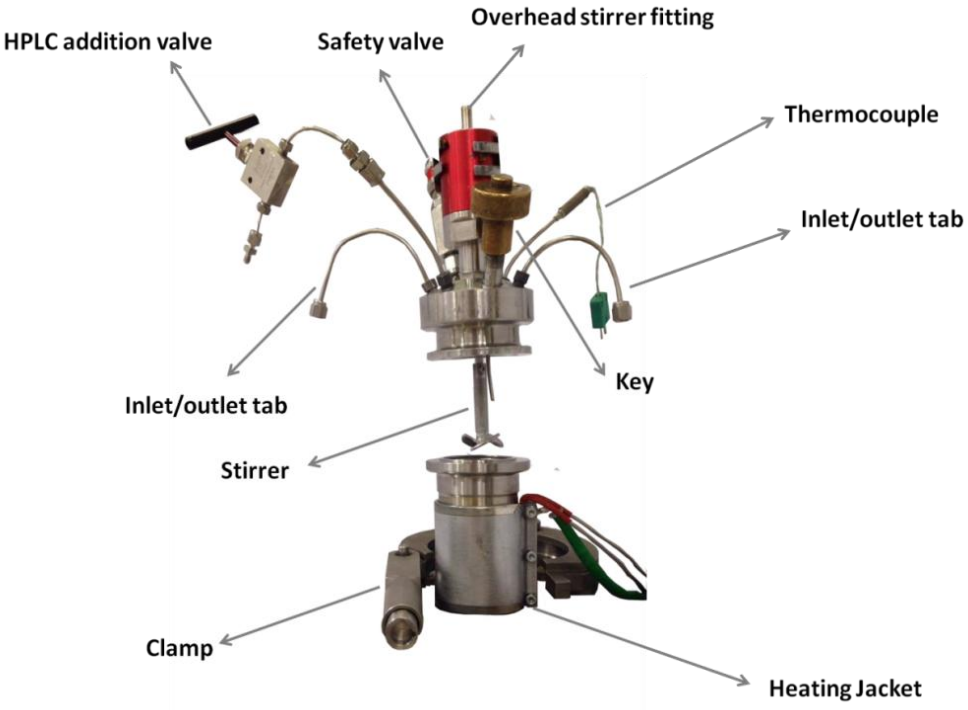


Figure 6: Photo of the MKIII clamp-seal autoclave and specific features are pointed out.

Temperature inside the cell is followed by a reader which is connected to the internal thermocouple. The autoclave is also equipped with a safety valve that prevents the

autoclave system not to exceed the pressures higher than 4350 psi. In unexpected situations with high temperature and pressure conditions excess amount of CO_2 will be released through the safety valve. In addition to this safety feature each individual high pressure autoclave set ups are connected to a trip switch which instantly cuts off the power to the heating monitor and heating jacket at the pressures above 4350 psi (300 bar).

2.2 High pressure variable volume view cell

Phase behaviour of the synthesised stabilisers in $scCO_2$ was investigated by using high pressure variable volume view cell (Figure 7-8) designed and produced by University of Nottingham.[1] Figure 8 shows the main parts of the variable volume view cell: Three ports are located on cell body; one on the top for the safety key and two remaining ports on the sides for internal thermocouple which extends out inside the solution and one for pressure transducer.

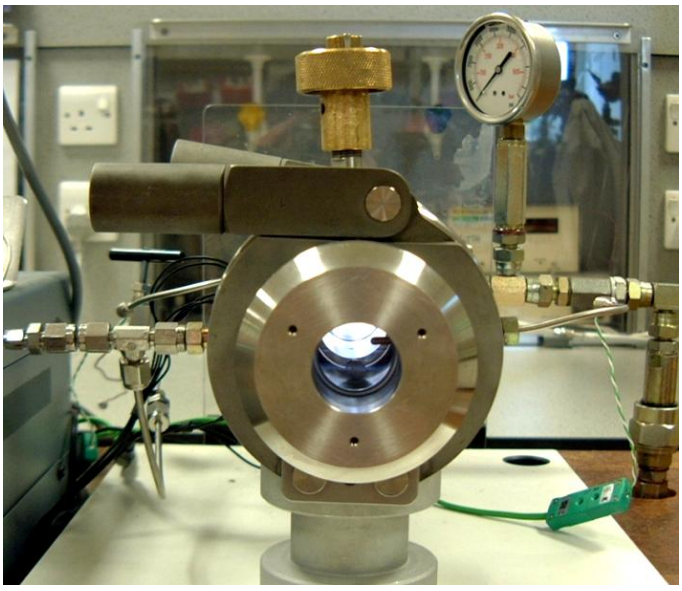
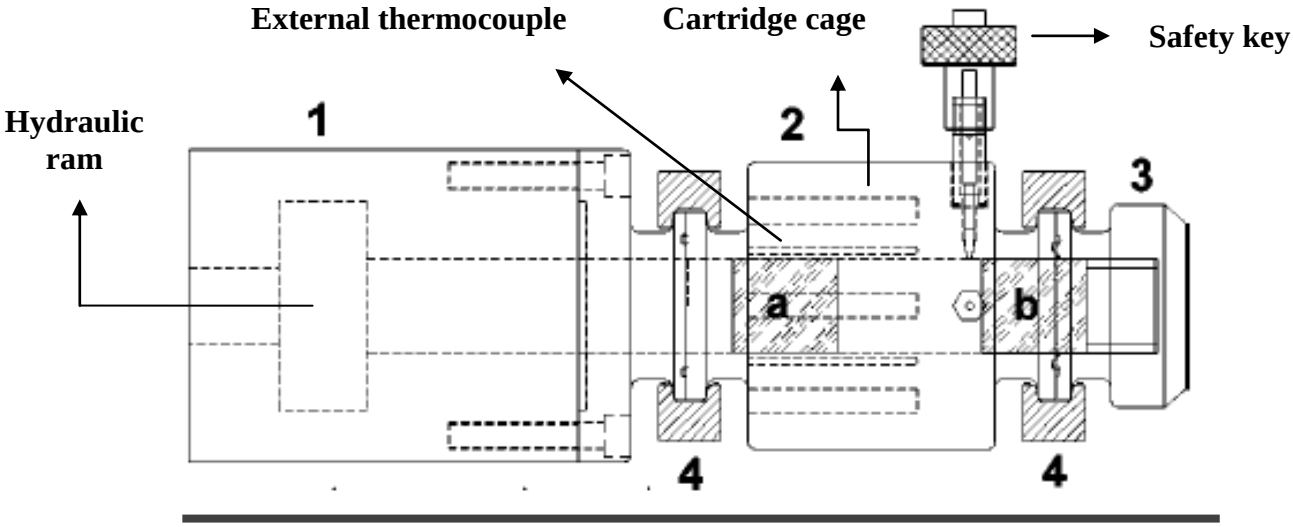


Figure 8: Front view of high pressure variable volume view cell.

The cell is heated with six cartridges that are allocated in the cages at the back of the body and additional thermocouple is fitted for to control the temperature. Last main part of the

view cell is the sapphire piston which moves back and forth thus changing the internal volume of the view cell. It is located at the very end of cell body and connected to hydraulic system with a safety clamp as in described for high pressure autoclave.



1) Hydraulic unit
2) Cell body
3) Window holder
4) Safety clamps
a) Sapphire piston
b) Static sapphire window

Figure 8: The scheme indicates the main parts of the high pressure variable volume view cell. Reproduced from reference.[1]

Internal parameters for the whole system is can be monitored and also adjusted by an electronic control unit. Additionally as in the case for high pressure autoclaves there is a trip switch for to cut off the power of the instrument if the cell temperature and pressure exceeds instruments limitations.

1. P. Licence, M. P. Dellar, R. G. M. Wilson, P. A. Fields, D. Litchfield, H. M. Woods, M. Poliakoff and S. M. Howdle, *Rev. Sci. Instrum.*, 2004, **75**, 3233–3236.